

**CENOZOIC SEISMIC STRATIGRAPHY OF THE CENTRAL NOVA SCOTIAN
CONTINENTAL MARGIN: THE INTERPLAY OF EROSION, DEPOSITION
AND SALT TECTONICS**

By

Adam W. MacDonald

Submitted in partial fulfillment of the requirements
for the degree of Masters of Science in
Applied Science Geology

at

Saint Mary's University
Halifax, Nova Scotia
January, 2006

© Copyright by Adam MacDonald, 2006



Library and
Archives Canada

Bibliothèque et
Archives Canada

Published Heritage
Branch

Direction du
Patrimoine de l'édition

395 Wellington Street
Ottawa ON K1A 0N4
Canada

395, rue Wellington
Ottawa ON K1A 0N4
Canada

Your file *Votre référence*
ISBN: 0-494-15257-5
Our file *Notre référence*
ISBN: 0-494-15257-5

NOTICE:

The author has granted a non-exclusive license allowing Library and Archives Canada to reproduce, publish, archive, preserve, conserve, communicate to the public by telecommunication or on the Internet, loan, distribute and sell theses worldwide, for commercial or non-commercial purposes, in microform, paper, electronic and/or any other formats.

The author retains copyright ownership and moral rights in this thesis. Neither the thesis nor substantial extracts from it may be printed or otherwise reproduced without the author's permission.

AVIS:

L'auteur a accordé une licence non exclusive permettant à la Bibliothèque et Archives Canada de reproduire, publier, archiver, sauvegarder, conserver, transmettre au public par télécommunication ou par l'Internet, prêter, distribuer et vendre des thèses partout dans le monde, à des fins commerciales ou autres, sur support microforme, papier, électronique et/ou autres formats.

L'auteur conserve la propriété du droit d'auteur et des droits moraux qui protègent cette thèse. Ni la thèse ni des extraits substantiels de celle-ci ne doivent être imprimés ou autrement reproduits sans son autorisation.

In compliance with the Canadian Privacy Act some supporting forms may have been removed from this thesis.

Conformément à la loi canadienne sur la protection de la vie privée, quelques formulaires secondaires ont été enlevés de cette thèse.

While these forms may be included in the document page count, their removal does not represent any loss of content from the thesis.

Bien que ces formulaires aient inclus dans la pagination, il n'y aura aucun contenu manquant.


Canada

Certification

Name: Adam MacDonald
Degree: Master of Science in Applied Science
Title of Thesis: Cenozoic Seismic Stratigraphy of the Central Nova Scotian Continental Margin: The Interplay of Erosion, Deposition and Salt Tectonics

Examining Committee:

Dr. Kevin Vessey, Dean of Graduate Studies

Dr. David H.S. Richardson, Program Co-ordinator

Dr. Grant Wach, External Examiner
Dalhousie University

Dr. Pierre Jutras, Senior Supervisor

Dr. David Piper, Supervisory Committee

Dr. David Mosher, Supervisory Committee

Dr. Andrew MacRae, Supervisory Committee

Date Certified: January 5th, 2006

© Adam MacDonald, 2006

Dedicated to Catherine,
for her patience, love and support.

TABLE OF CONTENTS

Table of Contents	iv
List of Figures	viii
List of Tables	xv
Abstract	xvi
Acknowledgements.....	xvii
1. Introduction.....	1
1.1 Study Area	3
1.2 Geologic Setting.....	7
1.3 Objectives	11
2. Methods	12
2.1 Two-Dimensional seismic reflection data	12
2.2 Three-Dimensional seismic reflection data	14
2.3 Seismic Stratigraphy	15
2.4 Seismic reflection facies	17
2.5 Synthetic Seismograms.....	17
2.6 Biostratigraphy.....	20
2.7 Gamma Ray	20
3. Introduction to Stratigraphic Architecture	23
3.1 General Statement.....	23
3.2 Seismic Stratigraphic Concepts	23
3.3 Sequence Stratigraphy	24
3.4 Sedimentation	28

3.5 Sub-Surface Salt.....	31
3.6 Paleochannels.....	33
3.7 Key Reflections.....	36
3.8 Seismic Reflection Geometry	40
4. Regional correlation and context	52
4.1 Biostratigraphy - Correlation to well data	52
4.1.1 Shubenacadie H-100	52
4.1.2 Newburn H-23	55
4.1.3 Glenelg N-49.....	57
4.1.4 Eagle D-21	58
4.2 Sequence Stratigraphy: Outer Shelf and Slope Relationship.....	59
4.2.1 Sequence One.....	59
4.2.3 Sequence Two.....	62
4.2.4 Sequence Three.....	63
4.2.5 Sequence Four.....	65
4.2.6 Sequence Five	65
4.3 Discussion	67
4.4 Stratigraphic Relationship to Salt Mobility	80
4.4.1 Sequence 1	80
4.4.2 Sequence 2	81
4.4.3 Sequence 3 and 4	81
4.4.4 Sequence 5	82

5. Facies types.....	83
5.1 Outer Shelf Deltas.....	84
5.2 Submarine Fans.....	85
5.3 Paleo-Channels	86
5.4 Mass Transport Complexes.....	89
5.5 Sediment waves I	93
5.6 Sediment waves II.....	95
5.7 Slope drape.....	95
5.8 Proglacial slope drape.....	98
5.9 Sediment drift.....	102
6. Integration of Stratigraphy and Facies Units	105
6.1 Sequence Unit 1	105
6.2 Sequence Unit 2	106
6.3 Sequence Unit 3	110
6.4 Sequence Unit 4	111
6.5 Sequence Unit 5	113
7. Discussion.....	117
7.1 Chronology of sea-level variation and associated depositional sequences.....	118
7.1.1 Paleocene through Early Eocene	121
7.1.2 Early Eocene through middle Early Oligocene	123
7.1.3 Middle Early Oligocene to end Middle Miocene	123
7.1.4 End Middle Miocene to Latest Miocene.....	127
7.1.5 Latest Miocene to end Quaternary.....	128

7.2 Timing of salt movement in relationship to the stratigraphic architecture	130
7.2.1 Paleogene	132
7.2.2 Neogene	134
8. Conclusions.....	136
References.....	140

LIST OF FIGURES

Figure 1.0	Location map of the study area, indicated by black box in center, in relation to the Scotian Basin.	4
Figure 1.1	Study area including well locations where biostratigraphic ties are correlated to seismic reflection data.	5
Figure 1.2	Seafloor surface render of the study area picked from 3-D seismic coverage and showing the canyons and ridges of the dissected slope.	6
Figure 1.3	Lithostratigraphy of the deepwater slope sediments.	8
Figure 2.1	Seismic stratigraphic features used to describe and interpret stratigraphy, depositional environment and facies distribution.	16
Figure 2.2	Synthetic seismogram progression from Checkshot to Interval velocity, Sonic velocities are multiplied by density for a given reflection coefficient, and then convolved with extracted wavelet to form a synthetic trace and synthetic profiles.	19
Figure 2.3	Simplified approach of lithologic interpretations based on Gamma Ray log signatures	22
Figure 3.1	A) Prominent reflectors of a seismic framework. B) Prominent reflections and established framework with internal reflection geometries and truncations.	25
Figure 3.2	Generalized sequence stratigraphic model analogues to the Scotian Slope and outer shelf relationship. Note the sequence boundary unconformity (orange) and deepwater (slope) conformities in the LST.	27
Figure 3.3	Generalized stratigraphic chart of the Cenozoic from the outer Scotian Shelf to Scotian Slope.	30
Figure 3.4	Seismo-stratigraphic deformation through uplift, collapse and faulting due to salt dynamics, and structural reorganization due to sub-surface movement.	32
Figure 3.5A	Interpreted paleo and modern day channel architecture from the upper slope as seen in seismic reflection profile.	34

Figure 3.5B	Interpreted paleo and modern day channel architecture from the lower-middle slope.	35
Figure 3.6	Type Section of the Cenozoic succession on the Central Scotian Slope, showing formation dip lines. Key reflectors are colored and line labeled as C10, E20, O30, M40, M50, P60 and P70.	37
Figure 3.7	Regional seismic line showing key reflectors from the slope to the shelf, and demonstrating seismic limitations at the shelf break. A) Reflector E20, draping over a convex lobe of internal chaotic reflections above C10.	39
Figure 3.8	A common loss of reflection continuity in the E20, M40, M50, P60 and P70 reflections due to paleochannel and paleo-canyon erosion.	41
Figure 3.9	The typical C10 reflection geometry relative to sub surface salt uplift and withdrawal, as well as shingle features (B) and the surface expression of a large withdrawal basin with bounding growth faults (A).	43
Figure 3.10	The M40 reflector and its faulted pattern in seismic reflection profile and in a 3-D time surface render.	46
Figure 3.11	The M40 reflector in relation to salt uplift in the middle slope with onlap and localized antiformal near the crest. Also to be noted are sediment wave features on the seaward side, above the salt high.	47
Figure 3.12	Seismic reflection profiles showing the high amplitude M50 reflector relative to salt highs in the middle slope and possible seafloor exposure due to uplift.	49
Figure 3.13	Seismic reflection profiles showing P60 draping a lower seismic unit of incoherent reflections. Also, the high, positive amplitude P70 reflection drapes the slope. Both reflectors are absent in the canyon area.	50
Figure 4.1A	Synthetic seismograms with key reflection correlations and biostratigraphic age picks of Shubenacadie H-100 and Newburn H-23 on the central Scotian Slope.	53

Figure 4.1B	Synthetic seismograms with key reflection correlations and biostratigraphic age picks of Glenelg N-49 and Eagle D-21 on the central Scotian Slope.	54
Figure 4.2	Multichannel seismic reflection profile from the outer shelf to slope in the northeastern part of the study area, with sequence boundaries identified and internal reflection geometries interpreted in relation to sequence boundaries.	60
Figure 4.3	Multichannel seismic and 3-D seismic reflection profile stitched together from the outer shelf to slope in the central portion of the study area with all five sequence boundaries identified and internal reflection geometries interpreted in relation to sequence boundaries.	61
Figure 4.4	3-D seismic reflection profile of the slope in the northeastern part of the study area, with sequence boundaries identified and internal reflection geometries interpreted in relation to sequence boundaries. (A) Packages of incoherent reflections on the lower slope.	64
Figure 4.5	3-D seismic reflection profile from the middle to lower slope, showing stacked packages of incoherent reflection interpreted as reoccurring mass transport deposits (MTDs) in Sequence 5.	66
Figure 4.6	Showing an alternative interpretation of sequence stratigraphy in the outer shelf to slope with many sub-sequences not fully addressed in this study.	68
Figure 4.7	Reflection geometry of Sequence 1, showing prograding reflections of the outer shelf delta and its coeval condensed section on the slope. Possibly forced regression of the delta front due to sea-level fall marks the Early Eocene upper boundary (C10) of the sequence.	70
Figure 4.8	(A) Submarine fan complex in relation to sequence boundaries in seismic profile.(B) Amplitude surface extraction of Sequence Boundary 1 (C10) showing the base of the fan complex with high amplitude paleo-channel fill and lower amplitude over channel deposits.	72

- Figure 4.9 Reflection geometry of Sequence 2 shelf margin regression and paleo-channel incision. On the slope, reflection, onlap the upper slope and thin seaward. A) submarine fan seen in Figure 4.8. B) central part of the study area in the same bathymetric setting as the submarine fan, but with more clinoform reflection geometry (inset). 74
- Figure 4.10 Reflection geometry of Sequence 3 showing, a relatively complete sequence stratigraphic succession of coastal margin regression FSST over upper slope reflections of the LST and TST. A) sediment waves in the upper to middle slope. B) Onlapping reflections on the upper to lower slope. 76
- Figure 4.11 Reflection geometry of Sequence 4, indicating a wedge of reflections onlapping the middle lower paleo-slope and downlapping reflections on the outer paleo-shelf in close proximity of the shelf break, forming a shelf margin wedge. A) Sequence Boundary 4 onlapping Sequence Boundary 3 on the upper paleo-slope. 77
- Figure 4.12 Reflection geometry of Sequence 5, showing complexity of onlapping / lapping and downlapping reflections of the paleo- slope in response to glacial influence. (A) scarps and associated erosional horizons. 79
- Figure 5.1 3-D seismic reflection profile flattened to the O30 unconformity reflection and to the base of a sheet-like lobe of a mature submarine fan of the Late Oligocene. 87
- Figure 5.2 A) 3-D seismic reflection profile from the upper slope, which is heavily incised by paleo-channel erosion and deposition. B) Interpreted paleo-channel evolution. 88
- Figure 5.3 3-D seismic reflection profile from the middle slope with multiple stage growth leveed paleo-channels. A-B: 3-D time slice showing the lateral lower amplitude nature of overbanking deposits. 90
- Figure 5.4A MTD outlined in yellow with depression filling geometry and hummocky upper surface. Typical incoherent internal reflections. Note: failure scarp labeled on inline profile and above draping unit. Crossline Profile A-B Figure 5.4B. 91

Figure 5.4B	Crossline seismic reflection profile with MTD outlined in yellow with a lense shape depression filling geometry with typical incoherent internal reflections.	92
Figure 5.5	(A) Type 1 sediment waves on the upper to middle slope recognized in seismic reflection profile as a convex lenses of aggrading reflections (inset top) internal to the upper and lower bounding high amplitude aggradation surfaces. (B) sediment wave trending ENE-WSW seen through 3-D seismic flattened time slice.	94
Figure 5.6	(A) Type 2 sediment waves in seismic reflection profile on the lower slope with aggrading reflections (inset) internal to the upper and lower bounding high amplitude aggradation surfaces. (B) sediment waves striking WNW seen on a 3-D seismic time slice.	96
Figure 5.7	Crossline and inline seismic reflection profile with a seismic unit of slope drape indicating relatively homogenous facies with low acoustic impedance, inferred here as fine grained sediment. Also, P60 draping of another acoustically weak sub-unit with considerably more upper surface morphology (Figure 5.9).	97
Figure 5.8	(A) Seismic reflection profile from the middle slope. (B) time surface render of P60.	99
Figure 5.9	(A) Slope-parallel striations seen in a 3-D amplitude extraction of the M50 reflector, which is also the top of a slope drape unit. (B) Striations in relation to the study area.	100
Figure 5.10	(A) Inline seismic reflection profile showing proglacial slope draping reflections that drape over paleo-failure scarp surfaces, and paleo-channels, which generally conform to the sub-surface morphology. (B) Time surface render of the P70, which is gently draping older retrogressive failure scarps.	101
Figure 5.11	(A) Crossline seismic reflection profile showing proglacial slope draping reflections that form a unit of high amplitude reflections over paleo-channels, and which generally conform to the sub-surface morphology. (B) P70 time surface render on the upper slope draping of paleo-channels.	103

- Figure 5.12. (A) Seismic reflection profile flattened to the M40 reflector and showing a thick sediment drift package above the O30 reflection and on top of a salt high. (B) Sediment drift model in the lower slope of the study area with aggrading sediment waves on top of a salt induced high. Paleo-current direction is inferred as parallel-to-slope. 104
- Figure 6.1. Strike section through the Newburn H-23 well site, with Gamma Ray log superimposed and used for indications of lithologic changes throughout the section. A) Sequence Unit 1 shows changes to a very low gamma signature at the C10 reflection, similar to Sequence boundary 0 (SB0) (Wyandot marker) below, which has been described as a chalky marl. 107
- Figure 6.2. Strike section through the Newburn H-23 well site, with Gamma Ray log superimposed and used for indications of lithologic change through out the section. A) Sequence Unit 2 shows changes in gamma signature at the C10 reflection, increasing toward the E20 reflection and again increasing from the E20 to the O30 reflection, indicating a fining-upward succession. 109
- Figure 6.3. Strike section through the Newburn H-23 well site, with Gamma Ray log superimposed and used for indications of lithologic changes through out the section. A) Sequence Unit 3 shows a change in gamma signature at the O30 reflection with a fairly homogeneous sandy gamma signature due to increased channel discharge and overbanking. 112
- Figure 6.4. Strike section through the Newburn H-23 well site, with Gamma Ray log superimposed and used for indications of lithologic changes through out the section. A) Sequence Unit 4 shows a change in gamma signature at the M40 reflection, with slightly sporadic values indicative of the overbanking deposits moving into to a more homogeneous signature of the slope drape. 114
- Figure 6.5. Strike section through the Newburn H-23 well site, with Gamma Ray log superimposed and used for indications of lithologic changes throughout the section. A) log signature at the M50 reflection into sporadic values indicative of interbedded turbidite muds and sands consistent with proglacial sedimentation. 117

Figure 7.1. Three oxygen isotope curves derived from global data (Zachos et al., 2001) and from the New Jersey Margin (Miller et al., 1996, 1998) as well as, the global eustatic curve from Haq et al. (1988) derived on the basis of sequence stratigraphy. Sea-level curves are correlated to key reflectors of this study and our sequence stratigraphic interpretations of relative sea-level.	119
Figure 7.2. Interpretive sealevel curve in relation to the study. Interpretation is based on stratigraphic architecture, paleo-shelf breaks and sequence stratigraphy.	122
Figure 7.3. (A) Seismic reflection dip profile through the middle of the study area, with features described in text relative to key seismic reflections. (B) features such as frictional drag (pull up), salt domes and tongues, antiform structures and dome crest collapse. MTD source is from out of page.	131
Figure 7.4. (A) Seismic reflection profile across a Oligocene channel. (B) time surface render of the O30 reflection indicating referential deposition into salt withdrawal basin from channel flow. Inset: Similar observations made by Booth et al., 2003 in the Gulf of Mexico and analogous to Figure 7.3.	133

LIST OF TABLES

Table 4.1 Biostratigraphic age picks and their measured depth at wellsite	56
---	----

ABSTRACT

Adam W.A. MacDonald

Cenozoic seismic stratigraphy of the central Nova Scotian continental margin: the interplay of erosion, deposition and salt tectonics

January 2006

The Cenozoic stratigraphy of the central Scotian Slope, part of the Mesozoic-Cenozoic Scotian Basin, is studied to understand influences of sea level change, salt tectonics and shelf-crossing glaciations on sedimentation patterns in a passive continental margin setting of the northern hemisphere. Interpretations are based on a recent 38 X 38 kilometer 3-D seismic data survey, extended by the study of regional 2-D multichannel seismic reflection, and correlated to biostratigraphic data and geophysical logs to provide new insights into the depositional history of this region. In the study area, Cenozoic strata have been dissected by deeply (500 m) eroded canyon systems during the Pleistocene. Broad inter-canyon regions also bear incomplete stratigraphic successions. These regions provide an opportunity to study the effects of erosional systems and salt tectonics on sedimentation patterns and stratigraphic development through the Cenozoic.

Cenozoic strata of the slope are subdivided into five large scale successions that are placed in a sequence stratigraphic framework by correlation of 7 key reflectors to the outer shelf. Paleo-channel erosion during lowstand sea-level deposited turbidite submarine fans, and formed lowstand wedge accumulations in the Middle Eocene, middle Oligocene and late Middle Miocene. Channel flow during these time periods was preferentially into salt withdrawal basins. During periods of highstand sea-level in the Early Eocene, Early Oligocene and Early Miocene, shelf margin progradation occurred on the outer shelf, and sedimentation on the slope was then minimized. The Cenozoic stratigraphy reveals a complex variety of extensional halokinetic structures recognized as periods of stratigraphic uplift, onlap, erosion and faulting that were most active in the Early Eocene, the Late Oligocene and the Late Miocene. Sea-level control was a critical factor controlling sedimentation on the slope, whereas paleoceanography, paleo-channel flow and salt tectonics affected the mode of deposition.

ACKNOWLEDGMENTS

I extend my greatest thanks to my supervisors David Piper and Pierre Jutras for allowing me to explore my ideas and develop this thesis while challenging my critical thought. I am indebted.

I have great appreciation for my other committee members David Mosher and Andrew MacRae for their patience and guidance through out the project.

My family was a crucial part of the support needed to undertake this project and I couldn't have done it without them.

I would like to thank the many people at the Geological Survey of Canada (Atlantic), at the Bedford Institute of Oceanography for giving me a place to conduct my research and who entertained my every question. Through my time at the GSCA I felt I have been with colleagues, friends and family.

I would like to extend my sincere thanks to John Hogg for supporting this project and his mentorship which made the overall experience possible. As well, Phil Nantais and Jonah Resnick in helping me gain access to data.

Digital 3-D seismic data was provided in kind by the EnCana Corporation. Without it this project would not have been possible. I am grateful for their interest in, and the support of, this research. 2-D digital seismic data was provided in kind by the companies of the Ex-PAREX Group whose generous understanding that digital data goes a lot further than paper copies these days. Many thanks to ChevronTexaco and its partners Petro-Canada and ConoccoPhillips, for releasing the Newburn H-23 exploration well data to me and supporting this research.

1. Introduction

The central Scotian Slope is a continental margin at mid-latitudes of the western North Atlantic Ocean, where the relationships of sea-level change, sediment supply, erosion, salt tectonics and glaciation can be examined. The Cenozoic sedimentary succession on the central Scotian Slope encompasses most of the Banquereau Formation (McIver 1972), which overlies the Upper Cretaceous Wyandot Formation and range from Campanian-Maastrichtian to Pliocene (Wade and MacLean 1990). The seismic character of the Cenozoic section generally consists of discontinuous and continuous events that prograded seaward on the outer shelf, and which aggraded upslope against the continental slope face as numerous sequences. Paleo-channel cut-and-fill sequences that formed below the modern day outer shelf edge and upper slope, during sea-level lowstands are recognized throughout the Cenozoic section. During highstands, sedimentation rates on the slope decreased and the outer shelf was dominated by delta or passive margin progradation. Glacial events have caused erosion on the central Scotian Slope, and the seafloor morphology recognized today is a coalescent pattern of canyons and ridges (Campbell et al. in prep).

Establishing a relationship between outer shelf and slope stratigraphy is difficult. Interpretation of seismic data through the shelf break is limited, because of complex geology, and multiple reflections from the dipping seafloor which cuts across primary reflections. Also, the upper slope area is often a zone of prolonged sediment bypass, making correlation across it difficult due to missing stratigraphic intervals.

Several unconformable surfaces are recognized throughout the Cenozoic section. Major unconformities, regionally recognized in the study area, are thought to be associated with sea-level fluctuations during the Early Eocene, Middle and Late Oligocene, Middle Miocene and Late Miocene (Haq et al. 1987; Wade and MacLean 1990; Miller et al. 1998; Zachos et al. 2001). These fluctuations controlled stratigraphic development below the outer shelf and slope. In the Scotian Basin, it is generally recognized that there is a widespread hiatus between the Early Oligocene and the earliest Miocene due to erosion of Oligocene strata. Two scenarios have been proposed to explain the extensive erosion: 1) a large eustatic drop in sea-level (Haq et al. 1987; Miller et al. 1998) and 2) localized reactivation of basin faults due to tectonic uplift (Pe-Piper and Piper 2004). The Western Boundary Undercurrent, active since the Late Oligocene but most intense during the Late Miocene, influenced sediment deposition on the central slope (McCave and Tucholke 1986). Minor disconformable surfaces are considered relatively local to the study area and are associated with occurrences of debris flow deposition and channel cutting during the Oligocene, Middle Miocene and through the onset of upland glaciation in the Pliocene. In the middle Pliocene, the Scotian Basin was a glaciated margin. Proglacial sedimentation and erosion influenced the slope by the Middle Pleistocene through the Quaternary. Finally, the Scotian Slope was strongly affected by salt tectonics, which caused the stratigraphic structural reorganization of Cenozoic sediment around active salt diapirs, pillows and allochthonous sheets (Wade and MacLean 1990; Shimeld 2004).

1.1 Study Area

The Scotian Slope lies seaward of the Scotian Shelf in the northwestern Atlantic Ocean (Figure 1.0). The Scotian Slope has a modern day mean gradient of 2-4° (Mosher et al. 2004). The Scotian Slope extends from the shelf break at a water depth of 100-200 meters below sea-level (mbsl) to a depth of 2000-2500 mbsl at the transition to the continental rise. The study area is southwest of the Sable Sub-basin, bound to the east by Logan Canyon and to the west by Dawson Canyon, encompassing the central-east Scotian Slope as well as part of the outer Scotian Shelf (Figure 1.1). For the purpose of biostratigraphic ties, regional lines of 2-D seismic reflection data were used to tie in offshore wells and correlate outer shelf stratigraphy.

The study area was chosen for the unique opportunity to study a relatively complete Cenozoic section in an otherwise highly dissected area of the central Scotian Slope (Figure 1.2). It is covered by approximately 1600 km² of high quality 3-D seismic data collected around the Weymouth prospect, which was an area of hydrocarbon exploration interest and resulted in exploration drilling (Weymouth A-45 well) of a sub-salt play in 2004. 3-D seismic data are tied with regional 2-D multichannel seismic reflection data, allowing for stratigraphic interpretation and biostratigraphic correlation with key surrounding offshore exploration wells with available, most recent or most complete biostratigraphy for the Cenozoic interval on the slope (Shubenacadie H-100 and Newburn H-23) and shelf (Glenelg N-49 and Eagle D-21) (Figure 1.1). The Weymouth A-45 exploration well has not yet been released for public access.



Figure 1.0. Location map of the study area, indicated by black box in center, in relation to the Scotian Basin. Modified from Shaw, 2002.

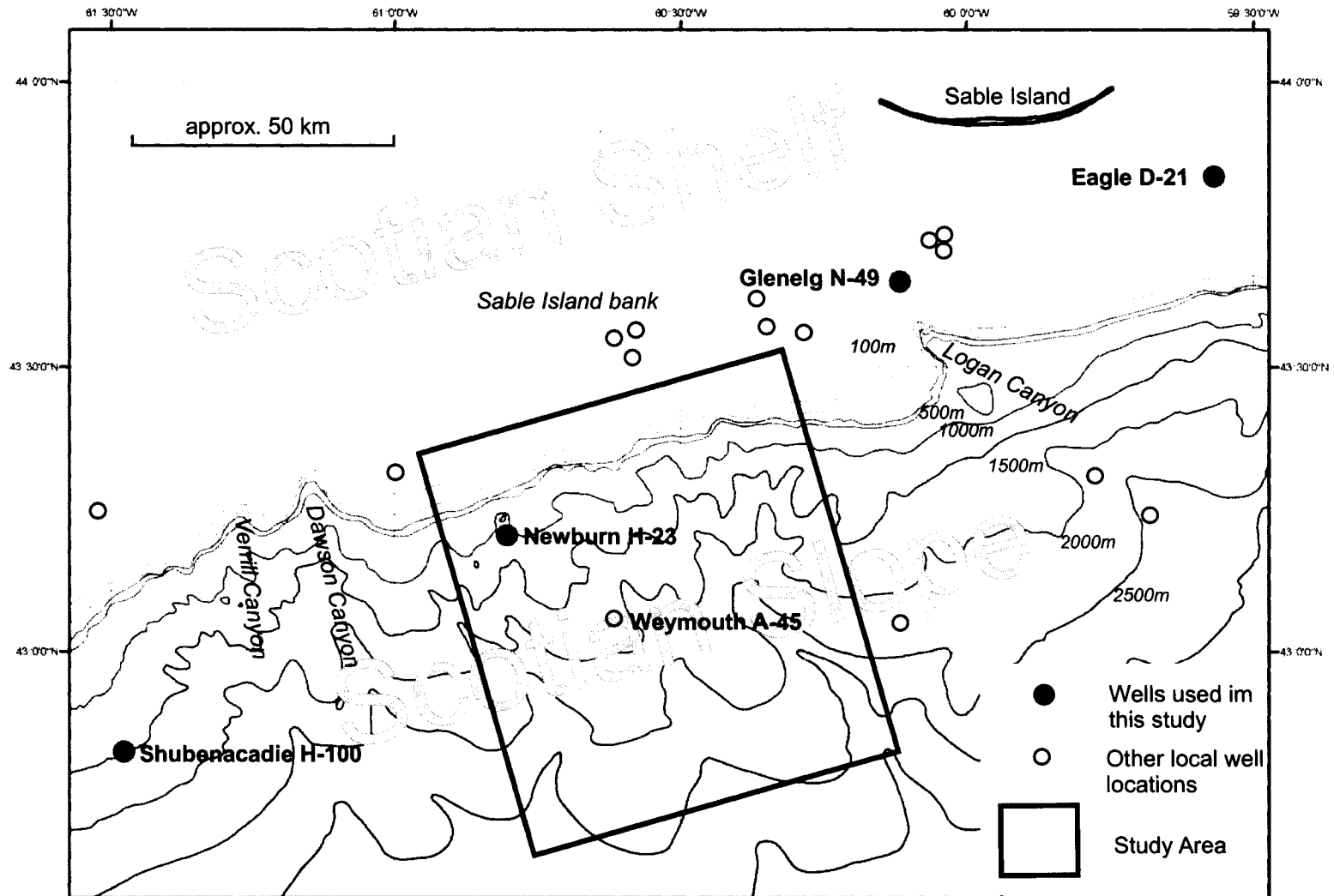


Figure 1.1. Study area including well locations where biostratigraphic ties are correlated to seismic reflection data. Note: Weymouth A-45 is not a biostratigraphic well location.

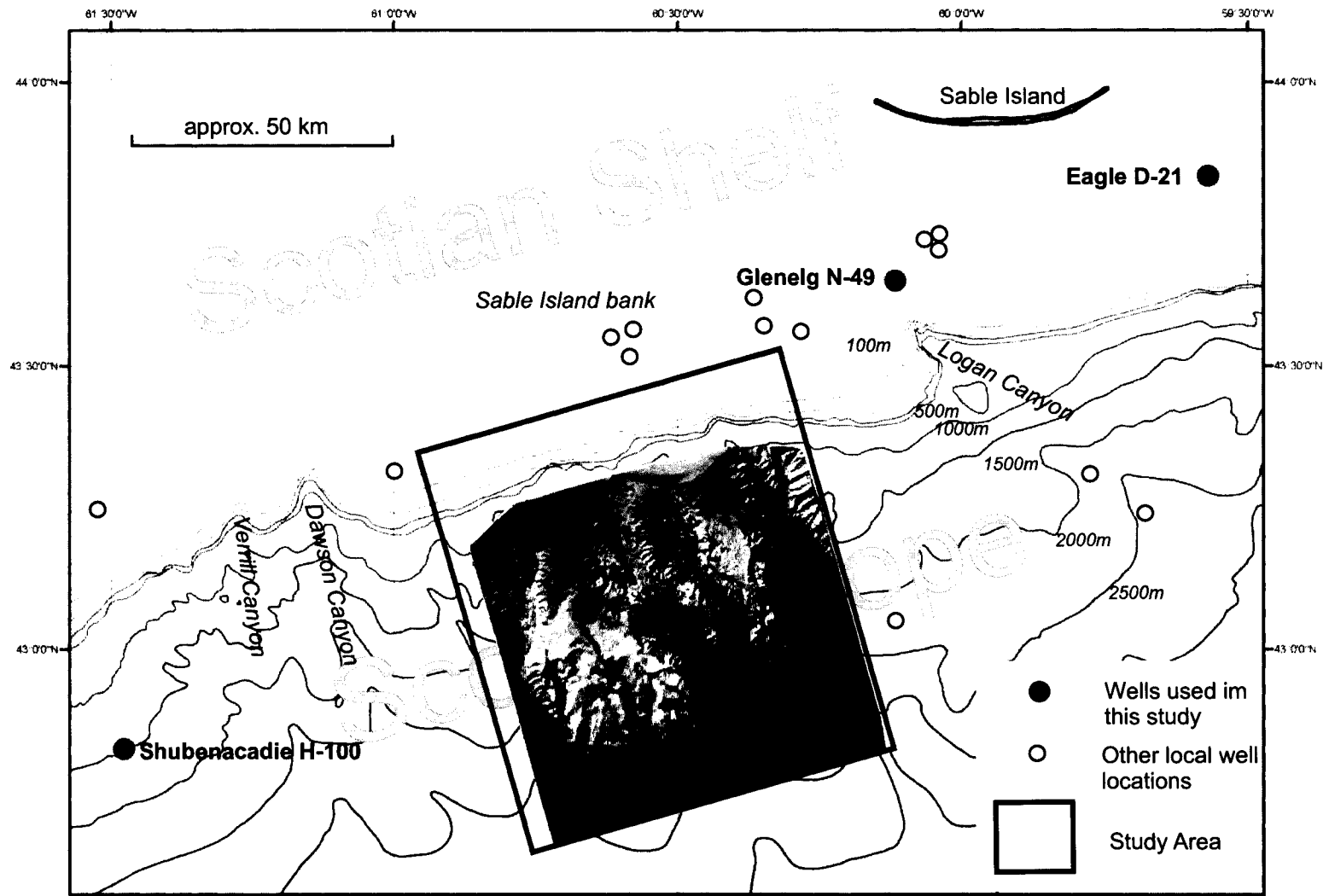


Figure 1.2. Seafloor surface render of the study area picked from 3-D seismic coverage and showing the canyons and ridges of the dissected slope.

1.2 Geologic Setting

The Scotian Slope is part of the Scotian Basin (Figure 1.0), a large passive-margin sedimentary basin that began to form during the early Mesozoic, approximately 230 million years ago (Jansa and Wade 1975; Wade and MacLean 1990; MacLean and Wade 1992). At that time, North America and Africa were part of the supercontinent Pangaea, and the present southeastern margin of Canada was adjacent to the Moroccan coast of Africa (MacLean and Wade 1992). Previous work by Wade and MacLean (1990) summarized the regional lithostratigraphic and structural history of the Scotian Basin from the Mesozoic to present (Figure 1.3). It is this model that is described herein, with added references.

The Scotian Basin rift phase began during the Late Triassic and continued into the Early Jurassic (Wade and MacLean 1990). The earliest deposition in the basin was that of the continental syn-rift red beds of the Eurydice Formation, followed by evaporites of the Argo Formation (Jansa and Wade 1975; Wade and MacLean 1990; MacLean and Wade 1992). By the late Early Jurassic, the rift phase of continental separation was completed (Uchupi and Austin 1979) and the drift phase of Scotian Basin development commenced above the Breakup Unconformity (BU) (Figure 1.3). From the late Early Jurassic to the Late Cretaceous, the Scotian Basin evolved as a passive margin with thermal subsidence rates accommodated by listric normal syn-sedimentary faults as the predominant structural feature (Hogg 2000). Deposition during the late Early to Middle Jurassic was characterized by the continental clastics of the Mohican Formation and the marine

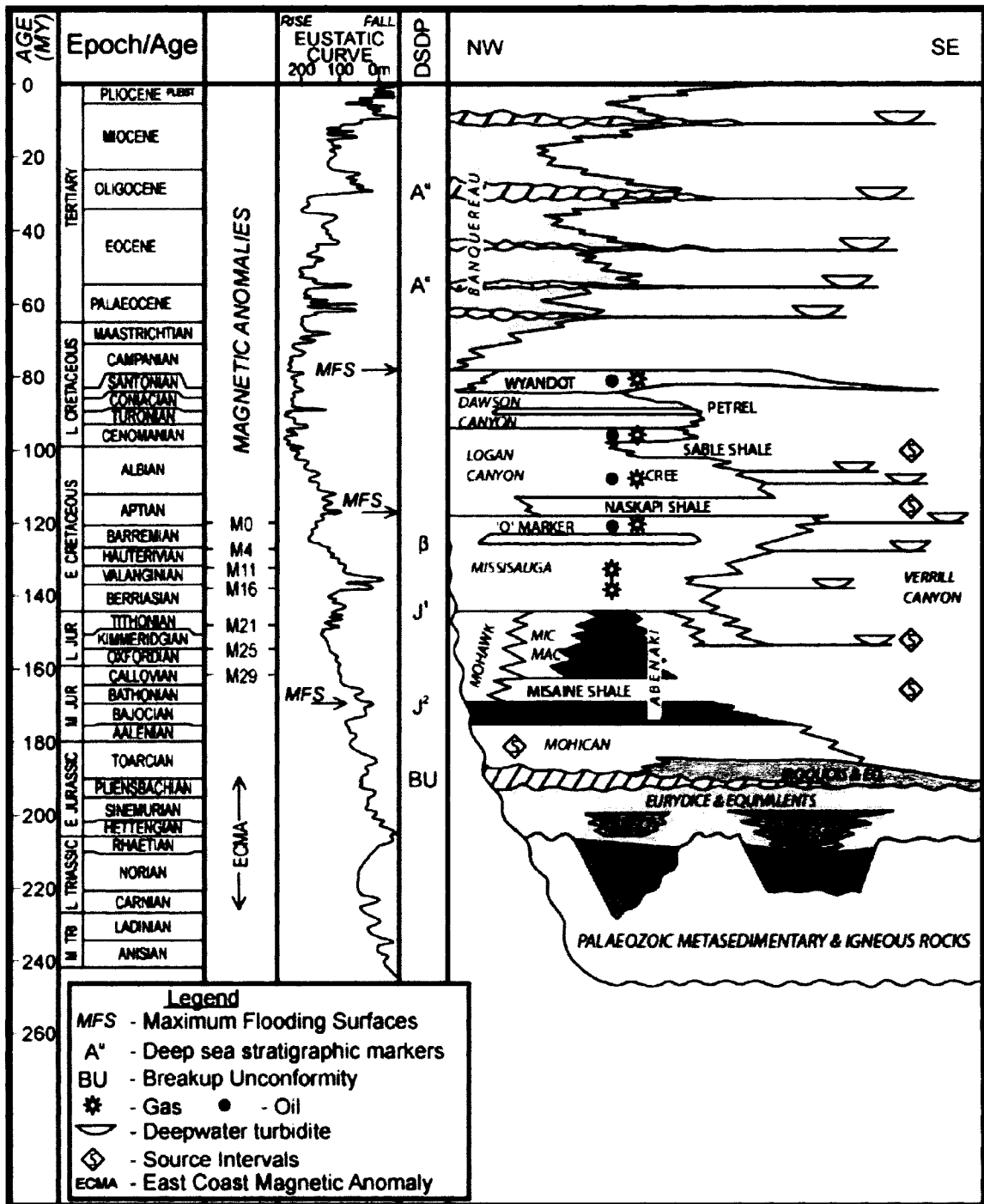


Figure 1.3. Lithostratigraphy of the deepwater slope sediments from Kidston et al., 2002. Original compiled from MacLean and Wade, 1993, 1995, and Haq et al., 1987.

dolostones of the Iroquois Formations. During the Late Jurassic, the Scotian Basin witnessed a period of regression and continental clastic deposition (the Mohawk Formation), evolving laterally into the deltaic clastics of the Mic Mac Formation, the carbonate reefs and banks of the Abenaki Formation, and the deep-sea mudstones of the Verrill Canyon Formation. Marine regression and high sediment influx during the Early Cretaceous resulted in the progradational deposition of fluvio-deltaic and prodeltaic sandy facies that are assigned to the Mississauga and Logan Canyon formations (McIver 1972; Wade and MacLean 1990). The Late Cretaceous was a period of general highstand and basin subsidence during which the marine shales, marls and minor chalk of the Dawson Canyon Formation and chalk and marl of the Wyandot Formation were deposited (McIver 1972; Wade and MacLean 1990). The Wyandot Formation is recognized regionally in the Scotian Basin and in most shelf areas has its top in the Campanian, though it may extend into the Maastrichtian on the eastern Scotian Shelf and slope. Eustatic sea level has been on a long term lowering trend from the Late Cretaceous to the present, with varying amplitudes of smaller-scale highstand and lowstand sequences through the Cenozoic (Haq et al. 1987). During the latest Cretaceous through the Cenozoic Period, seaward-thickening succession of mudstone, sandstone and marine shale that overlies the Wyandot Formation is assigned to the Banquereau Formation. The general mode of deposition on the Scotian Slope during the Cenozoic Period was mudstone dominated prodeltaic sedimentation, while on the shelf delta systems deposited significant sandstone and mudstone forming a thick Cenozoic sedimentary sequence of progradational successions (Wade and MacLean 1990; Mosher et al. 1994). Cenozoic sediments on the Scotian Slope are overlain conformably and unconformably by

Quaternary sediments, depending upon location (Swift 1985). The one exception for this clastic-dominated succession is an Early Eocene chalk unit.

On the slope, Cenozoic marine shales were deeply incised by canyon cutting during what is interpreted to be, periods of sea level lowstands (Uchupi and Austin 1979; Swift 1987). The Paleogene and Neogene periods were times of sea-level fluctuations in response to eustatic and glacio-eustatic change, which left several hiatuses (Haq et al. 1987; Miller et al. 1998; Zachos et al. 2001). Cenozoic transgressive sequences, by what are interpreted to be major drops in relative sea level, are expressed as major unconformities in the Paleogene, the Oligocene and the Miocene on the Scotian Slope (Uchupi and Austin 1979; Wade and MacLean 1990). Deepwater currents (McCave and Tucholke 1986) and paleochannel incision on the shelf and slope, have eroded away under-consolidated sediment and deposited it elsewhere in the deeper slope or rise (McIver 1972). The Late Pliocene saw the onset of terrestrial glaciation in North America and associated marine regression. Increased gully cutting took place into the early Pleistocene and high rates of prodeltaic sedimentation continued on the slope (Piper et al. 1987; Piper 2000). The middle to late Quaternary Period was dominated by proglacial deposition, with high sedimentation rates of glacial and marine sediments deposited on the outer continental shelf and slope. Quaternary sedimentary successions show a relatively continuous 'layer cake' stratigraphy, but are highly dissected, in some areas to the extent of exposing deeper Neogene and more uncommonly, Paleogene strata at or near the modern day seafloor (Mosher et al. 1994).

Salt structures in the central Scotian Slope are common architectural features (McIver 1972; Wade and MacLean 1990; Shimeld 2004). Stratigraphic architecture around and above salt highs consists of a complex variety of extensional halotectonic and syn-kinematic structures (Shimeld 2004). Large scale faulting along the edge of diapirs and on diapir crests is common. Salt has been suggested to have been active during the Cenozoic (MacLean and Wade 1993; Shimeld 2004).

1.3 Objectives

The purpose of this study is to develop an understanding of the Cenozoic stratigraphy of the central Scotian Slope and how it was influenced by sea-level change, paleo-channel erosion and deposition, and the influence of salt tectonics on the stratigraphic framework. This objective is accomplished by studying 2-Dimensional and 3-Dimensional reflection seismic data with biostratigraphic ties to offshore exploration wells and place stratigraphic evolution into a chronological context. The seismo-stratigraphic relationship of depositional facies is related to erosional, depositional, tectonic and paleoceanographic events that are placed within a sequence stratigraphic framework.

2. Methods

2.1 Two-dimensional seismic reflection data

With similar research objectives for the Jeanne d'Arc Basin of offshore Newfoundland, Deptuck (2003) described the basic methodology of collecting and understanding marine seismic reflection data. It is this model that is followed herein with added references.

The method for collecting seismic reflection data in marine settings involves the triggering of an acoustic pulse near the sea surface, which propagates through the water column and into the subsurface. Part of the acoustic pulse reflects off the sea floor, but some of the acoustic pulse transmits into the bottom and reflects off subsurface interfaces. Reflections from subsurface interfaces occur at boundaries between two media of different acoustic impedances (Mosher 1999); impedances being the product of velocity and density. The arrival times of the reflections are recorded by hydrophones towed behind the vessel, at or below the sea surface. These reflection data provide a cross-sectional representation of the subsurface based on reflected acoustic energy from subsurface stratal interfaces, and recorded in units of two-way travel time.

Acoustic energy is reflected at the boundaries between strata of contrasting acoustic impedance, which is the product of bulk density and seismic velocity (Kearey and Brooks 1991). In general, the harder the rock, the greater its acoustic impedance (Kearey and Brooks 1991). The magnitude of the change in acoustic impedance between two

stratigraphic units determines the strength (amplitude) of the reflection (Z). The ratio between the reflected and transmitted waves is the reflection coefficient (R) (North 1985). In addition to the amplitude of the reflection coefficient, equation (1), below, determines the polarity of the reflection coefficient based on whether the seismic pulse passes from a higher to a lower impedance layer, or vice versa. Therefore, if a low impedance layer (e.g. shale) overlies a high impedance layer (e.g. limestone), a positive reflection coefficient is generated, whereas if the deeper layer has lower impedance (e.g. salt), a negative reflection coefficient is generated.

$$R = \frac{Z_{\text{layer 2}} - Z_{\text{layer 1}}}{Z_{\text{layer 2}} + Z_{\text{layer 1}}}$$

*Zoepritz Equation from Yilmaz, 1987 in
Deptuck, 2003*

An individual seismic trace (wiggle plot) represents to convolution of the source function and the time-series of reflection returns from subsurface interfaces (the Earth's reflection coefficient series). An industry standard multi-channel seismic profile uses independent groups of hydrophones to record reflections along the streamer length. Each hydrophone group corresponds to a channel. Along track, each channel will receive pulses from a point that was also received by the previous channel. This is called a common-midpoint gathers (CMP). After sorting, each trace on a CMP gather it is then processed into an equivalent zero-offset trace and the traces in the gather can all be stacked (added) together (common-depth-point (CPD) stacking). By stacking the CMP reflections, seismic profiles can have an increased accuracy and a better signal to noise ratio.

2.2 Three-dimensional seismic reflection data

Marine 3-D seismic data are acquired by ships that tow multiple hydrophone arrays in a pattern across a survey area, to fully cover the area with a grid of shoot spacings. The in-line direction is parallel to the ship track, whereas the cross-line direction is perpendicular to the ship track. Rather than traces collected as CMPs, 3-D seismic data consist of traces collected as common-cell gathers, called “bins”. Bins represent traces brought together from 360 degrees around the center point. Typically, the traces in each bin are sampled vertically at either 2 or 4 ms intervals across each wavelength. Each vertical sample, combined with the horizontal bin area, defines a cube corresponding to a voxel. Each voxel represents a single amplitude value extracted from the bin.

3-D seismic data used in this study were time migrated in the pre-stack processing phase (PSTM) using a 3-D Kirchoff migration equation. Traces were binned at 37.5m x 12.5m and sub-sampled at 4 milliseconds (ms). A secondary site survey data set was also attained with similar processing but was sampled at 2 ms for higher resolution. All processing was done by EnCana Corporation (EnCana 2003), and data below 2 seconds of penetration were removed for confidentiality reasons.

Seismic surveys of 3-D data makes up a volume of information. Therefore, various methods and different strategies allow the interpreter to “slice” through the volume and extract specific information from a large quantity of data. In many cases, specific strategies were developed to investigate different aspects of interpretation. The most

common methods for viewing 3-D seismic data include vertical seismic sections, time-slices, and surface renders through time depth and amplitude extraction.

2.3 Seismic Stratigraphy

Seismic stratigraphy is the framework for seismic interpretation. It is the stratigraphic and facies recognition of reflection seismic data (Mitchum et al. 1977b; Kennett 1982). First, primary seismic waves are emitted and reflected back from physical surfaces in rock successions (e.g. bedding planes and unconformities – impedance boundaries). These allow the identification of boundaries between rock types that show contrasts in density and framework integrity. Recognition of reflection termination patterns, planiform and 2-D geometry reflection configurations are used to distinguish important surfaces, facies types and depositional environments in order to subdivide the stratigraphic record.

For the present study observations were made from seismic reflection interpretation based on differences in reflection characteristics and how they change across section. Prominent reflections within seismic section were chosen and correlated throughout the slope. This task established a basic framework for further observations. Bounding discontinuities, termination patterns (Figure 2.1 a), reflection configurations and seismic facies geometry were used to make inferences about depositional and erosional environments, such as paleo-channels, mass transport complexes, sub-marine fans and levee complexes. With a measured grid of interpreted 2-D or 3-D vertical profiles, auto correlation or gridding algorithms were applied to generate a rendered surfaces across

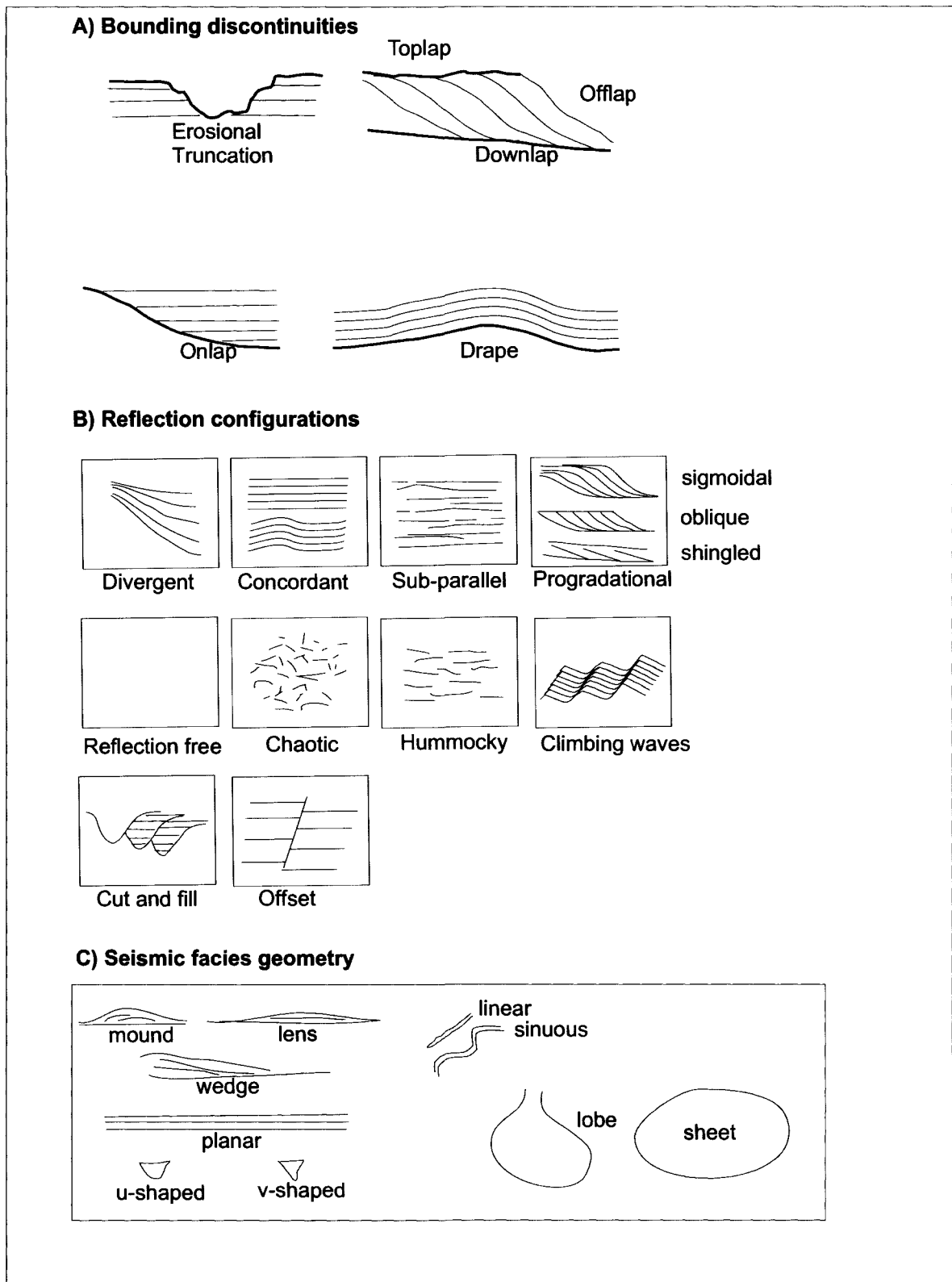


Figure 2.1. Seismic stratigraphic features used to describe and interpret stratigraphy, depositional environment and facies distribution. Modified from Deptuck, 2003.

stratigraphic reflections in time and with amplitude extracted. These surface and amplitude extracted renders were used to define the paleo-seafloor, slope and shelf break, as well as any other geomorphologic features.

2.4 Seismic reflection facies

As discussed above, seismic reflections are representative of the impedance contrasts between different rock types, sediment intervals or facies. Seismic facies are identified by their reflection character (geometry, strength, continuity), which is a function of their reflection coefficient and lateral coherency. A seismic facies is defined by its outer geometry and its relationship to the surrounding seismic stratigraphy. In identifying seismic facies, reflection characteristics such as internally chaotic, high or low amplitude, discontinuous, clinoform and mounding (Figure 2.1 b,c) were used as well as 3-D morphology and amplitude to make inferences on paleo-depositional environments.

2.5 Synthetic Seismograms

Synthetic seismograms are theoretically derived seismic traces generated from physical property information from wells. They are used to correlate well data, which is in the depth domain, to seismic data which is in the time domain. A synthetic log is a product of convolving the wavelet with the reflection coefficient in the time domain. The output synthetic trace is representative of the reflection response at the well site, and it can be covered back and forth from time to depth for seismic correlation.

Synthetic seismograms were generated using SynPAK software of The Kingdom Suite (TKS) software package which was operated through a student license granted by Seismic Micro Technologies (SMT) (Figure 2.2). Synthetic seismograms were used to correlate biostratigraphic data, recorded in depth, to seismic reflection data, recorded in time. To generate a synthetic seismogram a suite of well log data is needed, including sonic velocity or checkshot velocity, and density (bulk, or lithologically calibrated). The borehole sonic and density logs are converted into acoustic impedance data through simple velocity values multiplied by density. With acoustic impedance data, reflection coefficients (impedance contrasts between lithologic layers) are calculated and convoluted with an appropriate seismic wavelet representative of the seismic signal source. This wavelet can be calculated theoretically, or extracted at the well location from transecting seismic reflection data.

No log data were available in the upper section of most wells, as is the common case in offshore well data. For this reason no attempt could be made to make a log interpretation of lithology based on density and sonic log signatures. However, at the Newburn H-23 well site, the Gamma Ray log was done from seafloor to total depth (TD), thus allowing for observations.

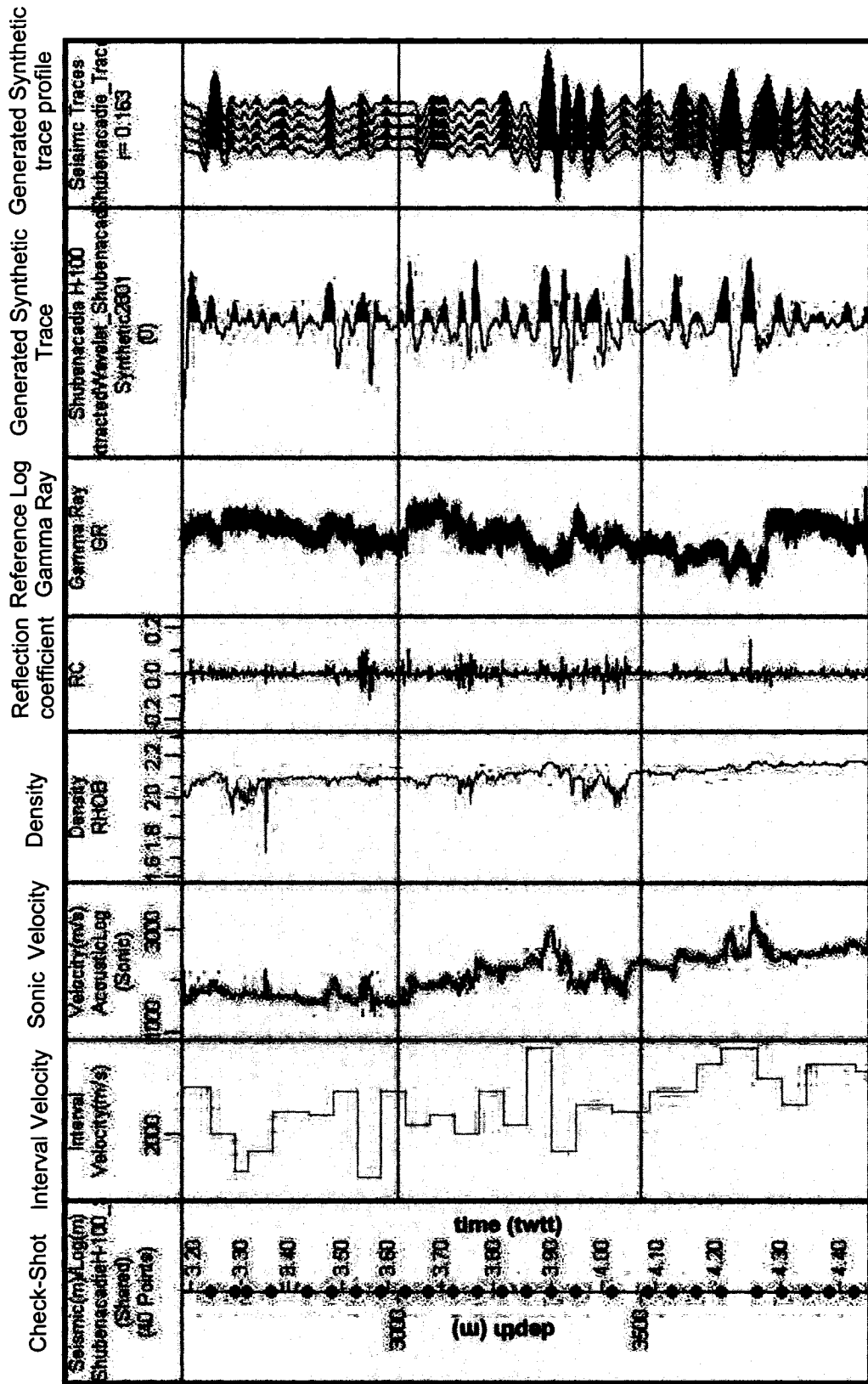


Figure 2.2. Shubenacadie H-100, synthetic seismogram progression from Checkshot (conversion between time and depth) to interval velocity, Sonic velocities are multiplied by density for a given reflection coefficient, and then convolved with extracted wavelet (not shown) to form a synthetic trace (seismogram) and synthetic profiles.

2.6 Biostratigraphy

Biostratigraphy is the process of dividing the stratigraphic record by correlating fossils based on age, type and abundance. Biostratigraphic “age control” for this study was based on palynomorphs (spores, pollen, dinoflagellates, acritarchs), nannofossils (calcareous fossil remains of single celled algae), and foraminifera, from four offshore exploration wells. Interpretations were made by various people, including R. Fensome, (2000) and F. Thomas, (1994) of the Geological Survey of Canada (Atlantic) on Shubenacadie H-100 and Eagle D-21. Sampling of the Cenozoic section for these two wells was from well cuttings only. Biostratigraphy in the additional two wells was done by petroleum industry contracts for Glenelg N-49 (Shell et al. 1986) and Newburn H-23 (Chevron et al. proprietary until 2007).

Where possible, stratigraphic markers from MacLean and Wade (1993) were used to further constrain or corroborate age picks correlated to seismic reflection profile.

2.7 Gamma Ray log

The Gamma Ray log is a measurement of the natural radioactivity of a formation. Gamma rays are bursts of high energy electromagnetic waves that are spontaneously emitted by some radioactive source. The three main earth elements that emit gamma rays are uranium, thorium and potassium, potassium being the most abundant. Feldspars, micas and clay minerals contain a large portion of the earth’s potassium. Since clay

minerals are the principal constituents of shales, they are generally radioactive. Conversely, quartz contains almost no radioactive elements and is the principal constituent of sandstone (low gamma emission) in the Scotian Basin. Gamma Ray logs are therefore used to determine vertical grain-size variations in well logs and are diagnostic to the depositional unit and / or depositional setting (Figure 2.3). Gamma Ray logs are expressed in American Petroleum Institute (API) units and, as discussed above, generally have values that are much higher in response to clay rich formations such as shale than non shales such as sandstones or carbonates. It can therefore be used as a loosely accepted lithological indicator. Caution is needed for inferring lithology based on gamma signatures only, as some minerals can produce similar to identical responses. An understanding of paleoenvironments and provenance is therefore needed to make any substantial inferences.

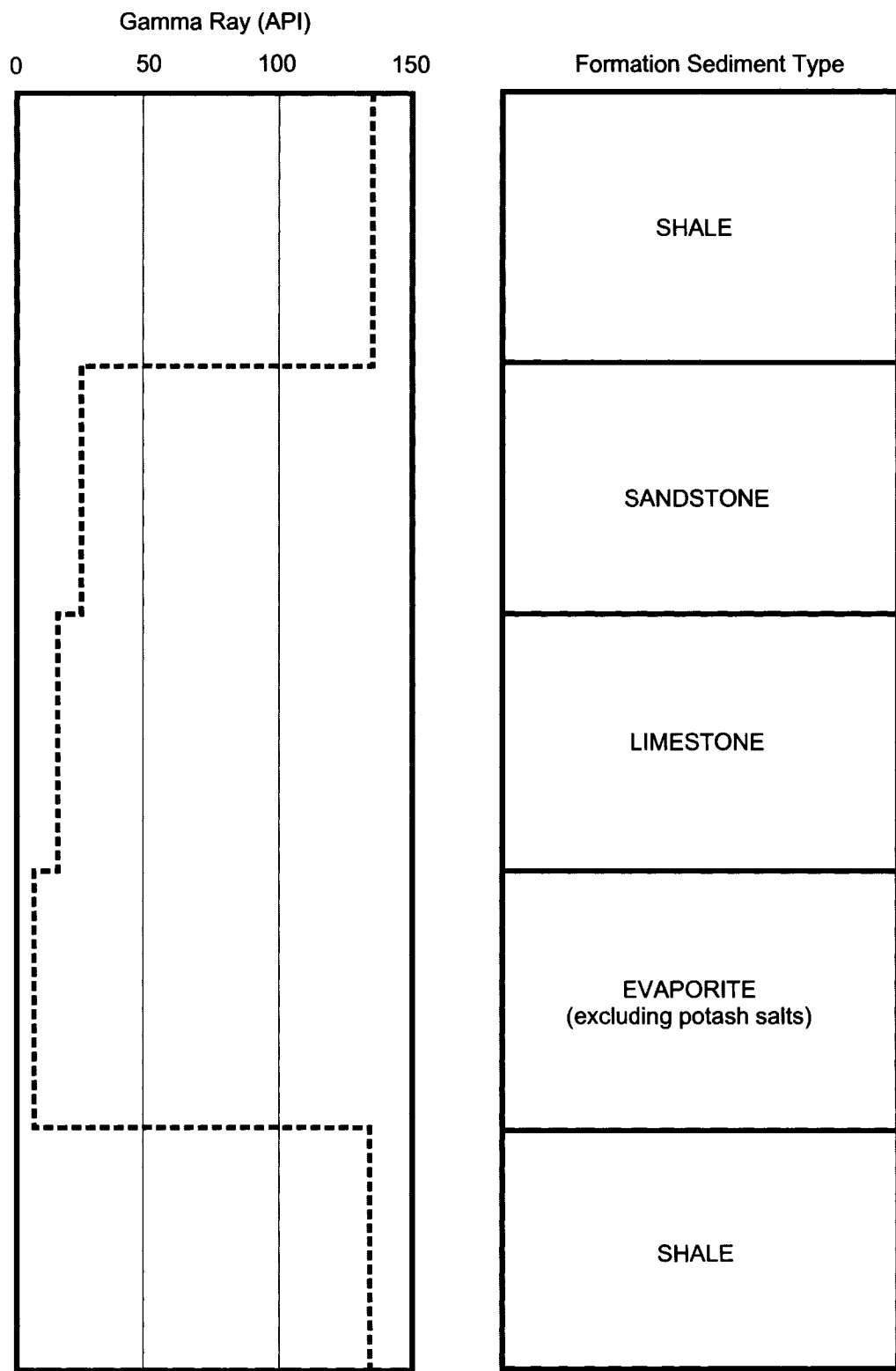


Figure 2.3. Simplified approach of lithologic interpretations based on Gamma Ray log signatures

3. Introduction to Stratigraphic Architecture

3.1 General Statement

Cenozoic sediments of the central Scotian Slope accumulated under variable conditions of sedimentation and it is here hypothesized that they were further influenced by salt tectonics and major channel-cutting events. By examining the seismic-stratigraphic architecture of the slope, a better understanding of their depositional history is achieved. The influence of salt on the stratigraphic architecture, by uplift and withdrawal, may have affected the mode of sedimentation, and it is herein studied in relationship to sedimentation and erosion.

3.2 Seismic Stratigraphic Concepts

The large-scale seismic-stratigraphic geometry indicates sedimentation through several depositional cycles. Each depositional cycle on the outer shelf and slope is inferred to represent a change in sea-level marked by the beginning of a marine cycle. Related sequences of seismic stratigraphy and sedimentary cycles of deposition are correlated by relative, principally eustatic, sea-level changes. These are widely accepted as major factors controlling sediment input to a passive margin system (Mitchum et al. 1977a; Haq et al. 1987; Posamentier and Vail 1988; Posamentier and Allen 1999; Posamentier and Kolla 2003).

The seismic stratigraphy of the central Scotian Slope and the outer Scotian Shelf through the Cenozoic period has undergone various cycles of sedimentation, which are interrupted by unconformities or correlative conformities identified in seismic-reflection data (Figure 3.1). Seismo-stratigraphic geometric features used in the study include onlap, offlap, undulations, and conformable and unconformable reflection surfaces (Figure 2.1). As nearly all sediment had to cross the outer shelf to be deposited on the slope, a genetic relationship exists between these two areas. Observations made on the sediment cycles from seismic stratigraphy on the outer shelf and slope provides a better understanding of the relationship between these coeval environments.

Non-eustatic influence is also considered in this study as a possible control of relative sealevel variation. The relative role of eustacy (global sea-level change), sediment supply and tectonics is very much a contentious debate. Although principally eustatic sea-level variation is compared to stratal geometry in this study, sediment supply or changes in tectonic uplift or subsidence could have influenced stratigraphic development in the Cenozoic.

3.3 Sequence Stratigraphy

Sequence stratigraphic concepts argue that changes in relative, principally eustatic, sea-level largely control stratigraphic geometries (Posamentier et al. 1992). A depositional sequence is defined as a conformable succession of genetically related strata bounded at their top and base by either an unconformity or its correlative conformity (Mitchum et al.

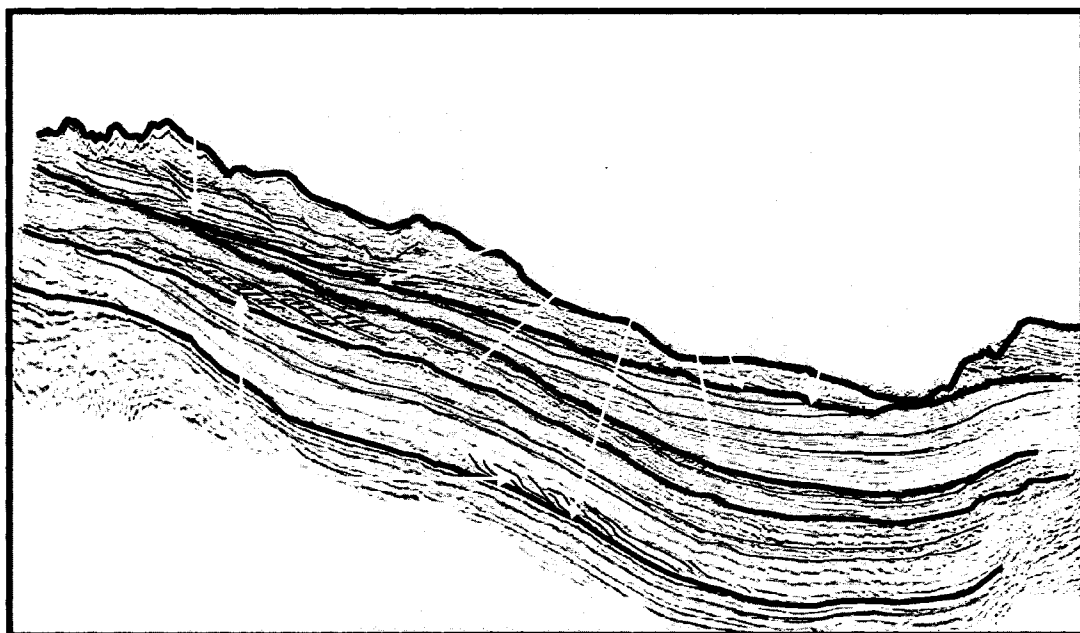
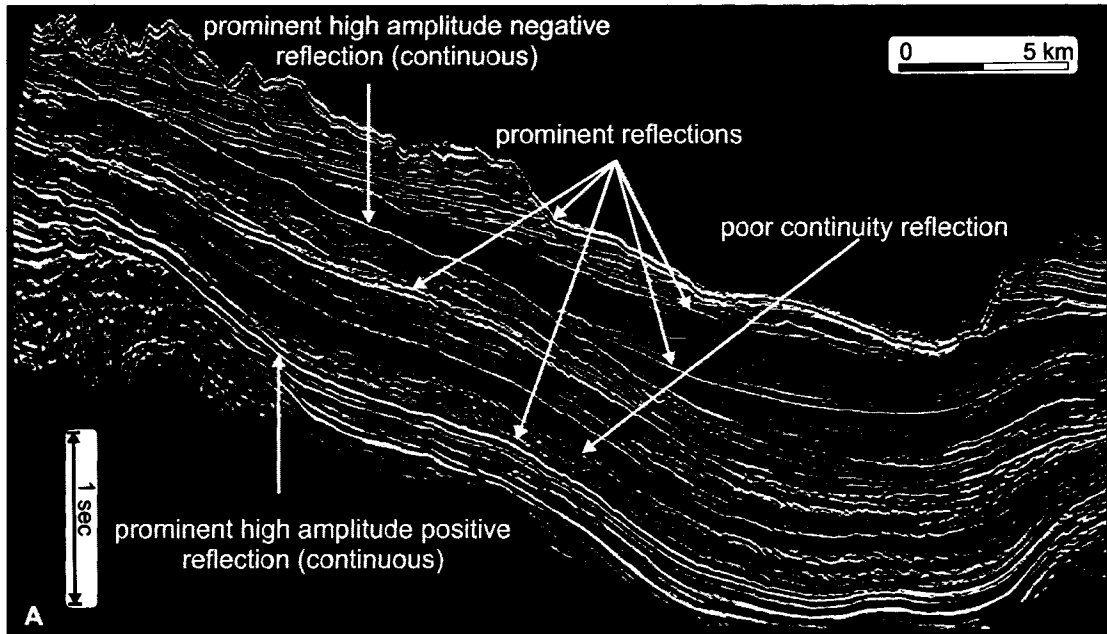
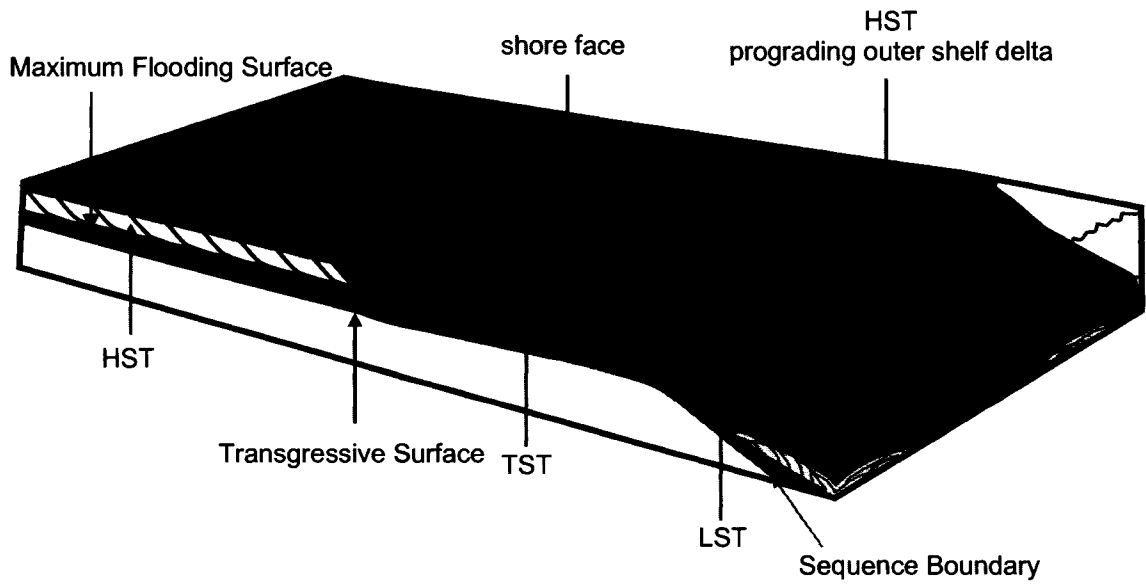


Figure 3.1. A) Prominent reflectors of a seismic framework. B) Prominent reflections and established framework with internal reflection geometries and truncations.

1977a). Sequence boundaries are representative of basinward shifts in onlapping reflections (Christie-Blick et al. 1998). Therefore, a sequence begins with a relative fall in sea-level, and a depositional sequence is the record of one cycle of relative sea-level change. Because of this predictability, assumptions on deposition can be made based on the internal structure of sequences. A depositional system may include coastal plain, shelf, alluvial plain and submarine fan sediments. In vertical succession, depositional sequences comprise of the following elements in this order: sequence boundary, lowstand system tracts, transgressive surface, transgressive system tracts, maximum flooding surface, highstand system tracts, and the following sequence boundary caused by a drop in relative sea-level (Figure 3.2).

Sequence boundaries are best identified by objectively determining an unconformity or a correlative conformity surface in a section either across strike or up dip (Posamentier and Allen 1999). This approach is a slightly different from the traditional “Exxon approach”, with type 1 and type 2 unconformity surfaces (Mitchum et al. 1977a; Posamentier and Vail 1988), where recognition of sequence boundaries are expressed in interpretive relationship to fluvial incision and tectonics (subsidence). It has been proposed that eliminating the processes of distinguishing between the two sequence boundaries will allow for better recognition of sequence boundaries in their paleogeographic setting and less confusion in the nomenclature (Posamentier and Allen 1999). The type 1 and type 2 sequence boundaries are not ignored but rather stated in observations made in relation to the up-, down- and across-section profile. It is this method of sequence stratigraphic

Relative sea-level highstand



Relative sea-level lowstand

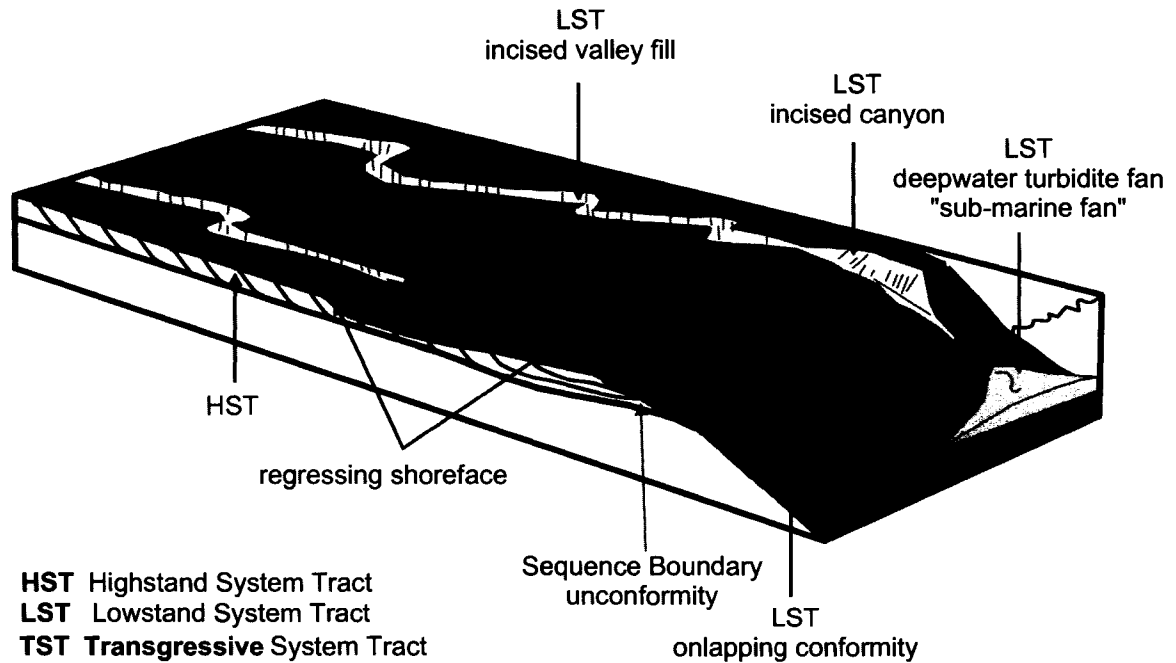


Figure 3.2. Generalized sequence stratigraphic model analogues to the Scotian Slope and outer shelf relationship. Note the sequence boundary unconformity (orange) and deepwater (slope) conformities in the LST. Modified from Posamentier and Allen, 1993.

principle that is applied and related to correlative deposits from the outer Scotian Shelf to the Scotian slope.

The sequences identified herein may result from differential preservation due to sea level changes, differential subsidence rates, and regional and local tectonics. If the relative sea level fall is faster than the rate of subsidence on passive continental margins, the sequence boundary will commonly be accompanied by fluvial incision and the deposition of a lowstand system tract consisting of possible outer shelf deltas, deepwater turbidites, and other forms of mass transport deposits on the slope (Posamentier and Allen 1993). If the rate of relative sea-level fall does not exceed subsidence rates, a shelf margin system tract characterized by a prograding system tract and little to no fluvial incision will be deposited (Mitchum et al. 1977a; Posamentier and Vail 1988; Posamentier and Allen 1999). As sea level rises, increased sediment accommodation occurs on the shelf and a maximum flooding surface (MFS) is created followed by a transgressive system tract (Figure 3.2). As sea-level rise slows or enters a period of still stand, sediment supply may again outpace subsidence, resulting in a shelf margin progradation of sediments and the development of a regressive highstand system tract.

3.4 Sedimentation

Sedimentation on the Scotian Slope varied during the Cenozoic period in a systematic manner. Transgressive and regressive periods affected sediment delivery from the Scotian Shelf to the Scotian Slope. In a passive continental slope sedimentation rates are

low when sea-level is high (highstand) and high when sealevel is low (lowstand) (Posamentier and Allen 1999). Each highstand and lowstand marine cycle is represented by a change in the mode of sedimentation on the outer shelf and slope. These changes are recognized in seismic units through the change of internal reflections and / or reflection geometry.

Factors controlling sediment delivery to the slope during lowstand periods include shelf crossing channels and glacial maximums. It has been recognized that the eastern Canadian margin has been glacially influenced with a proglacial emergent shelf in the Pliocene and shelf-crossing glaciation from the mid-late Pleistocene to the end of the Quaternary (King and MacLean 1976; Piper et al. 1990). Periodically through this time period, glacial maximum ice sheets reached the outer shelf edge and the upper slope (Shaw and Courtney 2002). During this period, high sedimentation rates of coarse glacio-fluvial prodeltaic deposits dominated the slope environment (King and MacLean 1976; Piper 1988; Mosher et al. 1989; Piper et al. 2002; Piper and DeWolfe 2003). Previous to being glacially influenced, slope sedimentation was dominated by deepwater turbidity systems such as submarine fans, draping sheets and lobes of turbidite deposits. During highstand periods, in the early Cenozoic, prograding outer deltas dominated the outer shelf to the near shelf edge. Highstand deposits generally consisted of prodeltaic clastics, with distal muds and marls on the slope (Figure 3.3).

Early Cenozoic facies of the Banquereau Formation, are described in earlier works as chalky marls and sandy mudstone (McIver 1972; Kidston et al. 2002). Cenozoic

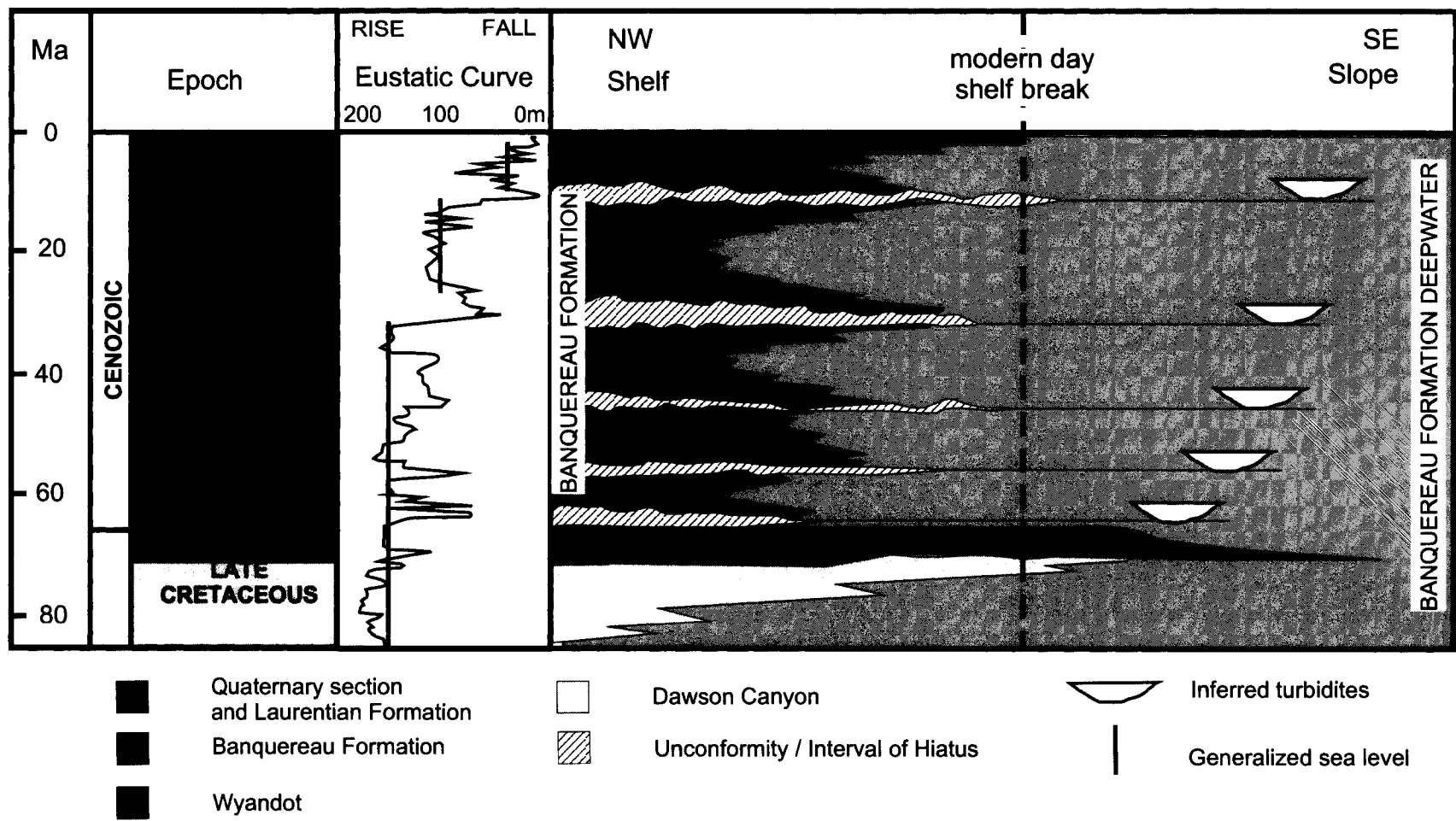


Figure 3.3. Generalized stratigraphic chart of the Cenozoic from the outer Scotian Shelf to Scotian Slope (modified from Kidston et al, 2002).

sediments on the outer shelf and slope are grossly separated into two sequences of highstand and lowstand system tracts following the work done by Crane (2003) in the southwestern Scotian Slope. These major system tracts are further subdivided in this study by the identification of additional sequence boundaries and stratigraphic cycles throughout the Cenozoic succession.

3.5 Sub-Surface Salt

Indications of salt structures are revealed by a drastic change in reflection character, and salt movement by highly deformed areas of the seismic section (Figure 3.4). Changes in reflection character are due to a strong impedance contrast as the seismic wave passes from high impedance sediment/rock to low impedance salt, generating a negative reflection coefficient. Generally, stratigraphic architecture changes with structural reorganization caused by salt movement or removal. The result of this reorganization are stratigraphic offsets (faults), stratigraphic pull-ups by frictional drag at the salt flanks, stratigraphic collapse, and a general spreading at the crest of an uplifted high (Parker and McDowell 1955; Turcotte 1982; Davison et al. 1996; Koyi 1998; Davison 2000). As surrounding strata sink into the space created by the evacuating salt, mini-basins are formed around salt diapirs (Figure 3.4). Sediment traveling down slope accumulates in these mini-basins.

Although negative reflection coefficients could result from lower density shale diapirs, sparse well data show that the halokinetic unit is the Argo Salt of the Triassic to Jurassic

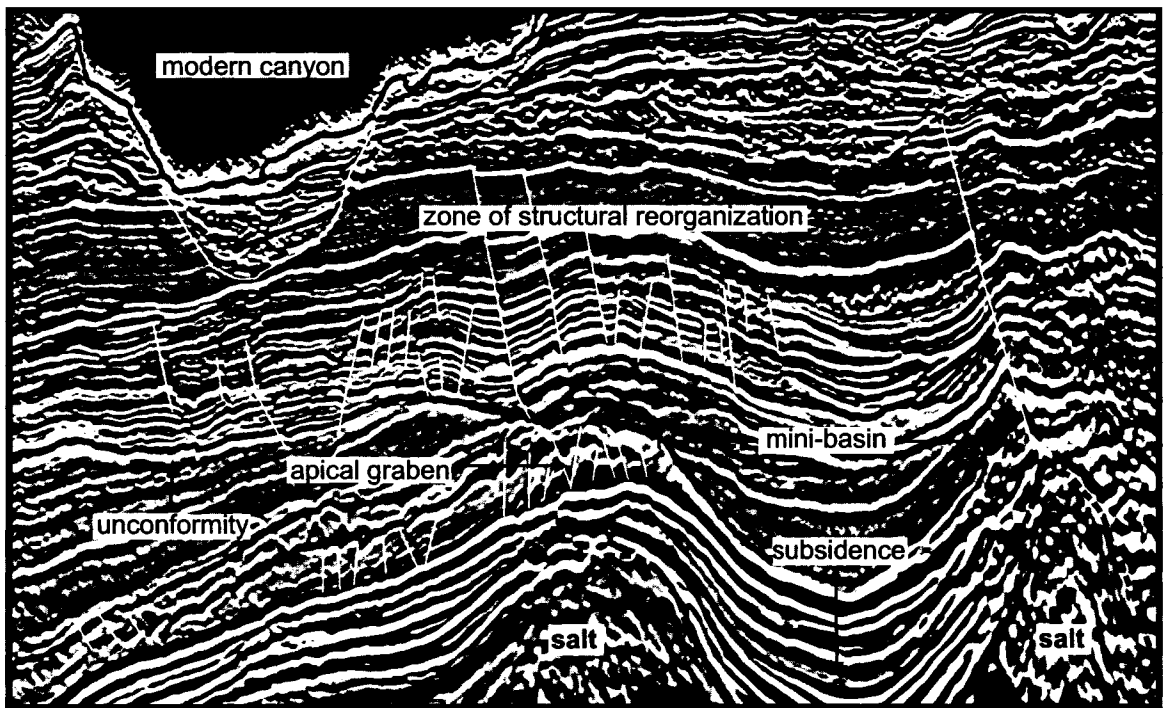
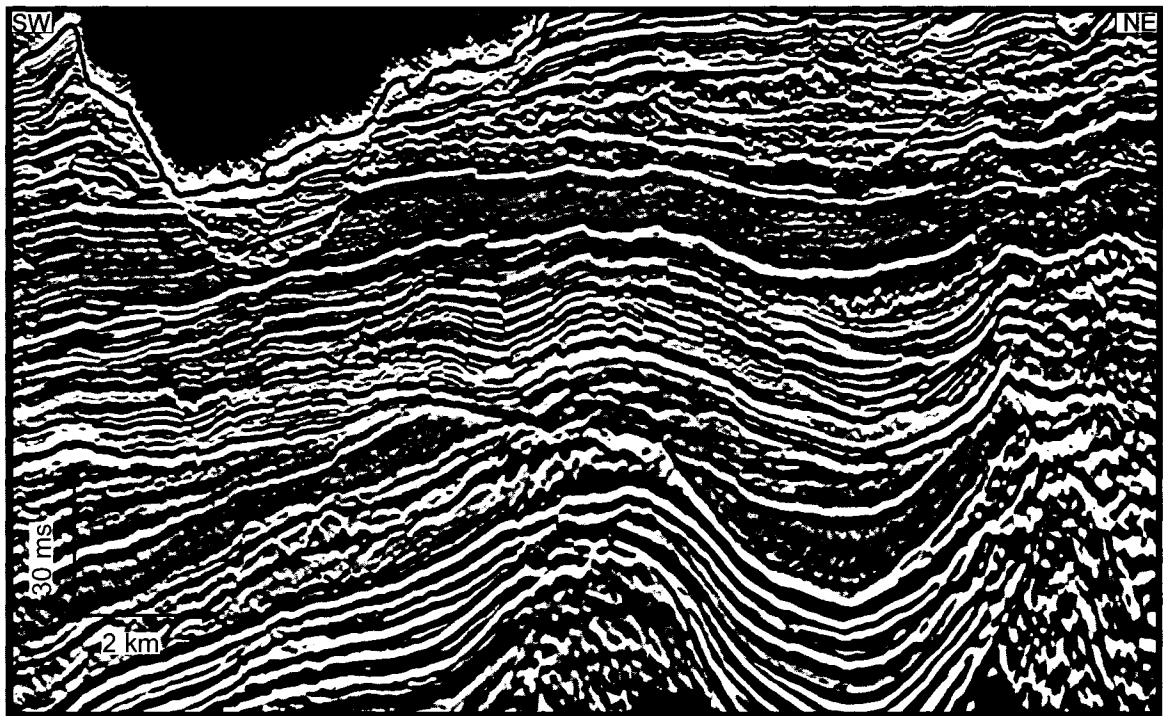


Figure 3.4. Seismo-stratigraphic deformation through uplift, collapse and faulting due to salt dynamics, and structural reorganization due to sub-surface movement.

Scotian Salt Province (McIver 1972; Wade et al. 1995; Shimeld 2004). With modern high quality seismic reflection data, both the upper and lower extents of salt in the study area are differentiated (Kidston et al. 2002). Identification of salt morphologies in subsurface, such as salt tongues, allochthonous bodies and diapirs, aid to better understand the dynamic nature of the salt migration and how it affects the evolution of the central Scotian Slope stratigraphy.

3.6 Paleochannels

Paleochannels are common erosive and depositional elements on outer Scotian Shelf and slope environment. In reflection seismic data, generalized characteristics of paleochannels are isolated or stacked reflections of an asymmetric to symmetric u- or v-shape geometry (Deptuck 2003) (Figure 2.1). These features are further defined by identifying high amplitude seismic reflections representative of coarse-grained channel fills and erosional boundaries of the channel walls (Figure 3.5a). Several architectural sub-elements are recognized on the outer shelf and slope: basal erosional fairways, slump blocks from failures along the channel walls, outer levees and inter-channel development, such as inter-channel levees and multi-stage growth (Deptuck et al. 2003; Posamentier and Kolla 2003). Large paleo-channels mapped on the outer shelf are correlated through the shelf break and onto the upper slope (Figure 3.5A), but are poorly imaged in seismic reflection profile at the shelf break. Generally, paleo-channels become less clearly developed in deeper water and are absent on the lower slope (Figure 3.5B).

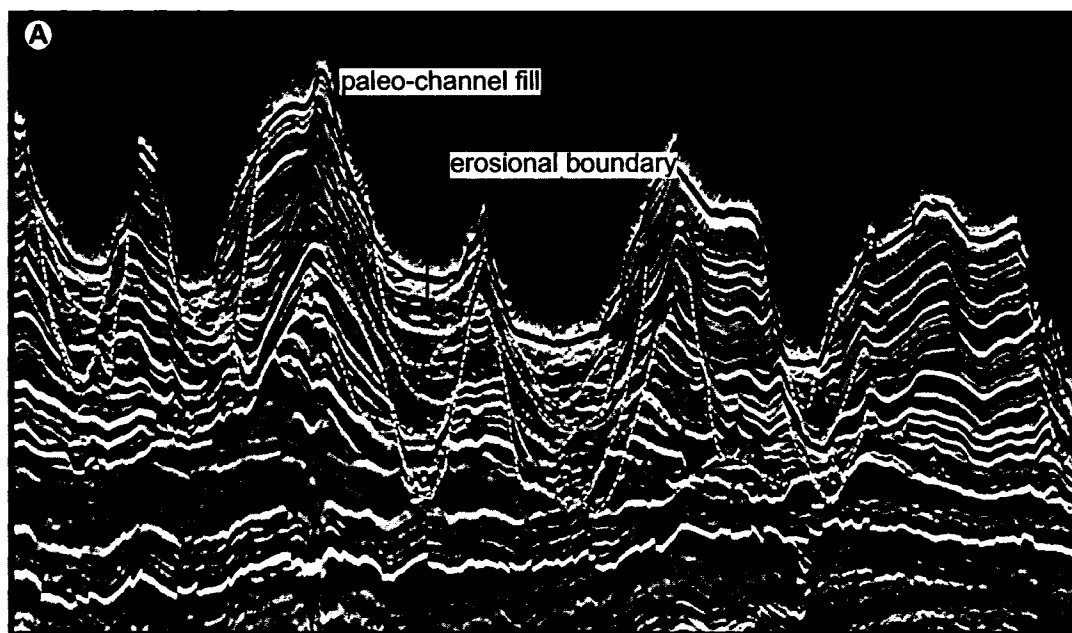
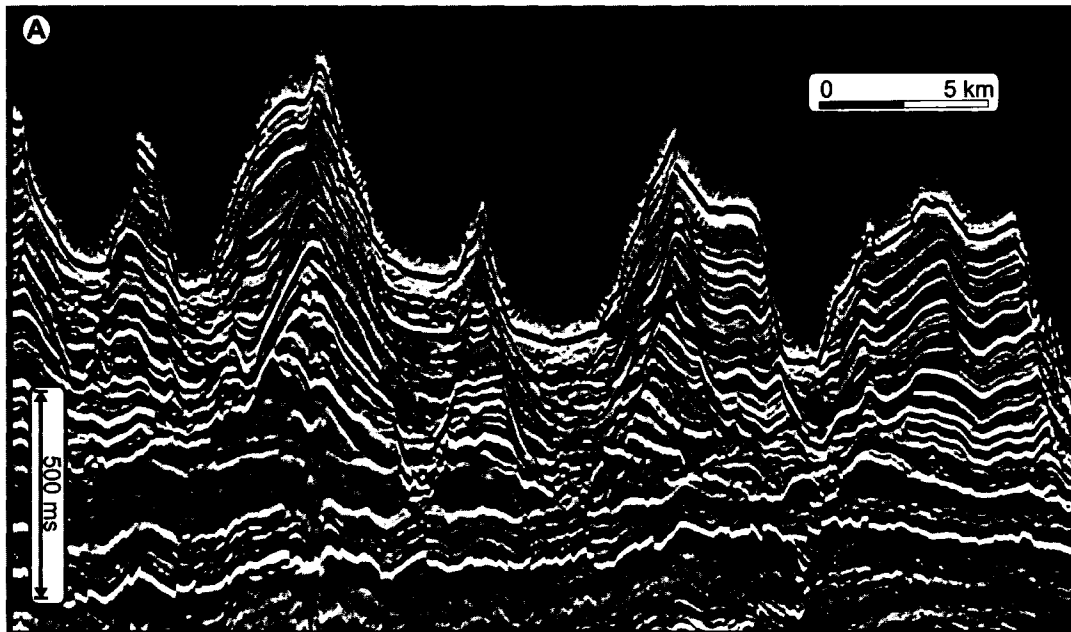


Figure 3.5A. Interpreted paleo and modern day channel architecture from the upper slope as seen in seismic reflection profile. Note: in the upper slope deeply incised (v shape) channel architecture and high amplitude channel fill and channel walls.

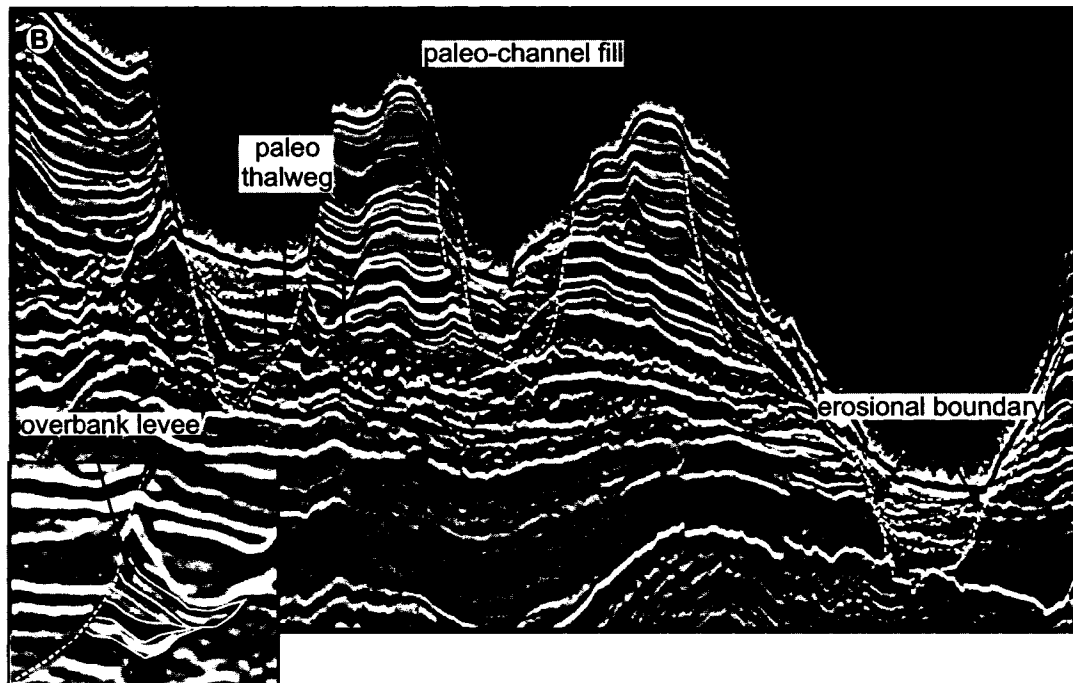
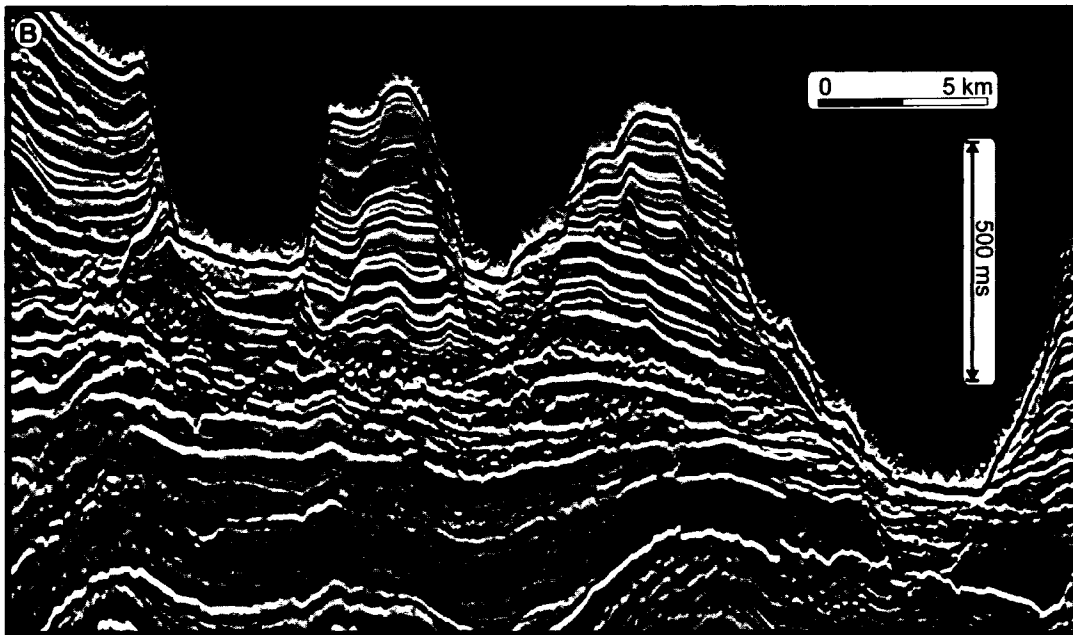


Figure 3.5B. Interpreted paleo and modern day channel architecture from the lower-middle slope. Note: in the lower-middle slope (u shape) in seismic reflection profile. The lower-middle slope displays levee deposits, high amplitude channel fill and channel walls.

3.7 Key Reflections

To establish a seismic reflection stratigraphy in the study area, seven key reflections are recognized in 3-D (Figure 3.6) and 2-D multichannel seismic reflection data (Figure 3.7). Key seismic reflections were chosen based on prominent reflection characteristics within the 3-D seismic reflection data on the slope, and then traced beyond the study area with 2-D seismic reflection data into offshore wells for biostratigraphic correlations. The wells on the slope are Shubenacadie H-100 and Newburn H-23. On the outer shelf, Glenelg N-49 and Eagle D-21 were used (Figure 1.1). From oldest to youngest, these key reflections are referred to as C10, E20, O30, M40, P60 and P70 on our seismic sections.

Across the slope, variations in reflection geometries are well recognized through 3-D surface renders. Faults, paleo-channels and depositional systems are common features when observed in vertically exaggerated plan view, from time depth or amplitude extraction. Above areas of salt uplift, concentric and extensional faulting is recognized in the middle to lower slope.

C10 (purple) is a positive reflection and corresponds to the deepest of seismic reflections picked. On the slope, C10 is interpreted to become the upper positive amplitude reflection of a package of regional high amplitude reflections recognized throughout the study area. On the outer shelf, the C10 reflector produces a strong positive amplitude reflection of consistent continuity. At the shelf break, the C10 reflection merges to form a condensed section on the middle to upper slope (Figure 3.6).

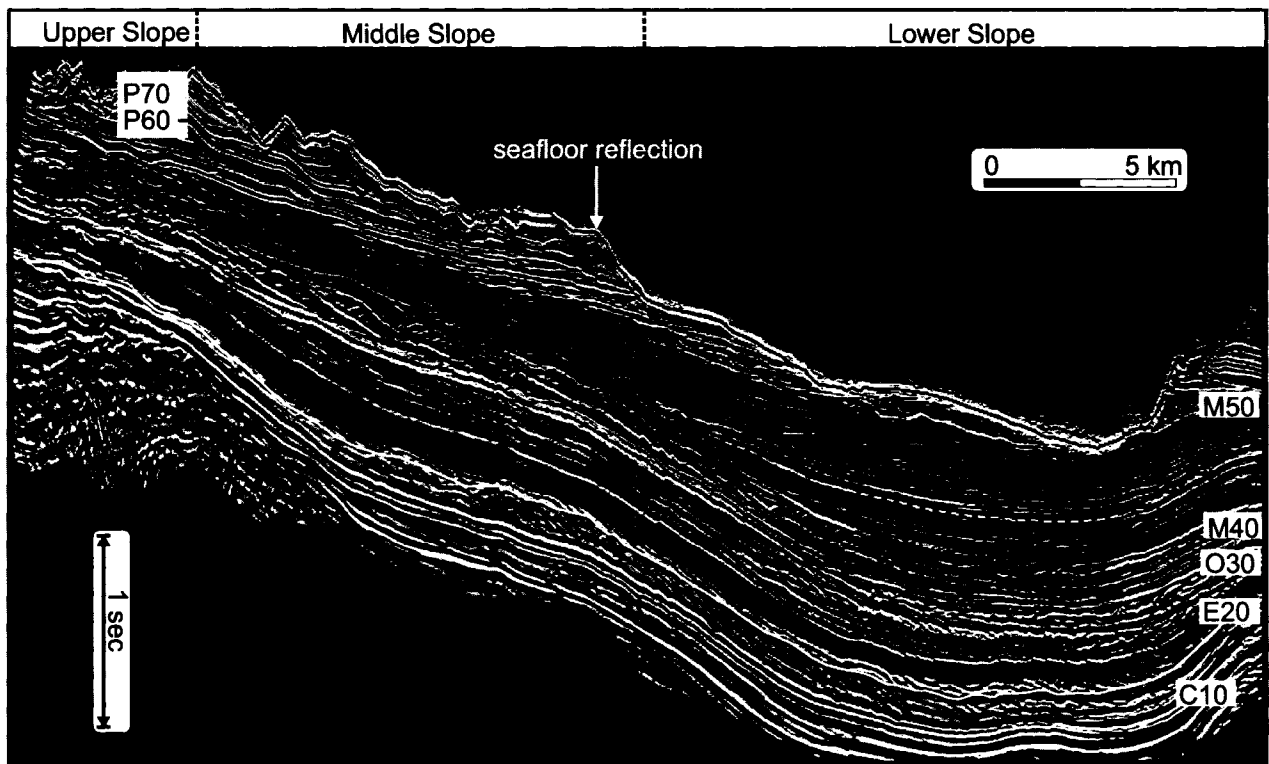
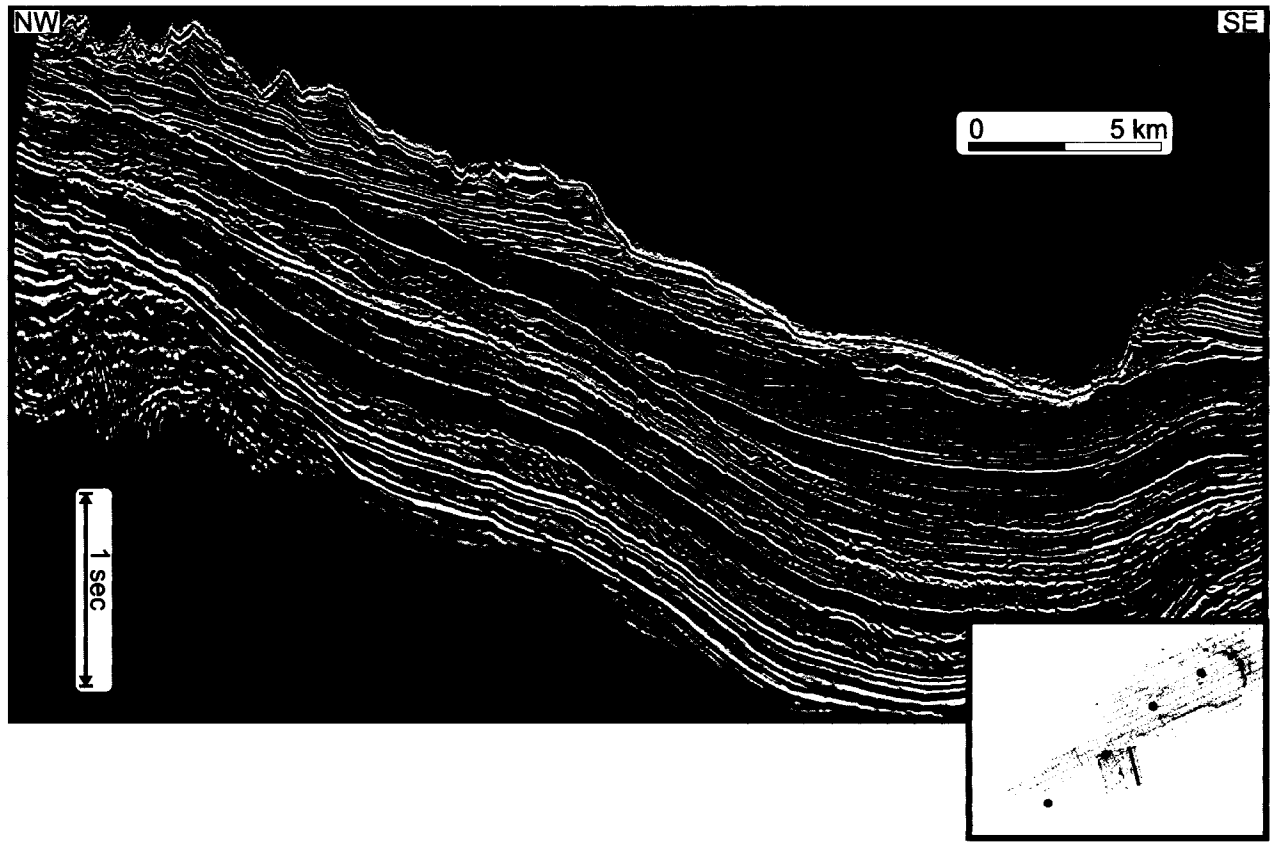


Figure 3.6. Type Section of the Cenozoic succession on the Central Scotian Slope, showing formation dip lines. Key reflectors are colored and line labeled as C10, E20, O30, M40, M50, P60 and P70.

The **E20** reflection is a positive reflection with poor continuity and irregular amplitude across the slope (Figure 3.6). Recognized across and down the slope, E20 is often missing or patchy at the shelf break and upper slope throughout the study area. When identified down-slope, it is recognized as a draped lowermost continuous reflection over a heavily faulted irregular package of reflections. Reflection character varies across the slope and on the outer shelf. However, it is well defined in areas without paleochannel erosion. On the outer shelf, the E20 reflection similarly shows a patchy amplitude variation across section. E20 becomes more consistent in amplitude signature and continuity to the northeast.

The **O30** (orange) reflection is a prominent high amplitude positive reflection. O30 is correlated from the slope up through the shelf break and into the outer shelf until it reaches the upper limits of seismic resolution near the sea floor. The O30 reflector truncates reflections down to the C10 reflection in the middle to upper slope and at the shelf to slope transition. The O30 reflection maintains its reflection continuity and high amplitude character across the study area.

The **M40** (red) reflection is a high amplitude negative reflection which maintains reflective continuity and character across the slope. M40 is tentatively traced through the shelf break onto the outer shelf, where signal to noise ratio is high (Figure 3.7).

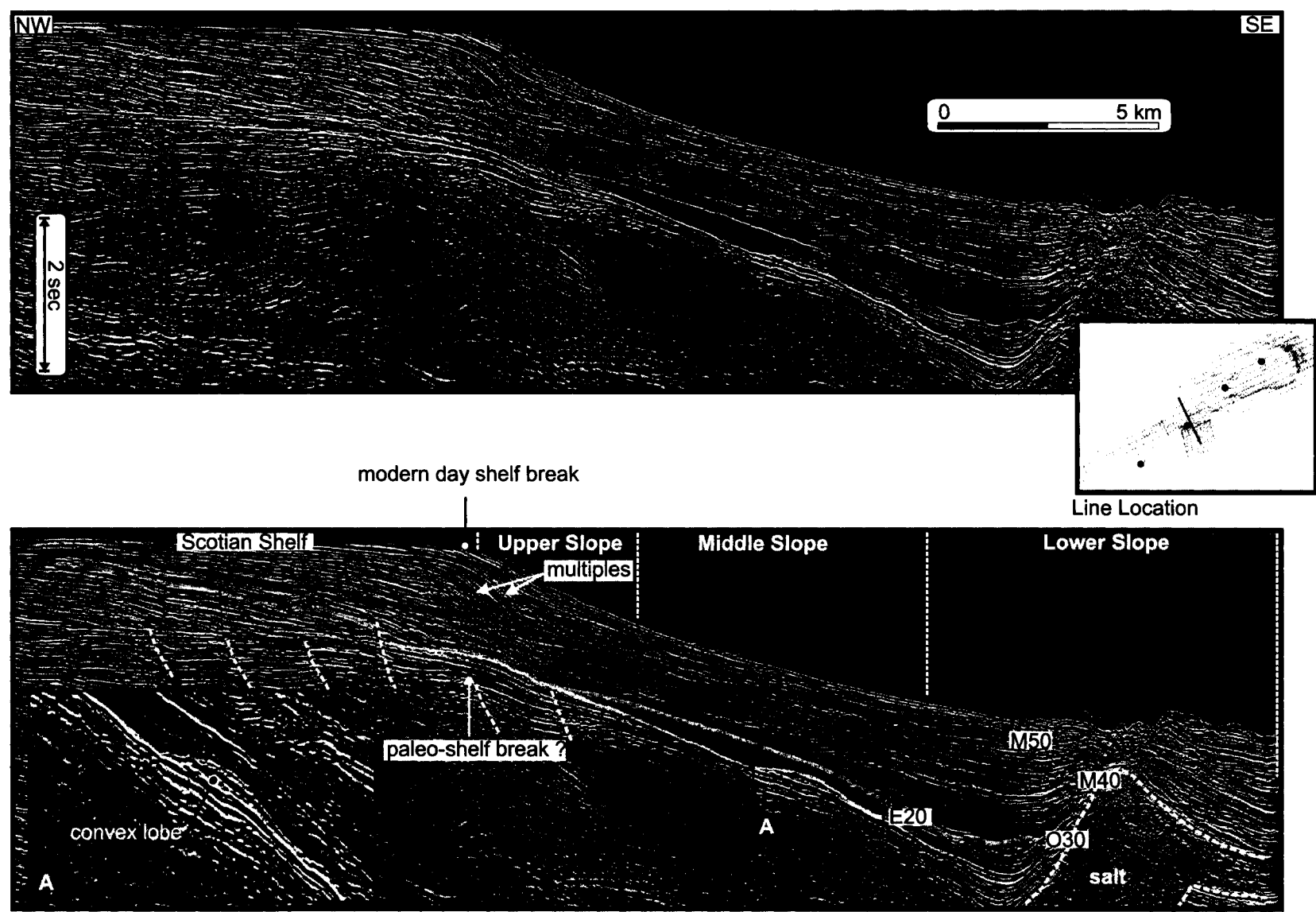


Figure 3.7. Regional seismic line showing key reflectors from the slope to the shelf, and demonstrating seismic image limitations at the shelf break with multiple reflections. A) Reflector E20, draping over a convex lobe of internal chaotic reflections above C10.

The **M50** (blue) reflection, also a high amplitude negative reflection, is incised by small channels on the middle slope and upper slope to shelf interface (Figure 3.8). The M50 reflection loses reflection strength and continuity in inter-canyon regions but is recognized under modern day canyon floors. The M50 reflection is recognized across the slope, but cannot be correlated with confidence through the shelf break. Its position on the outer shelf is speculative (Figure 3.7).

The **P60** (green) reflection is a strong high amplitude draping reflection recognized on the slope (Figure 3.6). Reflection continuity is often compromised by modern canyons and shelf edge erosion (Figure 3.8). **P70** is the youngest reflection picked and is based on a high amplitude signature. The P70 reflector has been cut in a similar way to P60 by canyons and is more often missing in sections throughout the study area (Figure 3.8).

3.8 Seismic Reflection Geometry

Correlation of the 7 key reflections was done through the 3-D seismic reflection data on the slope and regional 2-D multichannel seismic reflection data across the slope and outer shelf. At the Shubenacadie H-100 wellsite, approximately 60 km west of the 3-D seismic coverage, reflections P70, P60, M40, O30 and C10 were correlated relative to the regional horizons recognized as 1 (P60), 2 (M40), 3 (O30), 4 (E20) and 5 (C10) from the published stratigraphy of MacLean and Wade (1993). On the outer shelf, at the Glenelg N-49, the C10, E20 and O30 reflections correlated to horizons 3 (O30), 4 (E20) and 5 (C10) of MacLean and Wade (1993). Correlation from the slope to the outer shelf

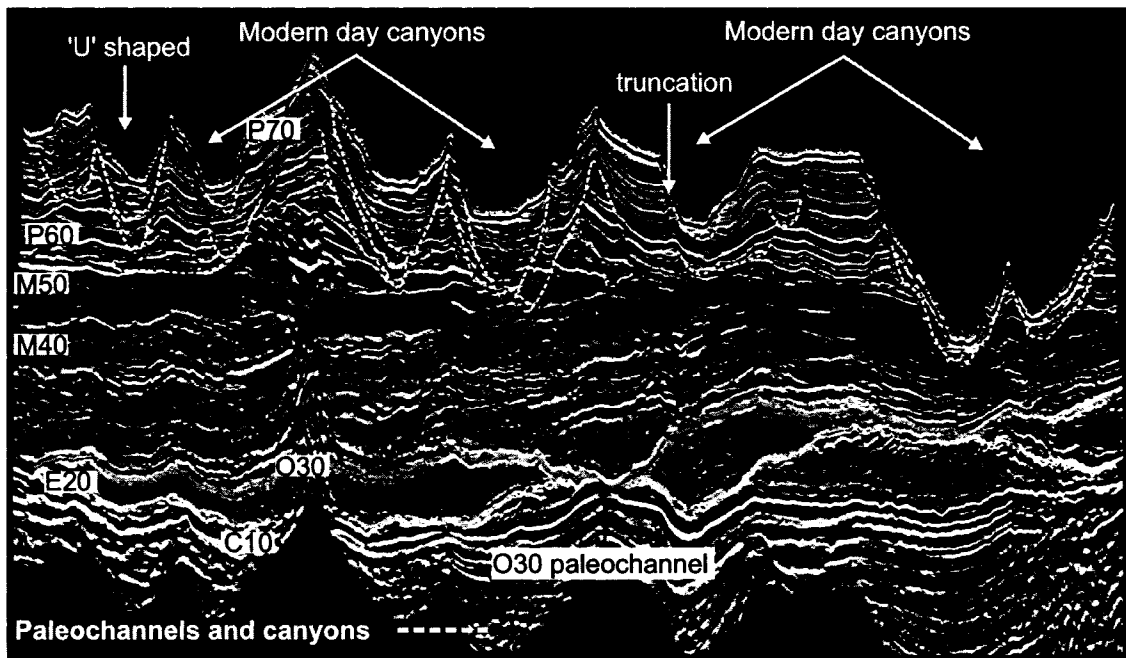
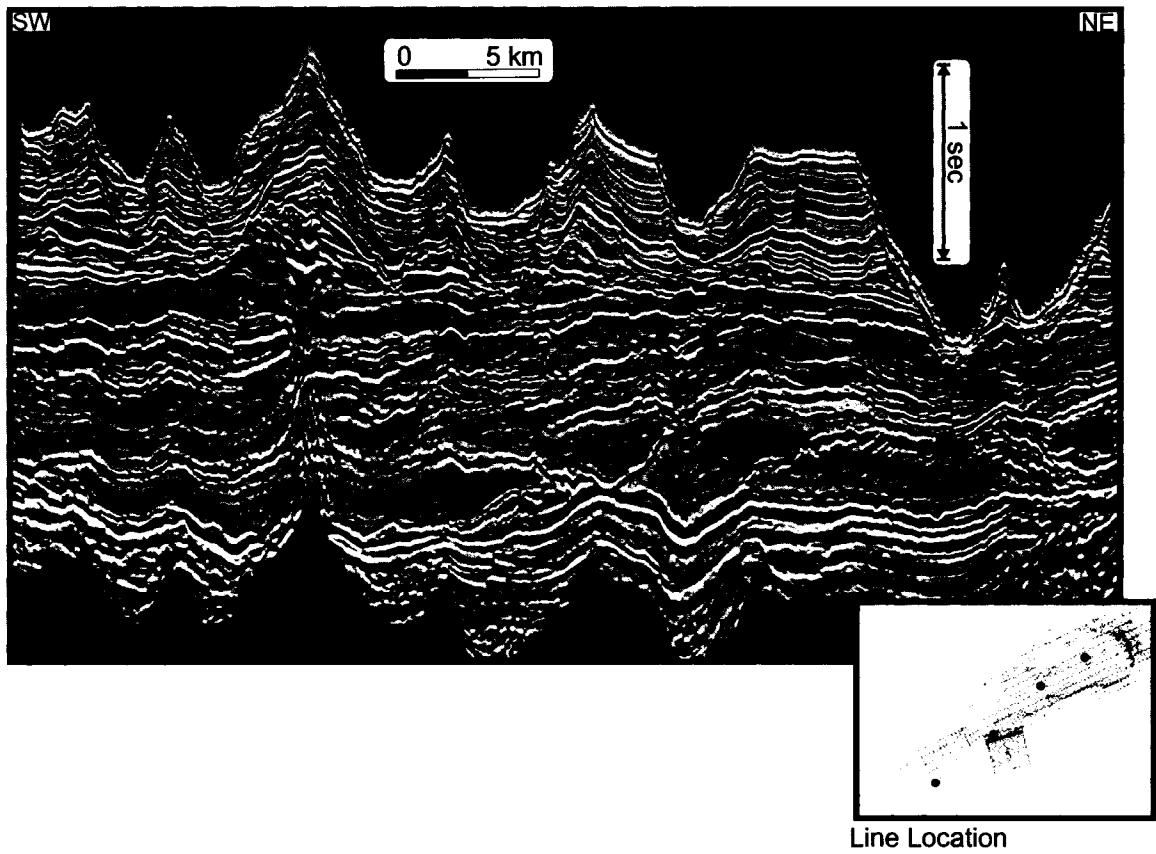
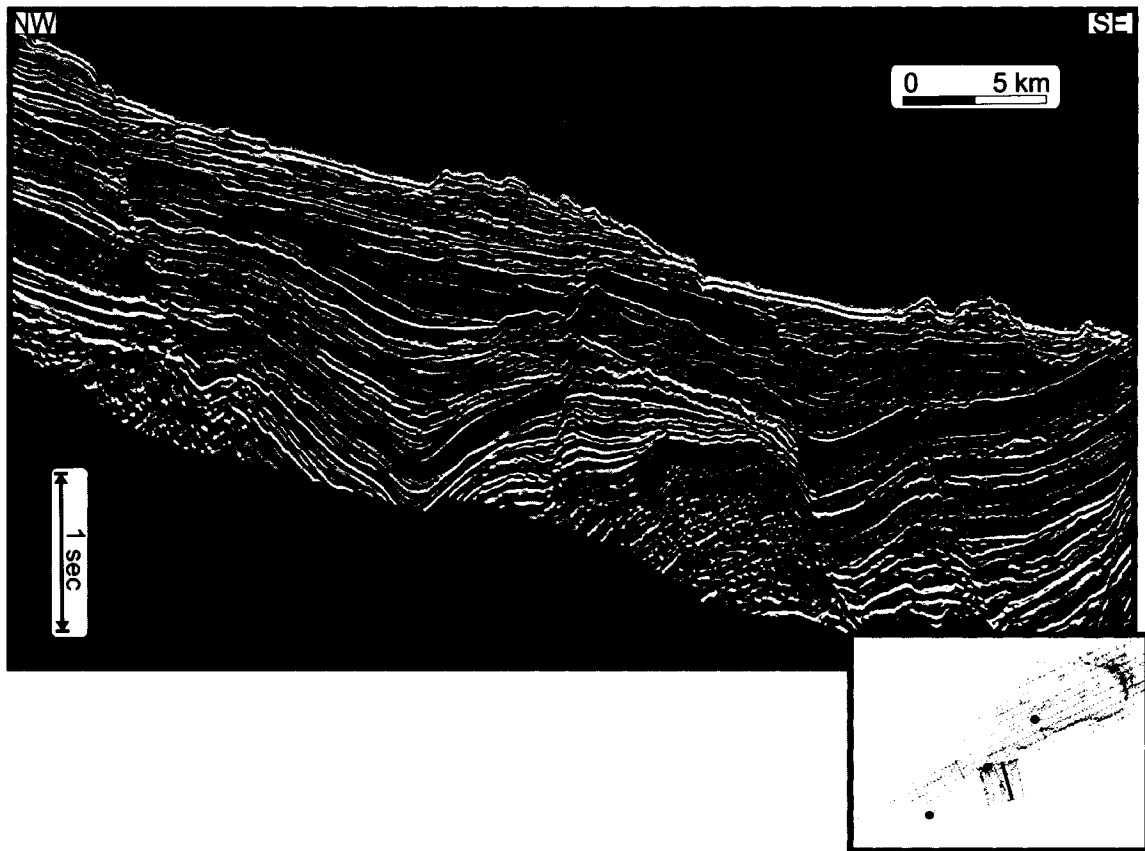


Figure 3.8. A common loss of reflection continuity in the E20, M40, M50, P60, P70 reflections due to paleochannel and paleo-canyon erosion.

allowed for an interpretation into the outer shelf to slope relationship and a regional sense of reflection character and geometry across the slope as far west as the Shubenacadie H-100 wellsite (Figure 1.2).

Across the upper slope, the C10 reflection characteristically displays discontinuity, subtle mounding and minor shingling. The C10 reflection is subsiding downward on the mid-slope into salt withdrawal basins, and offset by deep seated faults at the withdrawal basin flanks. In the withdrawal basin, the C10 reflection becomes more differentiated from its condensed package of reflections, and features such as mounding and shingles become more pronounced (Figure 3.9). Rimming salt highs, the C10 reflection is offset by normal faults around the basin edge and at the salt flanks. The C10 reflection either onlaps the flanks of the most pronounced salt highs, laps-out onto them, or overlies their upper limits. Commonly, above salt highs, rafted reflections older than C10 are present, and the C10 reflection is recognized as overlying or lapping out onto the rafted packages. The C10 reflection is only seen in the lower slope at the northeastern-most extent of the 3-D seismic data. Elsewhere in the study area, C10 drops below the 2 second sub-bottom mask applied to the 3-D seismic reflection data.

At the shelf break and upper slope, the C10 reflection is recognized as being partially eroded and faulted across the paleo-shelf break (Figure 3.7). On the outer shelf, the C10 reflection splits from a single reflection on the slope to the upper and lower high amplitude reflections of a prograding package of clinoform reflections on the outer shelf.



Line Location

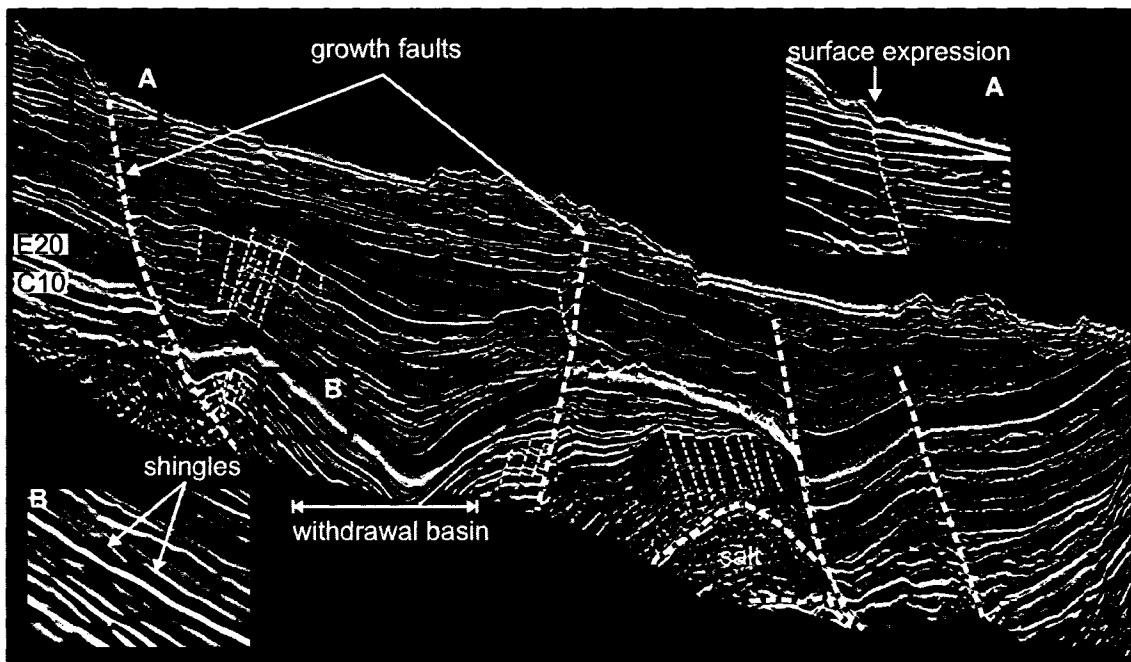


Figure 3.9. The typical C10 reflection geometry relative to sub surface salt uplift and withdrawal, as well as shingle features (B) and the surface expression of a large withdrawal basin with bounding growth faults (A).

Generally, the **E20** reflection appears in seismic reflection profiles sporadically, and reflection continuity is variable across the study area (Figure 3.8). In the upper slope, the E20 reflection is relatively high amplitude. It thins and laps out by the lower slope. The E20 reflection progressively decreases in reflection strength down-slope until it becomes indistinguishable in seismic section. Across the middle slope, the E20 reflection decreases in amplitude and continuity. In the northeastern middle slope, the E20 reflection reappears as an upper draping unit above an onlapping convex lobe which laps out seaward into the basin (Figure 3.7). In the lower slope, the E20 reflection is interpreted as a draping unit across the study area. In areas of salt uplift, E20 laps-out in the withdrawal basins before reaching the flanks of salt highs. Faulting affects the E20 reflection in a manner similar to C10, being offset locally by large growth faults, where structural reorganization around salt has occurred (Figure 3.9).

In the northeastern part of the study area, the E20 reflection onlaps the C10 reflection on the outer shelf with a relatively well defined high amplitude reflection. On the outer shelf, the E20 reflection forms the base of a sequence of downlapping reflections, which are recognized in the northeast but not in the southwest. The E20 reflection is eroded in places across the outer shelf and upper most slope, resulting in a decrease in amplitude and reflection continuity, with only small patches appearing between paleo-channels along the shelf to slope interface.

The **O30** reflection is a high amplitude regional unconformity, consistent in reflection character and continuity across and down slope. At the shelf break, O30 truncates

reflections and correlates to paleochannel architecture (Figure 3.8). Downslope, O30 truncates uplifted strata at salt flanks, onlaps the salt highs and off-laps the highs on the seaward side. In some areas of the lower slope, the E20 reflection is cross-cut by the O30 reflector. The O30 reflection is recognized on the outer shelf in areas not affected by paleo-channel erosion. Generally, the continuity of the O30 reflection is broken only by faults, paleo-channels and salt highs.

The **M40** (red) reflection is picked based on the regional continuity of a high negative amplitude reflection on the upper and lower slope. M40 is heavily faulted across the upper and middle slope and displays a polygonal fault pattern extending from the upper slope to the middle slope on 3-D surface render (Figure 3.10). In the lower slope, M40 is smooth and continuous where it is not offset by large growth faults that also affect deeper reflections. Correlation of the M40 reflection across these heavily faulted areas is possible based on its strong reflection continuity and amplitude. At salt highs, the M40 reflection onlaps, locally antiforms or pinches out along their flanks (Figure 3.11). The character and continuity of M40 is maintained across the slope. In 2-D multichannel seismic profiles it commonly is interpreted through the shelf break. On the outer shelf, the M40 reflection onlaps the O30 reflection at or near the shelf break. Further landward, on the outer shelf, the M40 reflection conforms to a package of downward dipping reflections.

The **M50** (blue) reflection is a high amplitude, unconformable, negative reflection incised by small channels, mass transport complexes and modern day canyon systems (Figure

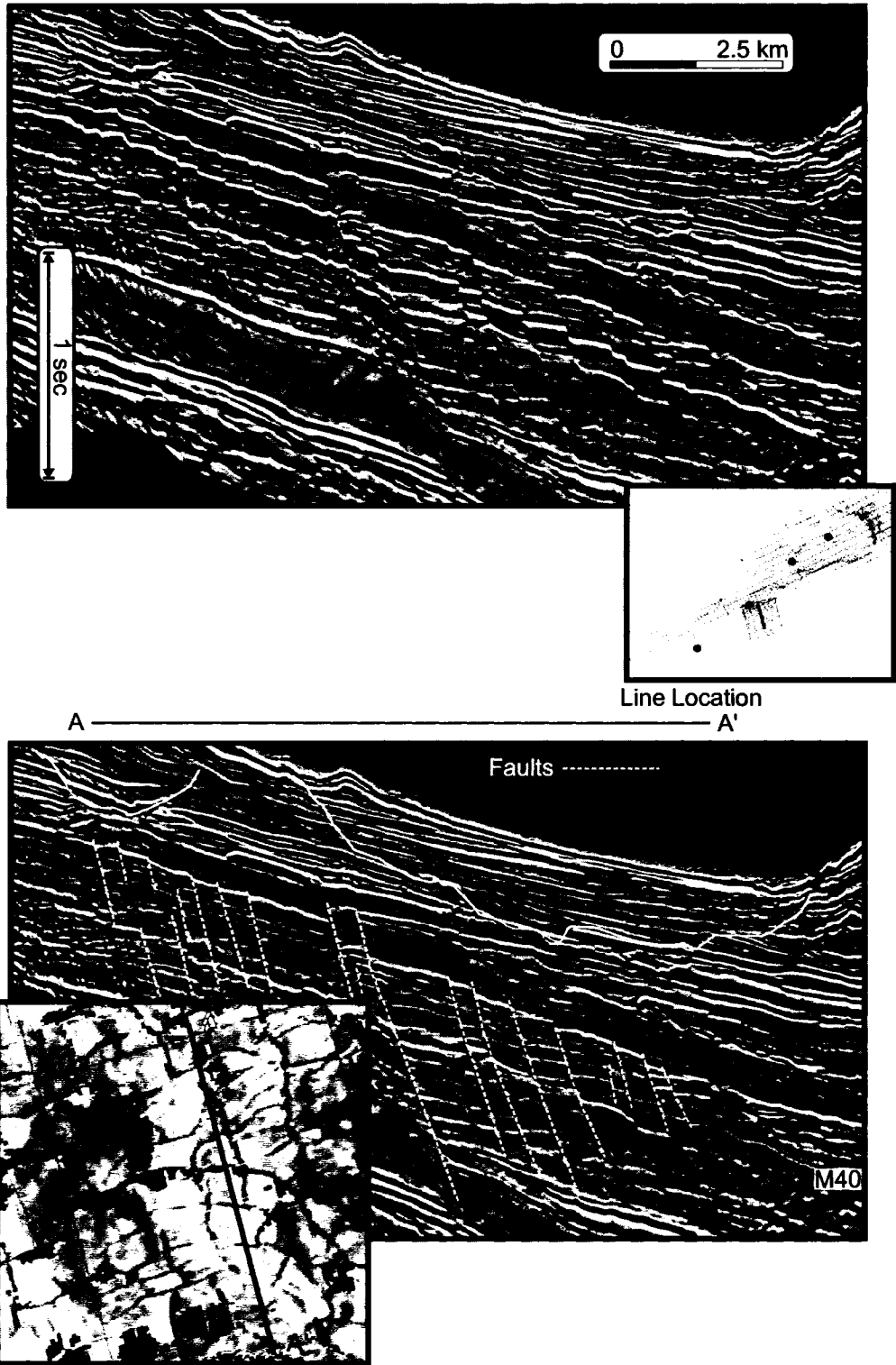


Figure 3.10. The M40 reflector and its faulted pattern in seismic reflection profile and in a 3-D time surface render.

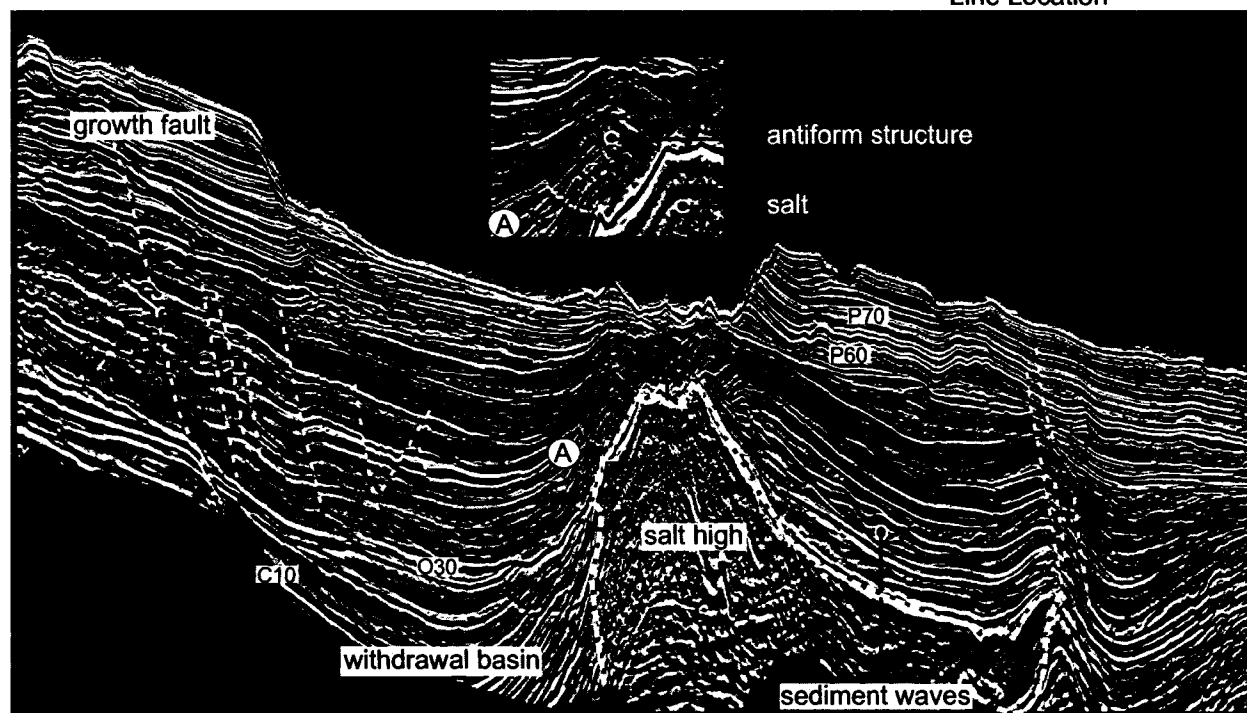
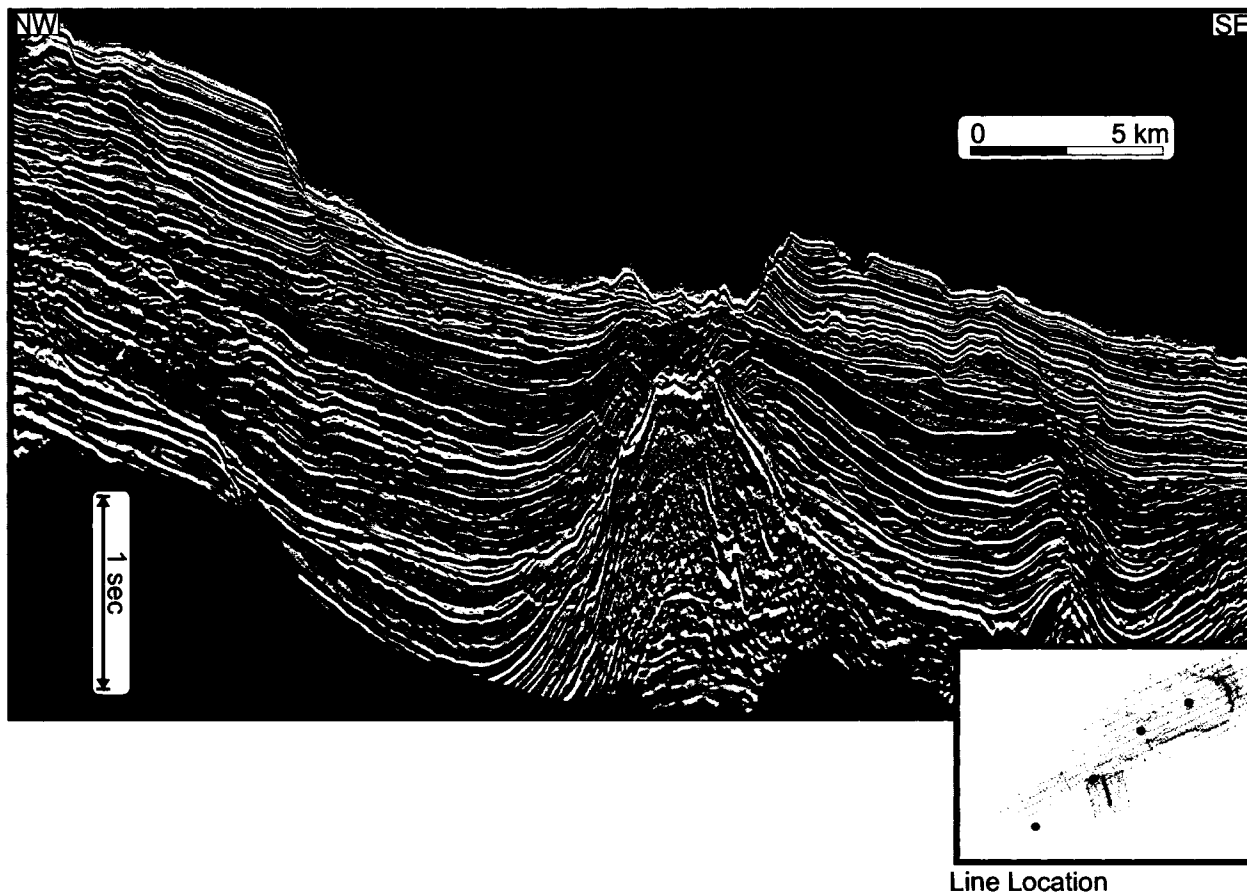


Figure 3.11. The M40 reflector in relation to salt uplift in the middle slope with onlap and localized antiform near the crest. Also to be noted are sediment waves features on the seaward side, above the salt highs.

3.8). The irregular nature of this reflection makes correlation problematic in some places. Faulting in the upper slope moderately affects the M50 reflection (Figure 3.10), but large scale growth faults clearly offset this reflection across the slope (Figure 3.12). At the crest and flanks of salt highs of the middle slope, the M50 reflection locally antilines to onlap the salt high, just as M40. The M50 reflection is heavily eroded in the upper to lower slope, where it is eroded by paleo-channels or uplifted by salt highs which are partially exposing it to the seafloor. The reflection character of M40 is maintained across the slope to the southwest and northeast in 2-D multichannel seismic profiles. In the upper slope, the M50 reflection onlaps the M40 reflection at the shelf break (Figure 3.6). The M50 reflector may offlap the M40 reflection, and conforms to a package of obliquely dipping reflections on the outer shelf.

The **P60** reflection is the lowermost draped reflection above a unit of undulating incoherent reflections. P60 is cut by modern day canyon systems, being recognized only in packages of relatively undisturbed intra-canyon areas of the study area (Figure 3.13). Above and around salt highs, linear normal faulting is recognized but little impact from salt movement is translated to the continuity of the P60 reflection. The growth faults on the flanks of the withdrawal basins cut across the upper slope and normally offset the P60 reflection to a lesser degree than older reflections.

The **P70** reflection is a smooth and continuous draping reflection in the upper and lower slope. Similar to P60, the P70 reflection is only visible in intra-canyon areas and where

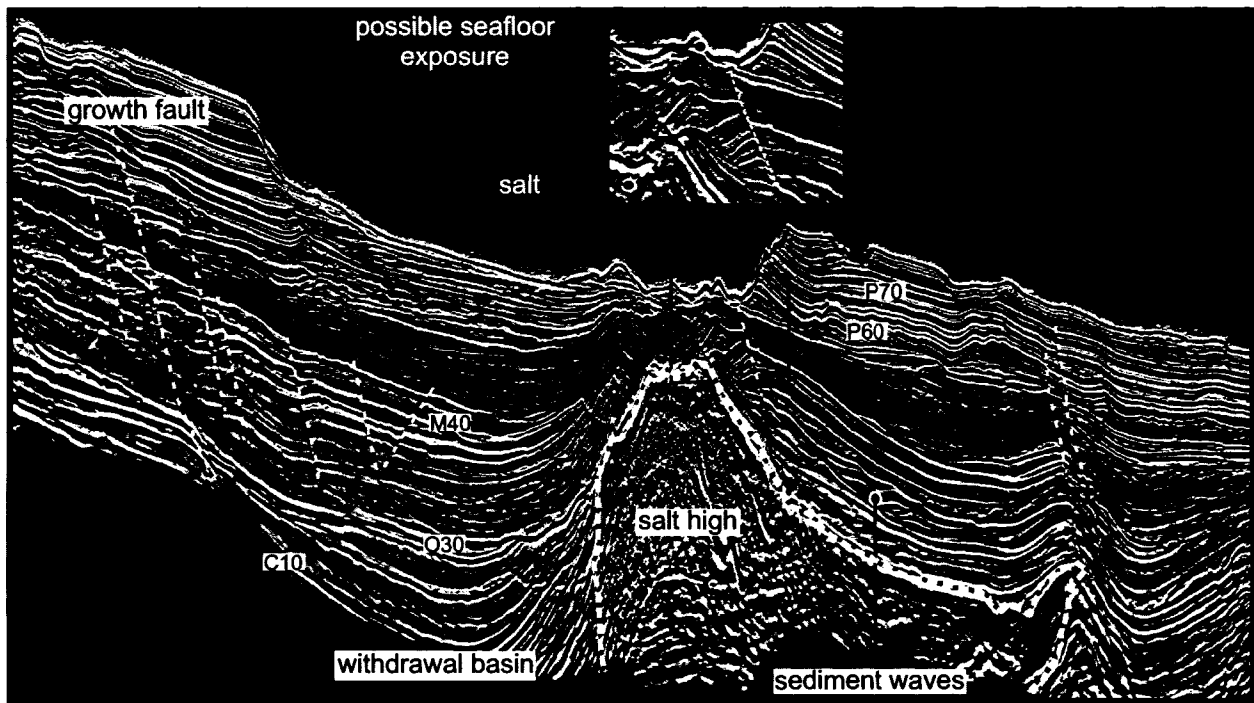
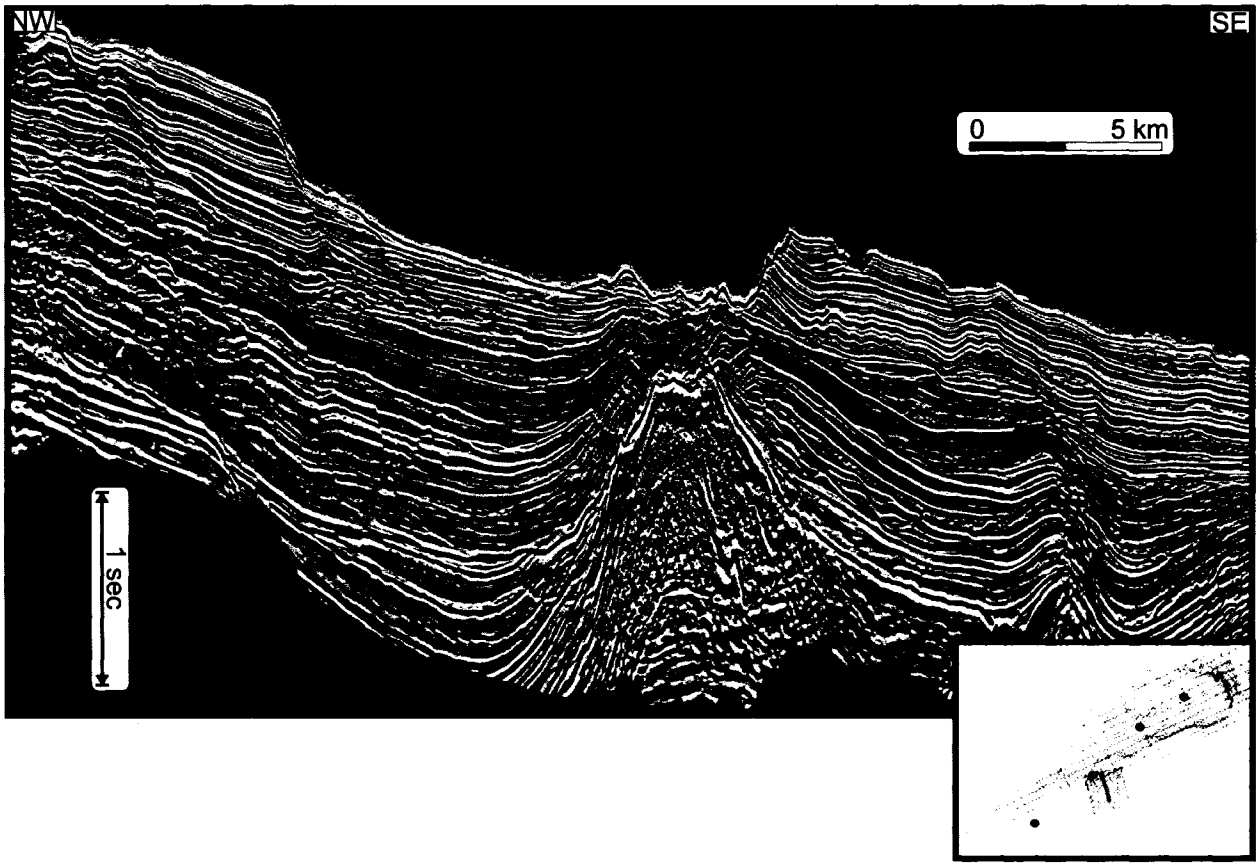


Figure 3.12. Seismic reflection profiles showing the high amplitude M50 reflector relative to salt highs in the middle slope and possible seafloor exposure due to uplift. Note that M50 is similarly deformed upward as an antiform on the northeast side of the salt high.

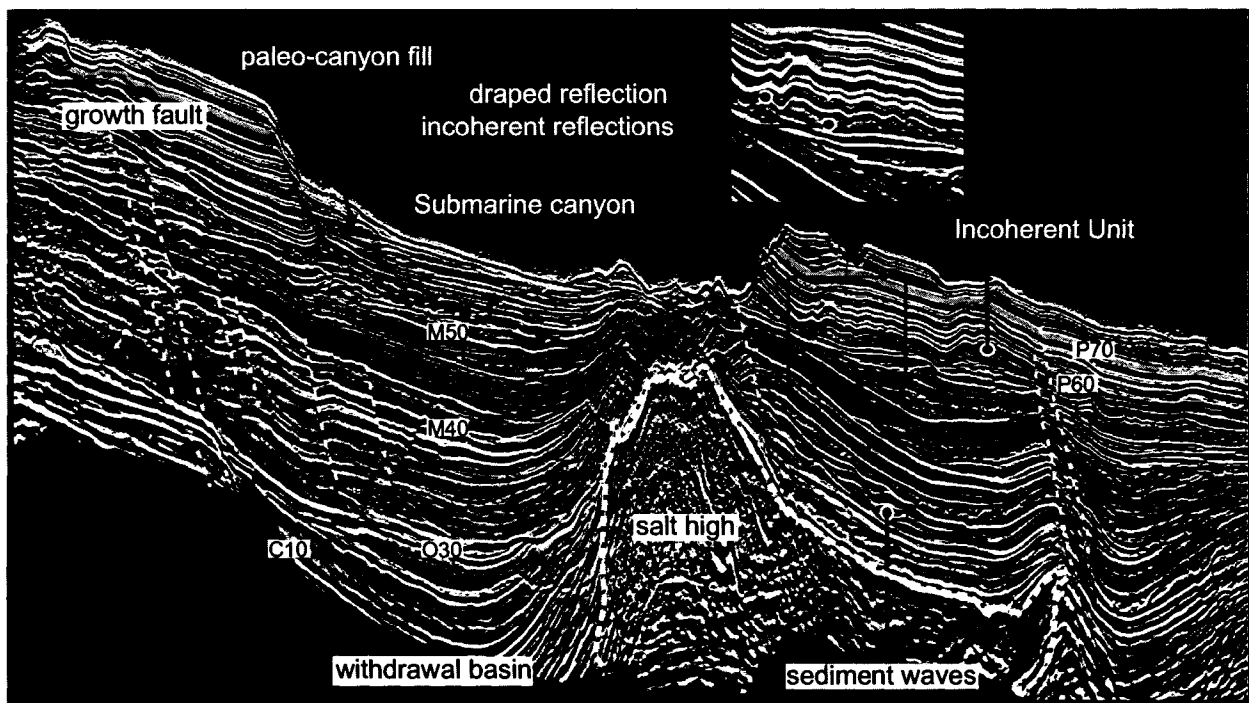
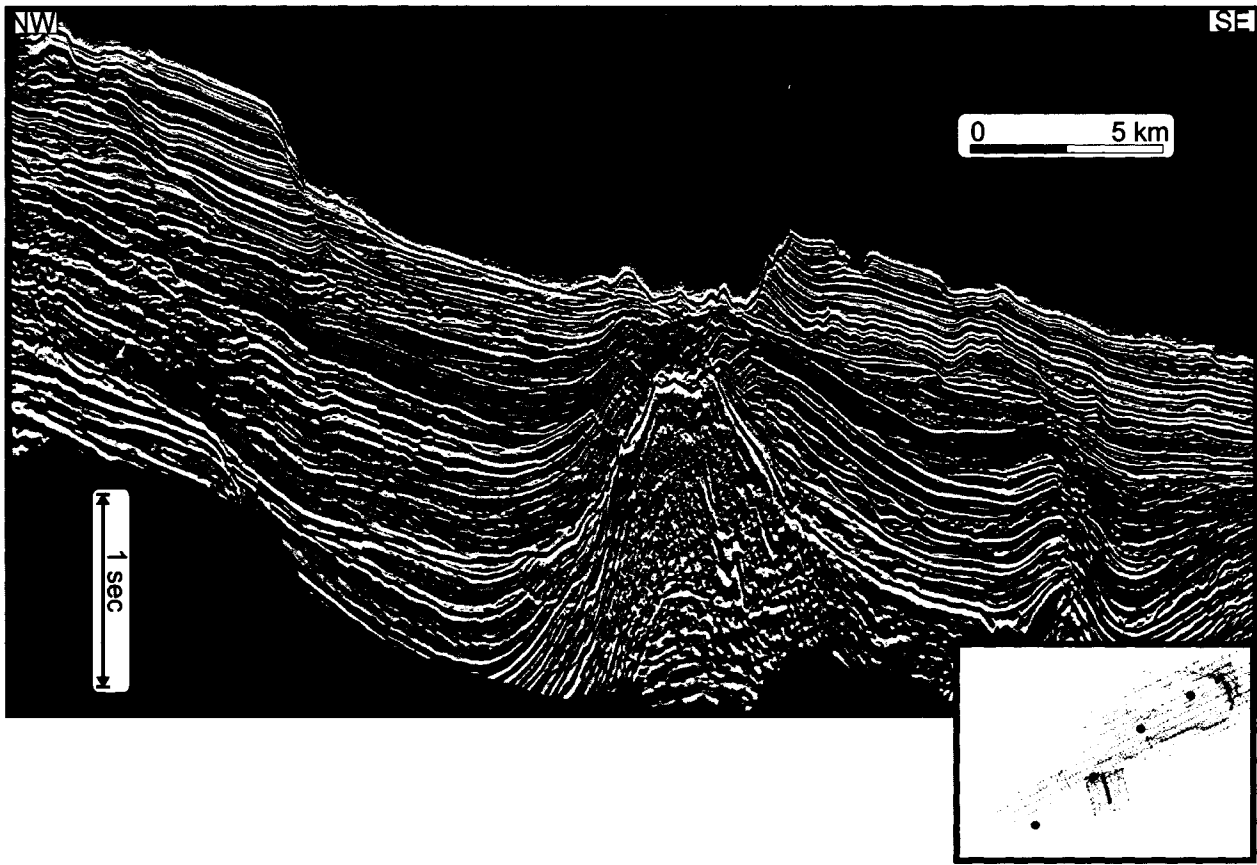


Figure 3.13. Seismic reflection profiles showing P60 draping a lower seismic unit of incoherent reflections. Also, the high, positive amplitude P70 reflection drapes the slope. Both reflectors are absent in the canyon area.

there has been minimal erosion by modern day canyons. Paleo canyons on the upper to middle slope are common, cutting the P70 reflection across the slope. Reflection strength and continuity is maintained into the lower slope (Figure 3.13).

4. Regional correlation and context

4.1 Biostratigraphy - Correlation to well data

Chronostratigraphy of the study area was established by correlation of seismic reflection markers to time-depth-corrected synthetic seismograms and biostratigraphic picks on the slope at the Shubenacadie H-100 and Newburn H-23 wellsites (Figure 4.1A) and on the shelf at the Glenelg N-49 and Eagle D-21 wellsites (Figure 4.1B). Confident correlations are provided with generation of synthetic seismograms at the well sites. The biostratigraphy at these wells are based on palynomorphs and nannofossils. Biostratigraphic data at the Newburn H-23 well is propriety to Chevron et al. and will be released in 2007. At Shubenacadie H-100, picks are based on palynology (Fensome 2000) and microfossils. The biostratigraphy of Glenelg N-49 is based on the Shell et al., (1986) well site report. At Eagle D-21 well site biostratigraphic age picks are principally based on planktonic foraminifera (Thomas 1994), using zonations from (Bolli and Saunders 1985; Toumarkine and Luterbacher 1985; Thomas 1994).

Several sources of error may exist in constructing synthetic seismograms. Time-depth conversion is based on velocity information. Synthetic seismograms allow confirmation of the velocities determined during seismic processing by simulating the seismic trace using well data. With the seismogram derived from well data, possible sources of error are the result of: 1) no well bore data collected through the upper (Cenozoic) section forcing the use of assumed velocities or density values 2) the vintage of the data and the

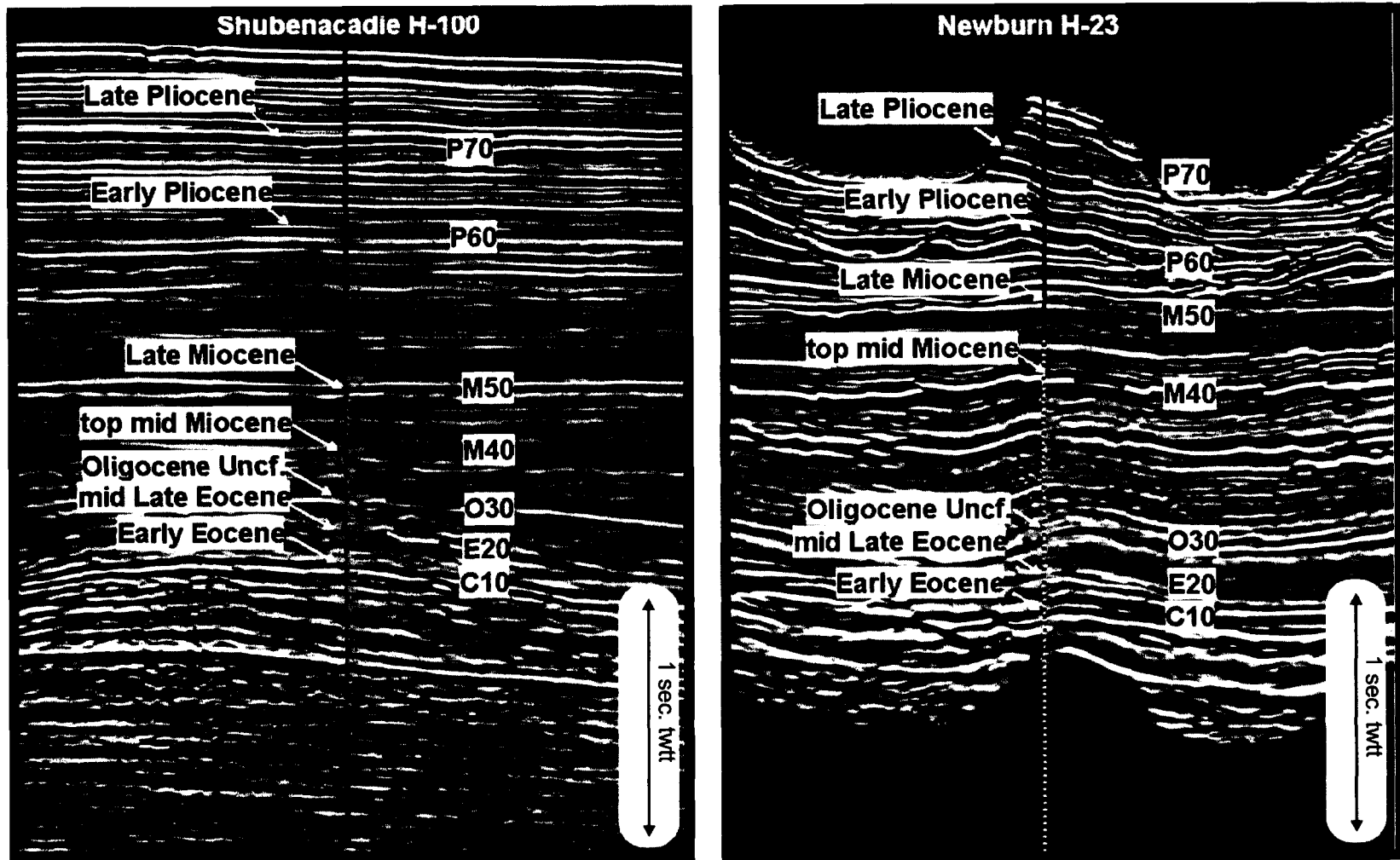


Figure 4.1A Synthetic seismograms with key reflection correlations and biostratigraphic age picks of Shubenacadie H-100 and Newburn H-23 on the central Scotian Slope.

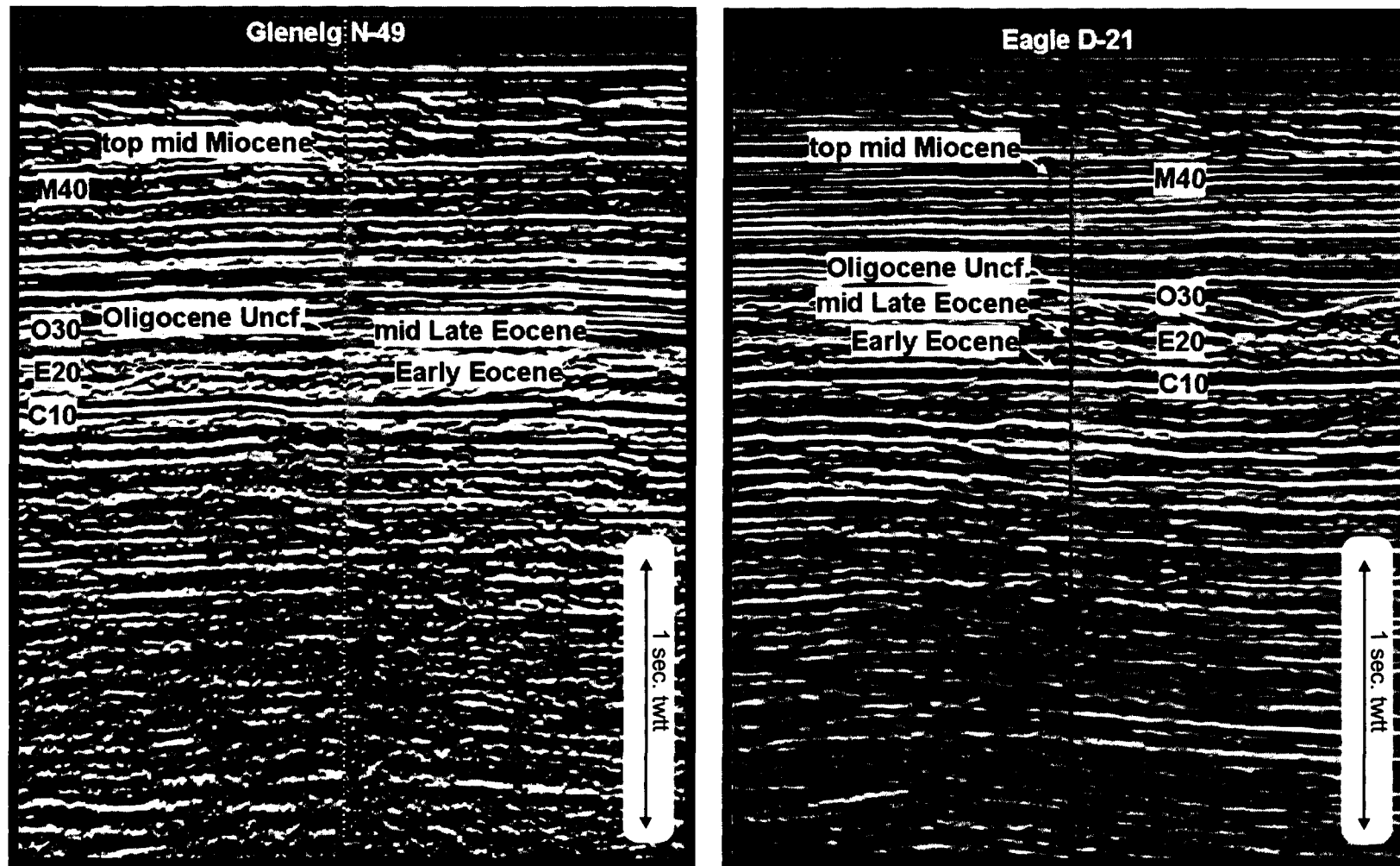


Figure 4.1B Synthetic seismograms with key reflection correlations and biostratigraphic age picks of Glenelg N-49 and Eagle D-21 on the outer Scotian Shelf.

limited technological capability of that time and 3) the availability and interval of check shot data. As mentioned in earlier in Chapter 2, it is not uncommon for wells to have limited log data collected in the upper section, outside the area of hydrocarbon interest. Well data used in this study is a variety of vintages. The magnitude of any errors in determining the time to depth correlation may be as great as 50 – 100 ms (twtt). Although correlations to synthetic seismograms are confident, the greatest confidence is in wells with the best log and velocity data, namely Newburn H-23 and Shubenacadie H-100.

4.1.1 Shubenacadie H-100

Age estimations at Shubenacadie H-100 are as follows: M50: late Miocene; M40: top mid Miocene; O30: late Eocene to early Miocene unconformity; E20: middle late Eocene; C10: early Eocene (Table 4.1). The P60 and P70 reflectors correlate to horizons 2 and 1 of MacLean and Wade (1993), which dated them respectively as late Middle Pliocene and Late Pliocene based on the biostratigraphic work of Williams (1975) and Barss et al. (1979). Although these two dates are based on much earlier works, the P60 date is supported by the fact that the P60 reflection (2064m) lies just above the earliest biostratigraphic picks of late Piacenzian (mid-late Pliocene) at 2140m (Fensome 2000).

4.1.2 Newburn H-23

Biostratigraphy of Newburn H-23 is based on calcareous nannofossils and palynomorphs. Zonal interpretations of Cenozoic nannofossils were made by Chevron et al, (2007) to

Table 1**Shubenacadie H-100**

C10	early Eocene	3323m	M40	top middle Miocene	2903m
E20	middle late Eocene	3189m	M50	late Miocene	2640m
O30	Oligocene Unconform.	3049m			

Newburn H-23

C10	NP15	2784m	M40	NN7	1947m
E20	NP18	2557m	M50	late Miocene	1681m
O30	NN3 – NP19	2522m			

Glenelg N-49

C10	early Eocene	1423m	M40	early / late Miocene	542m
E20	middle late Eocene	1253m	M50	?	
O30	Oligocene Unconform.	966m			

Eagle D-21

C10	early Eocene	1276m	M40	earliest Pliocene	544m
E20	middle Eocene	1139m	M50	?	
O30	Earliest Miocene	964m			

match the Neogene Nannofossil (NN) and Calcareous Nannofossil (NP) zones using the (Martini 1971) scheme, as modified by (Hardenbol et al. 1998). Reflections of the late Miocene (M50), upper Middle Miocene (M40), Late Eocene to Early Miocene (O30), middle Late Eocene (E20) and Early Eocene (C10) were correlated from Shubenacadie H-100. Using these nannofossil zonations, ages are applied to seismic reflectors. They are as follows: M40 is late Burdigalian (NN7), O30 is middle Burdigalian to middle Priabonian (NN3-NP19), E20 is early to middle Priabonian (NP18 –NP19) and C10 is Ypresian (NP15). At the O30 unconformity, zone NP 20 is recognized directly below the lowest NN2 pick. Reflectors P60 and P70 are not biostratigraphically dated at Newburn H-23, but correlated into the Newburn H-23 well site.

4.1.3 Glenelg N-49

The Glenelg N-49 wellsite is on the outer shelf (Figure 4.1). Biostratigraphic data for Glenelg N-49 is by Shell et al. (1986). O30 (“Oligocene Unconformity”), E20 (middle late Eocene) and C10 (early Eocene) reflections correspond relatively well respectively, to horizons 3, 4 and 5 of MacLean and Wade (1993). The M40 reflection, however, does not directly correlate to any published seismic stratigraphic markers in the Scotian Basin but does correlate to published Miocene picks at offshore well sites (MacLean and Wade, 1993).

4.1.4 Eagle D-21

Biostratigraphy data at Eagle D-21(Thomas 1994)are primarily focused on the Cenozoic section (Thomas 1994) and relied on planktonic foraminifera. The C10 reflection correlated to the Early Eocene, E20 to the Middle Eocene, the O30 to Middle Oligocene to earliest Miocene and the M40 to the earliest Pliocene. The M40 reflection is thus younger than in the other wells. As a possible explanation, Thomas (1994) indicated that some foraminiferal species occur higher in the stratigraphic section on the shelf than on the slope. Thomas (1994) suggested that well sites on the shelf would have “shoaled out” earlier in the Cenozoic section, eliminating the preferred depth interval for the diagnostic foraminifera while it was still maintained on the more seaward outer shelf and slope.

4.2 Sequence Stratigraphy: Outer Shelf and Slope Relationship

The Cenozoic architecture of the Scotian Slope and outer Scotian Shelf is placed in a sequence stratigraphic framework, integrating analyses of seismic reflection data and published offshore biostratigraphy studies. The Cenozoic section is subdivided into 5 sequences across the central outer shelf and slope.

4.2.1 Sequence 1

Sequence 1 is recognized on the outer paleo-shelf and across the slope. On the outer paleo-shelf, Sequence 1 is a parasequence of clinoform reflections downlapping the lower sequence boundary (Sequence Boundary 0) (Figure 4.2). Sequence Boundary 0 is interpreted as the maximum flooding surface (MFS) and correlated to the Wyandot marker (MacLean and Wade 1993). On the outer paleo-shelf, the C10 reflector forms the top unconformable sequence boundary of Sequence 1. Sequence Boundary 1 thus represents a change in sea-level and hence a change in the mode of deposition on the outer paleo-shelf. On the slope, Sequence Boundary 1 merges into the underlying high amplitude Sequence Boundary 0 (Wyandot marker) in the lower and middle slope to form a condensed package of Sequence 1 reflectors (Figure 4.3).

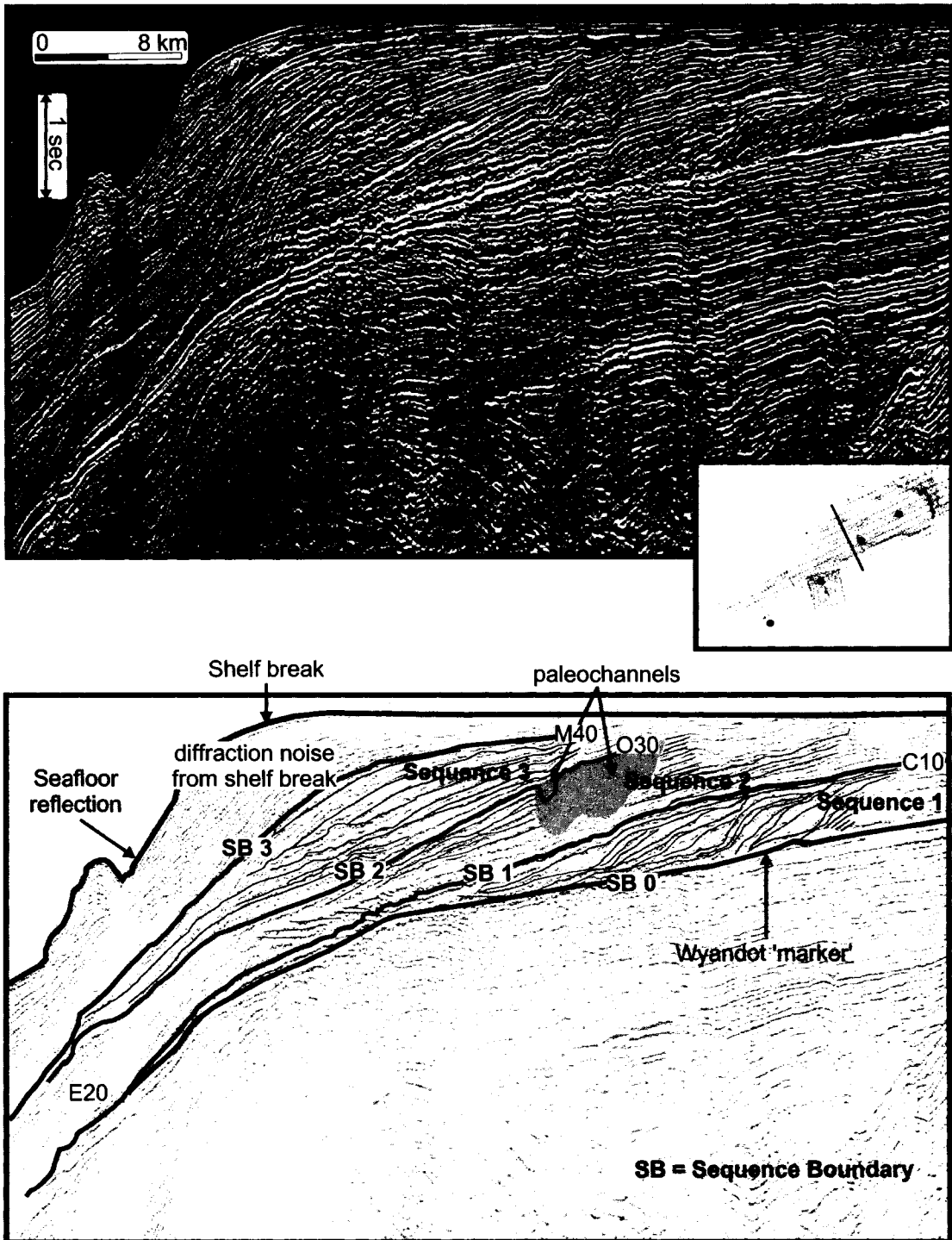


Figure 4.2. Multichannel seismic reflection profile from the outer shelf to slope in the northeastern part of the study area, with sequence boundaries identified and internal reflection geometries interpreted in relation to sequence boundaries.

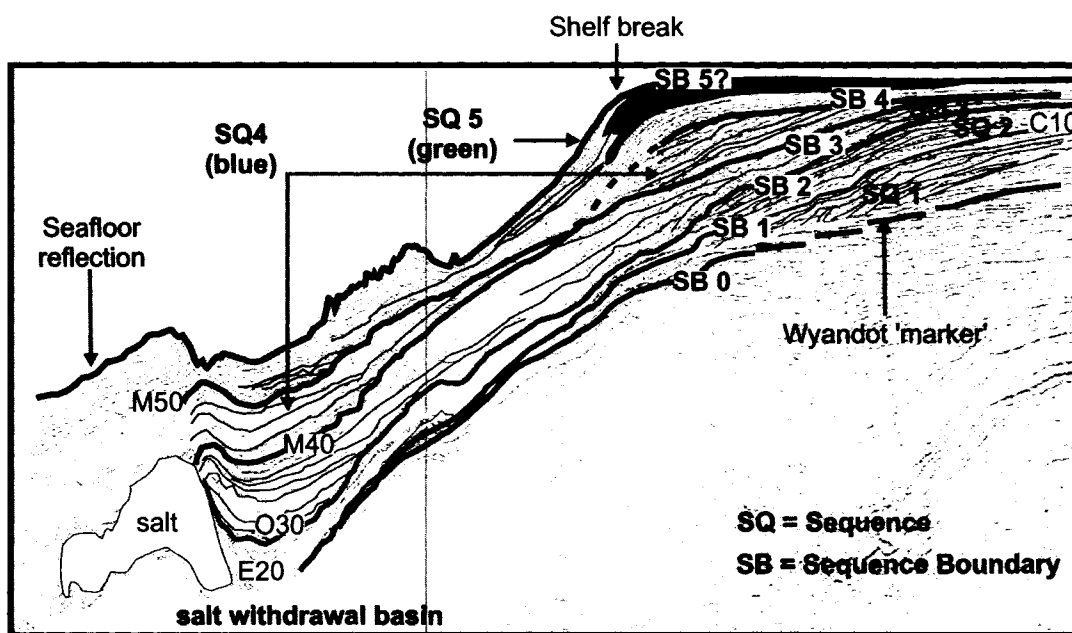
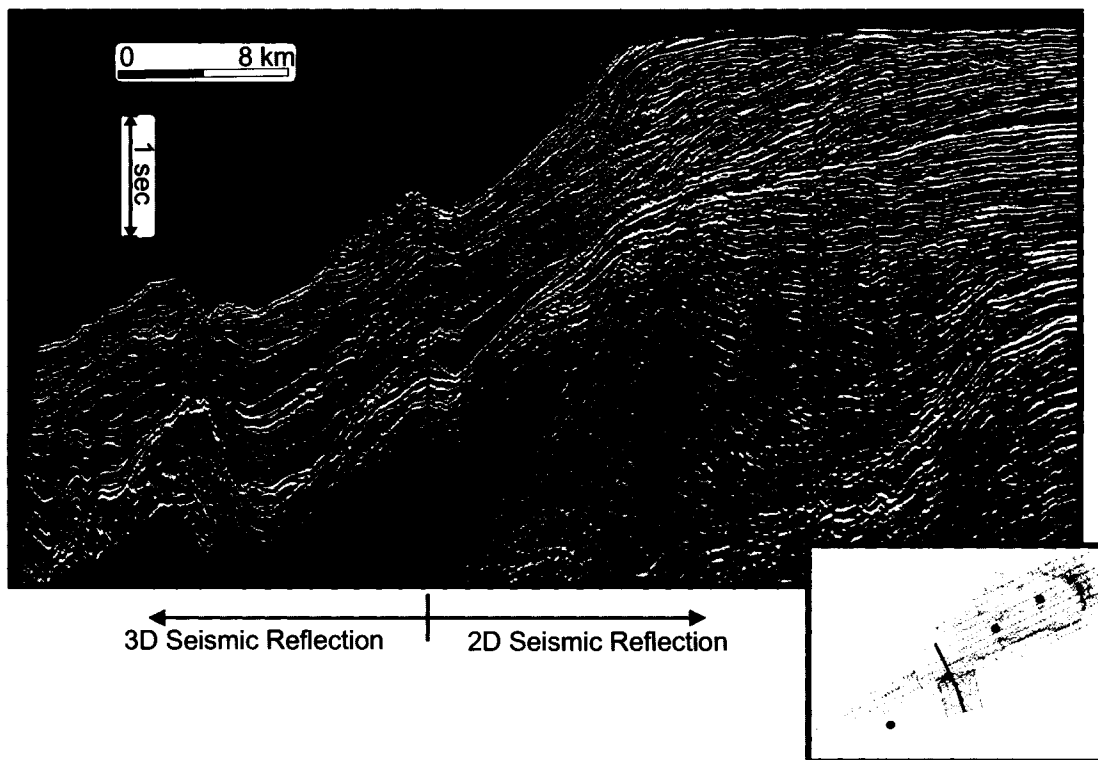


Figure 4.3. Multichannel seismic and 3-D seismic reflection profile stitched together from the outer shelf to slope in the central portion of the study area with all five sequence boundaries identified and internal reflection geometries interpreted in relation to sequence boundaries.

4.2.3 Sequence 2

Sequence 2 is recognized on the outer paleo-shelf and across the slope. On the outer paleo-shelf, Sequence 2 is a series of seaward dipping reflections that are downlapping and laterally migrating from the outer paleo-shelf to the upper slope (Figure 4.2). On the outer paleo-shelf, internal reflections of Sequence 2 are gently downlapping oblique reflections which migrate out as far as the upper slope. On the upper slope, an onlapping succession of aggrading reflections is recognized, with Sequence 2 onlapping Sequence Boundary 1 (the C10 reflection) at the paleo-shelf break. Downslope, internal reflections lap out or become unresolved in seismic profile in the lower slope. Sequence 2 reflections on the slope form a wedge-shape geometry of aggrading reflections onlapping the paleo-shelf break (Figure 4.2). In the middle to lower slope, the E20 reflector is recognized internally as a draping horizon over a mound of reflectors that offlap Sequence Boundary 1 in the middle slope, and then lap out on Sequence Boundary 1 in the lower slope (Figure 4.3). The E20 reflection is widely eroded and difficult to define across the slope and outer paleo-shelf. However, it separates two seismic reflection styles in Sequence 2, although it is not defined as a sequence boundary. It is discussed later in this chapter.

Paleochannels incise Sequence 2 in the upper slope and at the paleo-shelf break. On the outer paleo-shelf and upper slope, paleochannels are recognized and in some instances have removed Sequence 2 entirely. Stratigraphically, the outer paleo-shelf reflection geometry of Sequence 2 would suggest a regressive coastal margin setting. Sequence Boundary 2, the O30 reflection, unconformably cuts Sequence 2 on the outer paleo-shelf

and paleo-slope. In some instances Sequence 2 is completely removed (at this level) on the upper slope and outer shelf. On the upper slope, Sequence Boundary 2 cuts through Sequence 2 into Sequence 1 at the paleo-shelf break. Paleochannel incision across the outer paleo-shelf and upper slope is correlative with the onset of Sequence Boundary 2 and the change into Sequence 3.

4.2.4 Sequence 3

Sequence 3 is recognized on the outer paleo-shelf and across the slope. Upper slope and outer paleo-shelf reflections are aggradational and onlapping along Sequence Boundary 2 (Figure 4.2), forming a wedge geometry on the upper slope. Similar to Sequence 2, on the outer paleo-shelf, gently downlapping oblique reflections are recognized, as well as similar onlapping and aggrading reflections on the slope (Figure 4.2). In the lower middle and lower slope, intervals of incoherent and irregular reflections are recognized interbedded with smooth and continuous internal reflections (Figure 4.4). Across the slope, Sequence Boundary 3 (the M40 reflection) marks a distinct change in seismic character. The Sequence Boundary 3 reflection unconformably cuts the paleo-upper and paleo-middle slope, and conformably overlies the paleo-outer shelf. The transition from Sequence Boundary 3 to Sequence Boundary 4 is gradual on the outer paleo-shelf with Sequence 3 and Sequence 2 converging up dip towards the coastal margin.

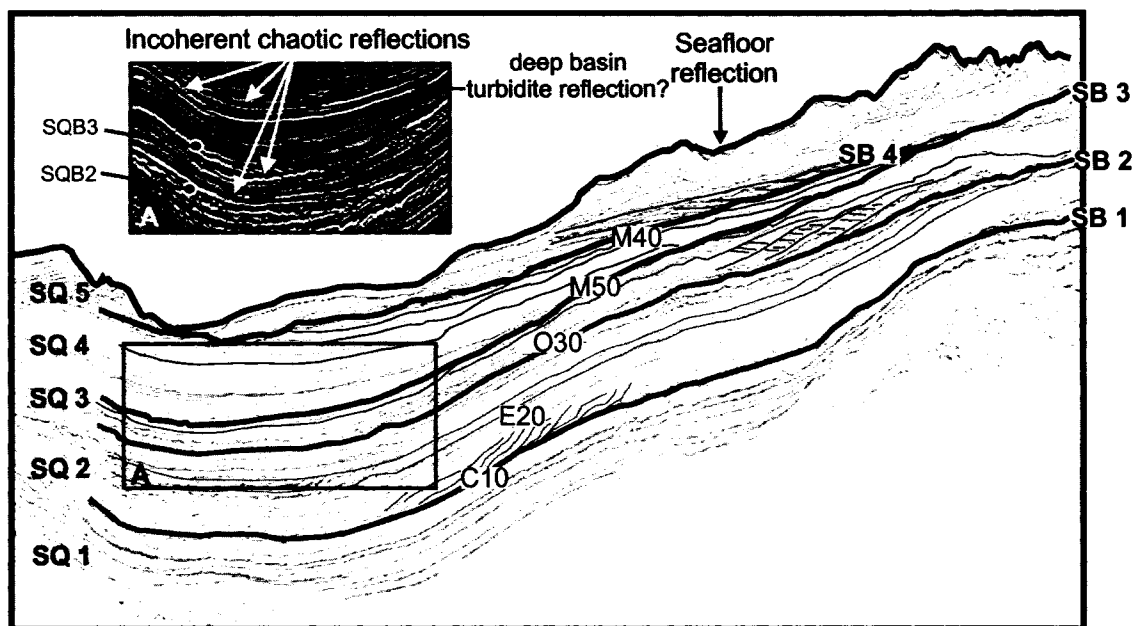
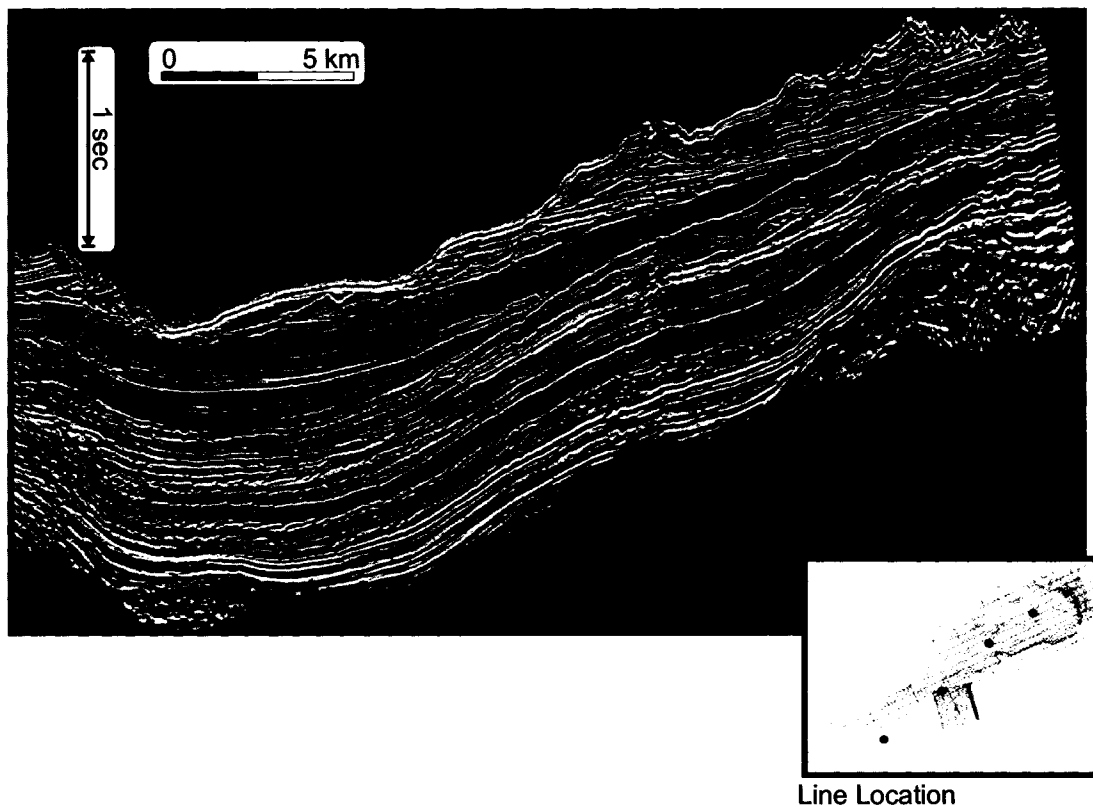


Figure 4.4. 3-D seismic reflection profile of the slope in the northeastern part of the study area, with sequence boundaries identified and internal reflection geometries interpreted in relation to sequence boundaries. (A) Packages of incoherent reflections on the lower slope.

4.2.5 Sequence 4

Sequence 4 is recognized on the outer paleo-shelf and across the slope. Reflections on the outer paleo-shelf are oblique and gently downlapping. On the slope, reflections are aggrading and onlapping on the upper slope face. The lower slope package of onlapping reflections is interrupted by smaller packages of incoherent and irregular reflections (Figure 4.5). Sequence Boundary 4 (the M50 reflection) is an unconformable horizon cut by paleochannels on the outer paleo-shelf and upper slope. Sequence Boundary 4 is not well imaged on the paleo-shelf break but is seen onlapping Sequence Boundary 3 on the uppermost slope.

4.2.6 Sequence 5

Sequence 5 is recognized on the outer paleo-shelf and across the slope. On the outer paleo-shelf to upper slope, Sequence 5 is dominated by paleo-channel incision and erosion. In the middle and lower slope, Sequence 5 consists of a series of stacked packages of irregular to incoherent reflections indicative of mass transport deposits (MTD) (Figure 4.5) (Mosher et al. 1994; Piper and McCall 2003). Seismo-stratigraphic geometries on the outer paleo-shelf and slope are similar to the previous three sequences, with stacked aggradational reflections onlapping the middle to lower slope. However, in multichannel seismic reflection profiles, a shelf edge prism with low amplitude reflectors and poor continuity is seen as downlapping the outer paleo-shelf and the upper slope (Figure 4.3). In the middle to lower slope, stacked packages of incoherent reflections

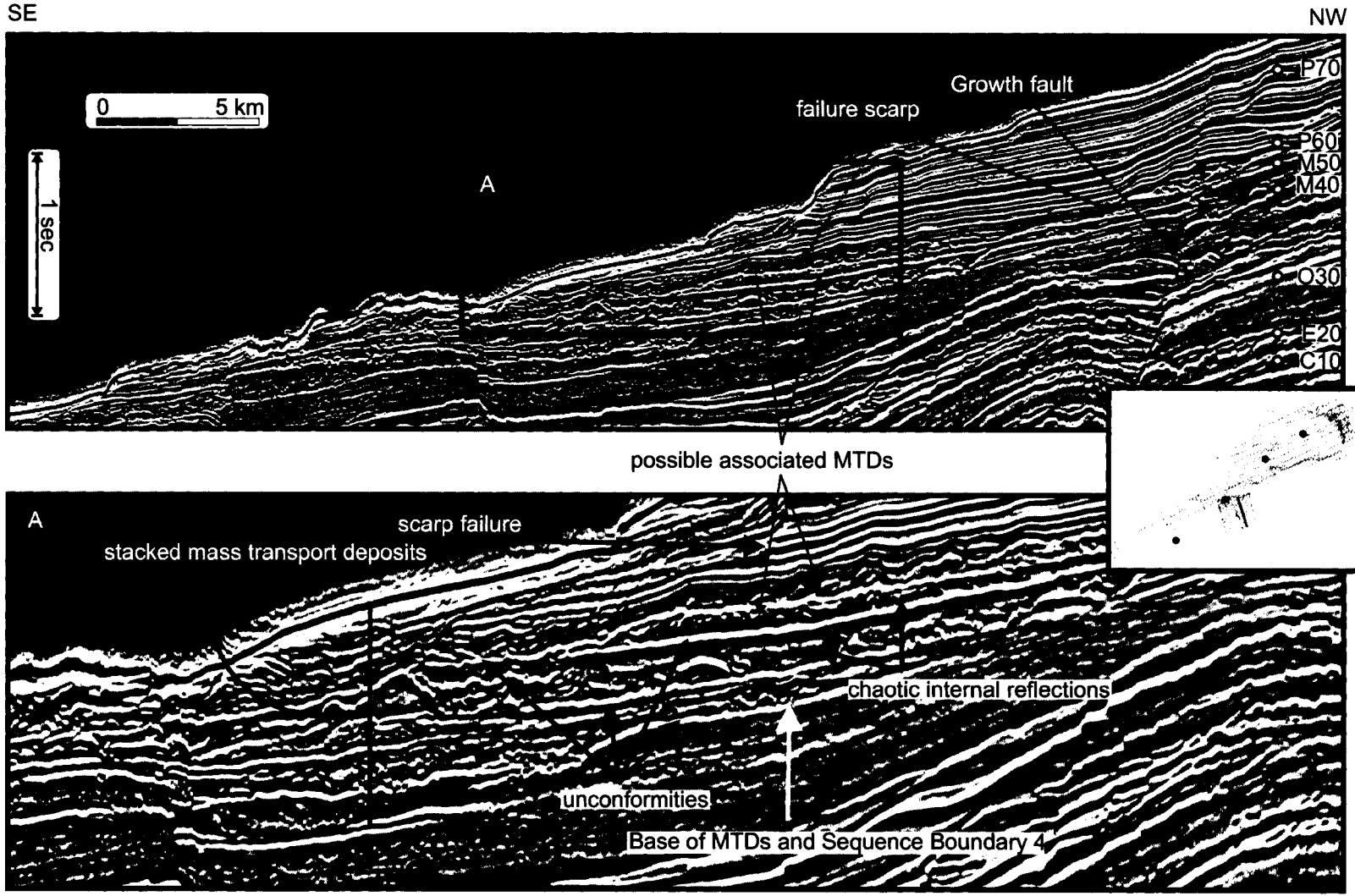


Figure 4.5. 3-D seismic reflection profile from the middle to lower slope, showing stacked packages of incoherent reflection interpreted as reoccurring mass transport deposits (MTDs) in Sequence 5.

from multiple MTDs are recognized. The confining upper sequence boundary of Sequence 5 is defined on the slope and outer shelf as the seafloor reflection.

4.3 Discussion

Five sequences and correlative sequence boundaries are recognized in this study. Each sequence boundary represents a major change in sea-level in the Cenozoic section. Although the stratigraphic element is identified independently of any assumptions concerning sea-level, interpretation of the timing and nature of slope deposition requires inferences related to sea-level, sea-level change and oceanographic processes.

Although five sequences are identified and discussed herein, it is recognized that within each of these five major sequences, other smaller sequences are recognized (Figure 4.6). Sea level change does not have the same effect on each of the five sequences. Major sequences discussed above and below are considered as representations of deposition related to major sea-level cycles during the Cenozoic. With a decrease in relative sealevel each sequence has likely gone through falling stage system tract (FSST) as they moved into a lowstand system tract (LST), as well as transgressive system tract (TST) with the raising of sea-level, which culminates with a maximum flooding surface (MFS) into a highstand system tract (HST) before the sea-level lowers again. Major unconformities also affect the interpretation of sequence stratigraphy. Hiatuses in stratigraphic successions have removed complete or near complete system tracts, truncating unconformities and correlative conformities. Figure 4.6 shows an interpretation of system

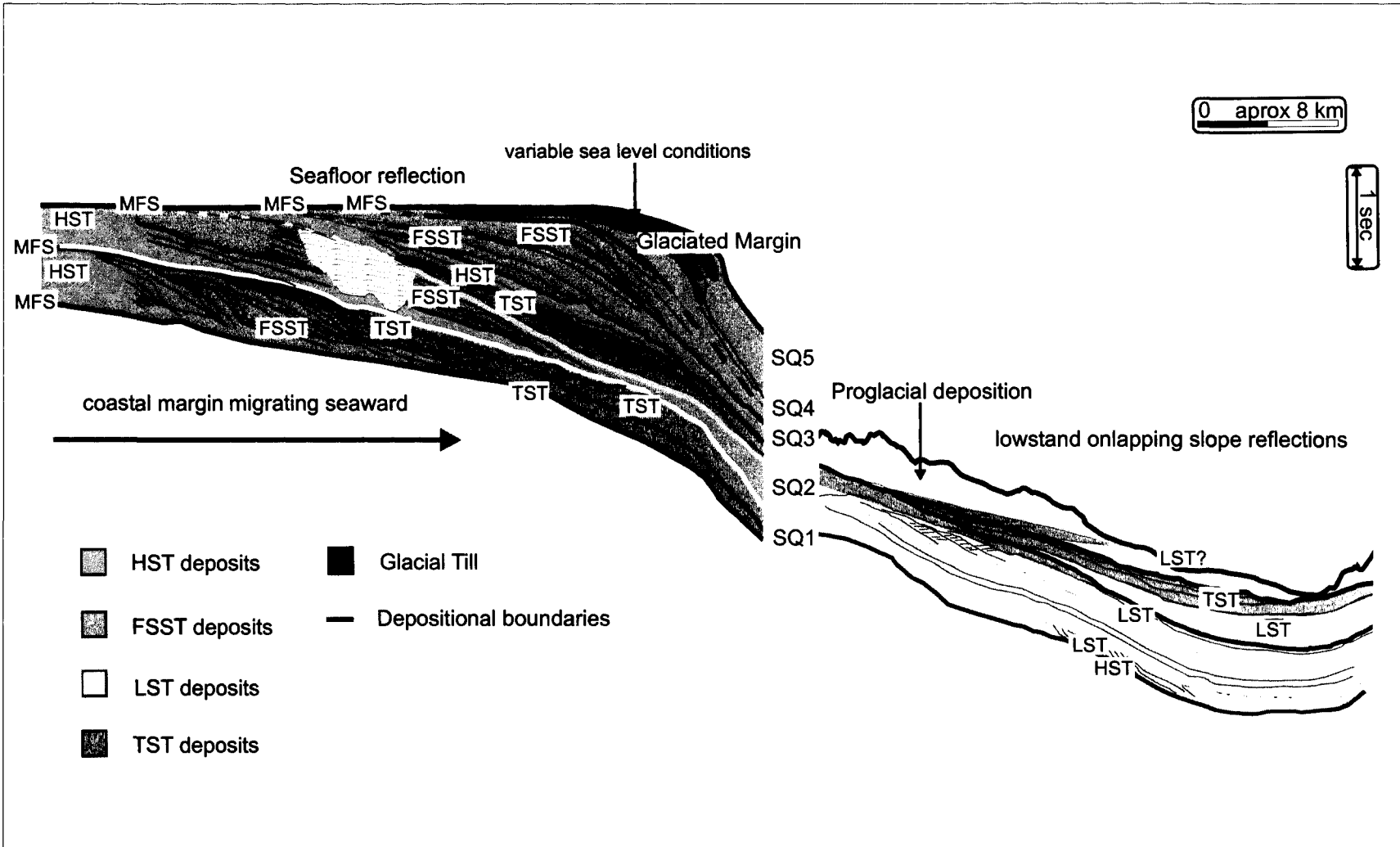


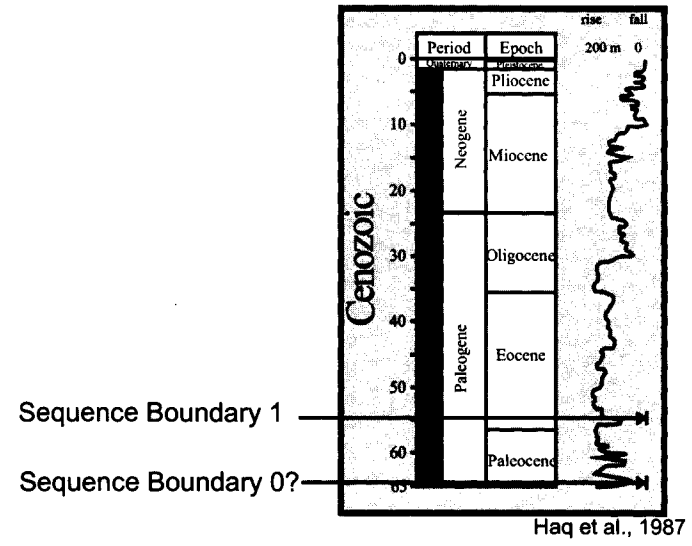
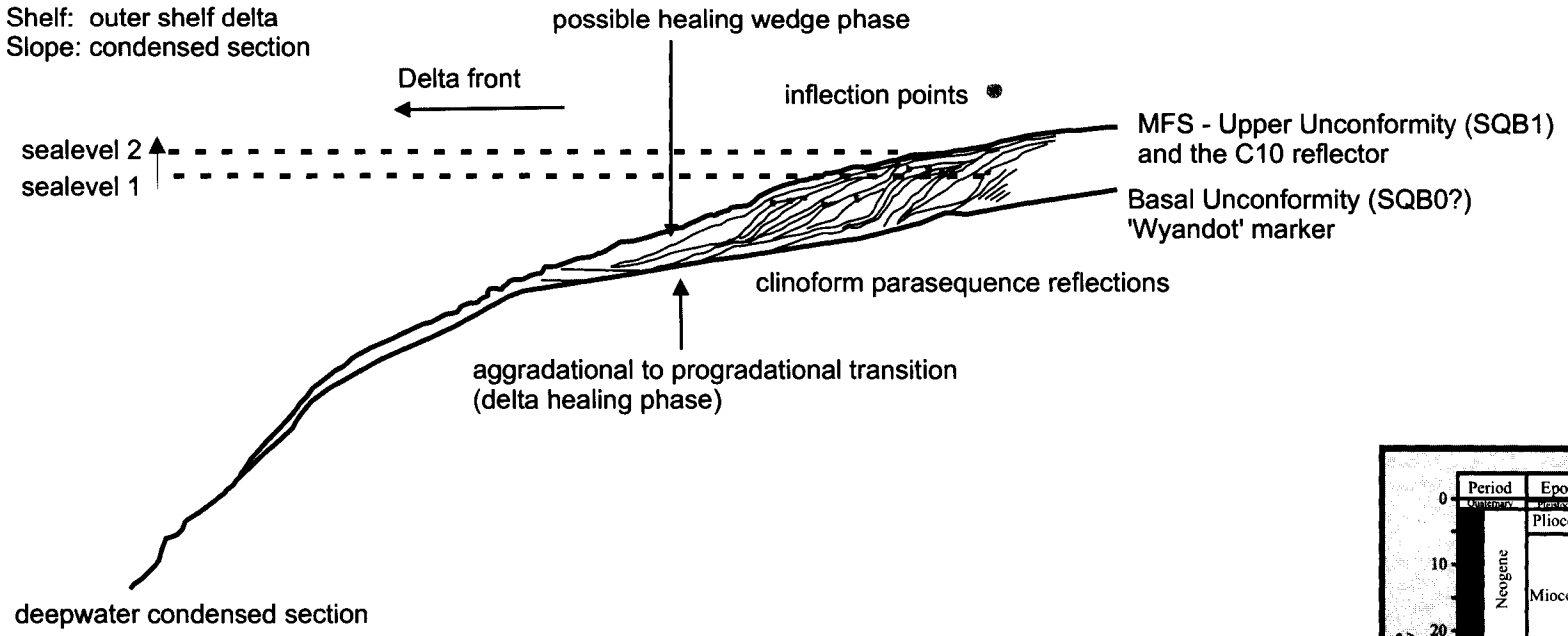
Figure 4.6. An alternative interpretation of sequence stratigraphy in the outer shelf to slope with many sub-sequences not fully addressed in this study.

tracts within the large scale sequence stratigraphy of Figure 4.2, where TST are placed above LST and MFS above TST. Any FSST would have to take place after a HST and be followed by a LST. Assumptions can be made on the development of facies in each system tract in relation to the reflection geometry and the amplitude of sea level change.

Sequence 1 ranges from the latest Cretaceous (Wyandot marker) to the Early Eocene (C10). The reflection geometry of Sequence 1 on the outer paleo-shelf is interpreted as an outer shelf delta (Figure 4.7). The lower bounding surface, the Wyandot marker (Sequence Boundary 0), is a chalky horizon (Wade et al. 1995) correlative to a maximum flooding surface on the eastern Canadian continental margin. Outer shelf deltas landward of the paleo-shelf break are characteristic of highstand or falling stage systems tracts. The depths of inflection points suggest fluctuating sea level, possibly creating an overprint of several small order sequences. Similarly, condensed deepwater sections consisting of the upper and lower bounding surfaces of an outer shelf delta are also characteristic of a highstand system tract. Reflection geometry in the outer shelf delta succession indicates a complex sea-level history with three or more periods of delta progradation with sea level rises and falls. Sequence Boundary 1 (Figure 4.7) represents a relative unconformity directly above the outer shelf delta succession and a change in sedimentation. The general change reflection geometry from downlapping clinoforms Sequence 1 to very low angle downlapping reflections of Sequence 2 on the shelf and slope is the basis for recognizing Sequence Boundary 1 and the change to Sequence 2.

Sequence One:

Shelf: outer shelf delta
Slope: condensed section



Haq et al., 1987

Figure 4.7. Reflection geometry of Sequence 1 (Figure 4.2), showing prograding reflections of the outer shelf delta and its coeval condensed section on the slope. Possibly forced regression of the delta front due to sea-level fall marks the Early Eocene upper boundary (C10) of the sequence.

Sequence 2 spans from the Early Eocene C10 reflection (Sequence Boundary 1), to the Late Oligocene O30 unconformity (Sequence Boundary 2). The change to Sequence 2 is marked by a change in reflection geometry on the slope to an onlapping and toplapping sequence of reflections typical of a lowstand system tract (Figure 3.2). On a 3-D surface render of the base of Sequence 2, seismic amplitude shows well defined submarine fan morphology on the upper slope (Figure 4.8). With increased sediment delivery to the slope in the early stages of Sequence 2, the Scotian Slope became a deepwater depocenter for submarine fans and turbidite flows. Submarine fans are deposited in deep marine settings (>800 meters), including slope basins (Bouma 1969; Deptuck 2003). With the fall in sea level, the regime of sedimentation on the shelf and slope changed. The E20 reflection, Sequence 2 internal reflection on the slope, is a sub-sequence boundary possibly related to an Early Eocene lowstand and the onset of a TST in the middle to late Eocene (Figure 4.8).

Sequence Boundary 2 corresponds to the O30 reflection, which is recognized as a hiatus event that removed great amounts of sediment on the outer shelf and slope during the middle to late Oligocene, eroding down as far as the middle Eocene strata. Sequence Boundary 2 truncates internal reflections of Sequence 2 and is often correlated, in this study, to complete packages of missing Oligocene strata at the paleo shelf break and upper slope. Further landward on the inner shelf, however, the O30 reflection is dated at the Onondaga E84 well site as middle Late Oligocene (MacLean and Wade 1993). This age constraint could not be applied at the other wellsites due to the absence of biostratigraphic data.

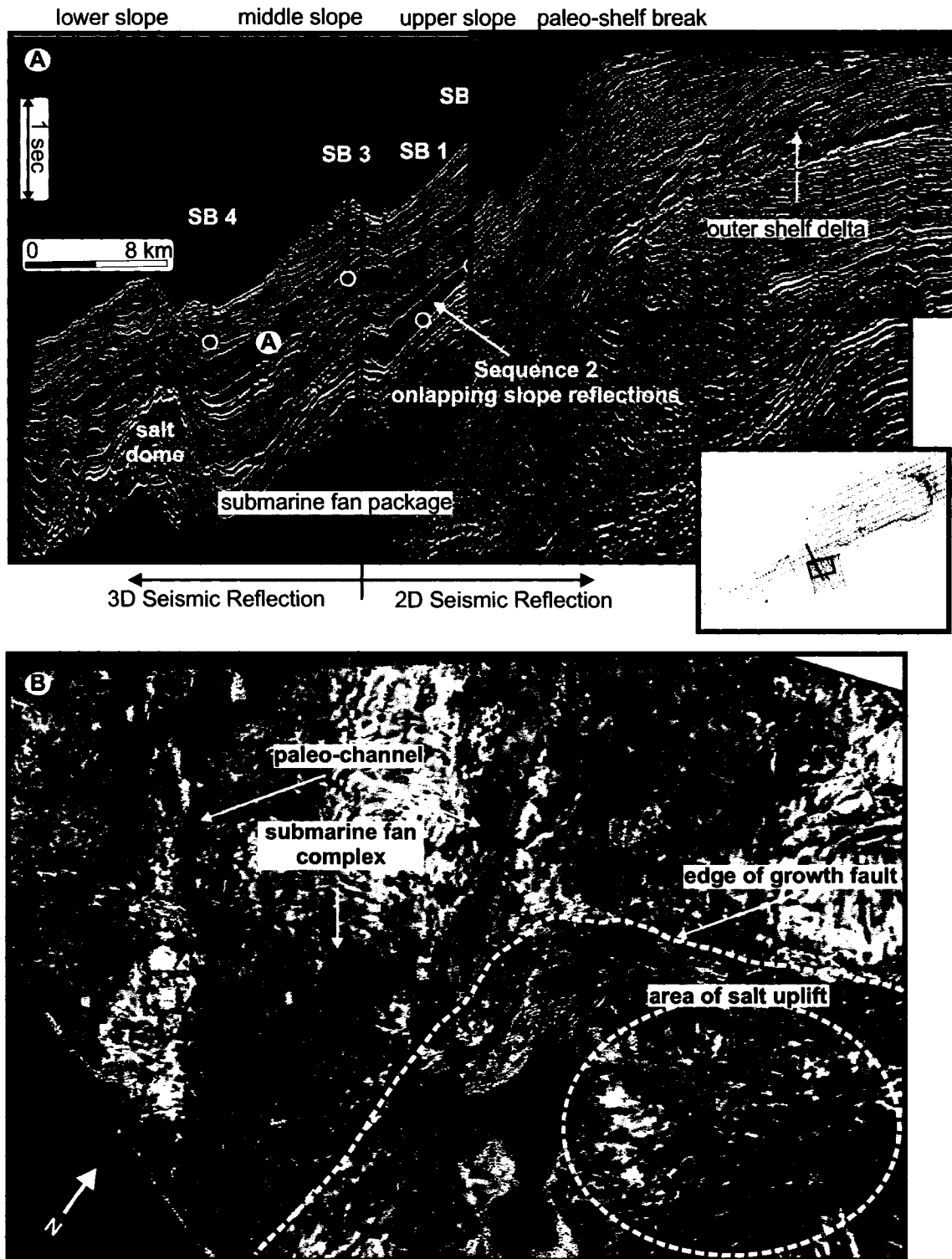


Figure 4.8. (A) Submarine fan complex in relation to sequence boundaries in seismic profile. (B) Amplitude surface extraction of Sequence Boundary 1 (C10) showing the base of the fan complex with high amplitude paleo-channel fill and lower amplitude over channel deposits. Note: Blue = high amplitude, Yellow = lower amplitude

Pronounced paleo-channel incision is observed below Sequence Boundary 2 on the outer shelf and upper slope (Figure 4.9). Sequence Boundary 2 marks the end of the middle Oligocene erosion, and the end of sediment bypassing on the outer shelf and slope. With such a large hiatus through the middle Oligocene, indications of a LST or a transition period between Sequence 1 and Sequence 2 are not recognized on the slope or outer shelf in the seismic reflection geometry. However, in the seismic reflection profile across the Onondaga E84 well site on the inner shelf, the O30 reflection is directly followed by a sequence of prograding shelf margin reflections. This pattern suggests that erosion during the hiatus was greatest at the shelf break and upper slope while a HST or FSST was developing on the inner shelf during the late Oligocene.

Sequence 3 is confined between the O30, Sequence Boundary 2, and M40 Sequence Boundary 3 reflectors. Sequence Boundary 3, is an unconformable surface on the paleo-slope, but a conformable surface on the paleo-outer shelf (Figure 4.2). Paleochannel incision on the outer shelf and upper slope in Sequence 3 was the result of another relative lowering of sea-level.

Gently dipping and seaward migrating reflections of Sequence 3 on the outer shelf are typical of a HST or FSST. Reflection geometry of the paleo-slope, indicates a “lowstand wedge” of onlapping reflections aggrading upslope towards the shelf break (Figure 4.10), which are more consistent with a FSST. The outer shelf reflections of Sequence 3 prograde out to the shelf edge and downlap the TST above the lowstand wedge (Figure

Sequence Two:

Shelf: Shelf margin progradation
Slope: Onlapping Stacked reflections and gravity flows

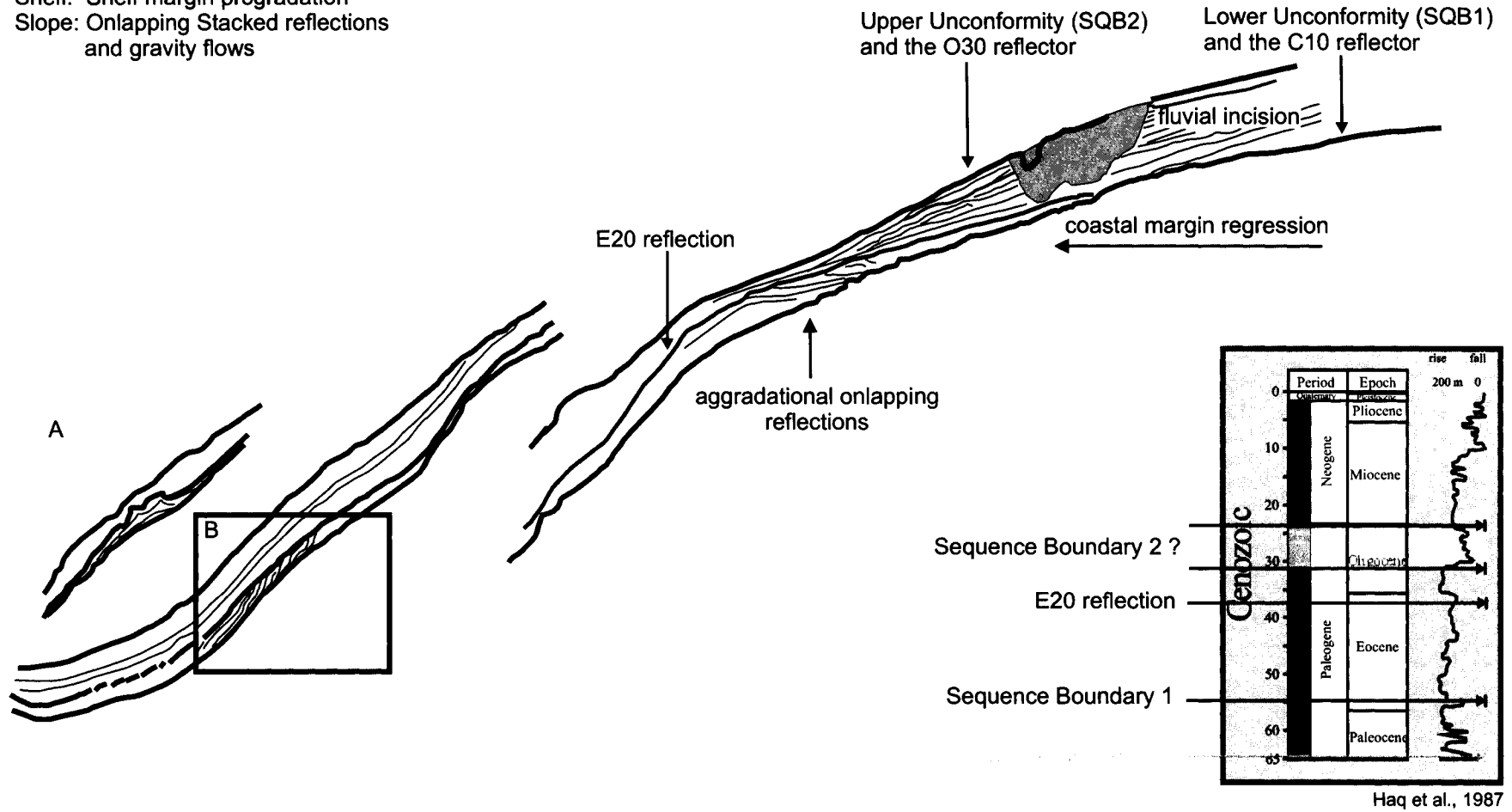


Figure 4.9. Reflection geometry of Sequence 2 (Figure 4.2), shelf margin regression and paleo-channel incision. On the slope, reflections, onlap the upper slope and thin seaward. A) sub-marine fan seen in Figure 4.8. B) central part of the study area in the same bathymetric setting as the sub-marine fan, but with more clinoform reflection geometry (inset).

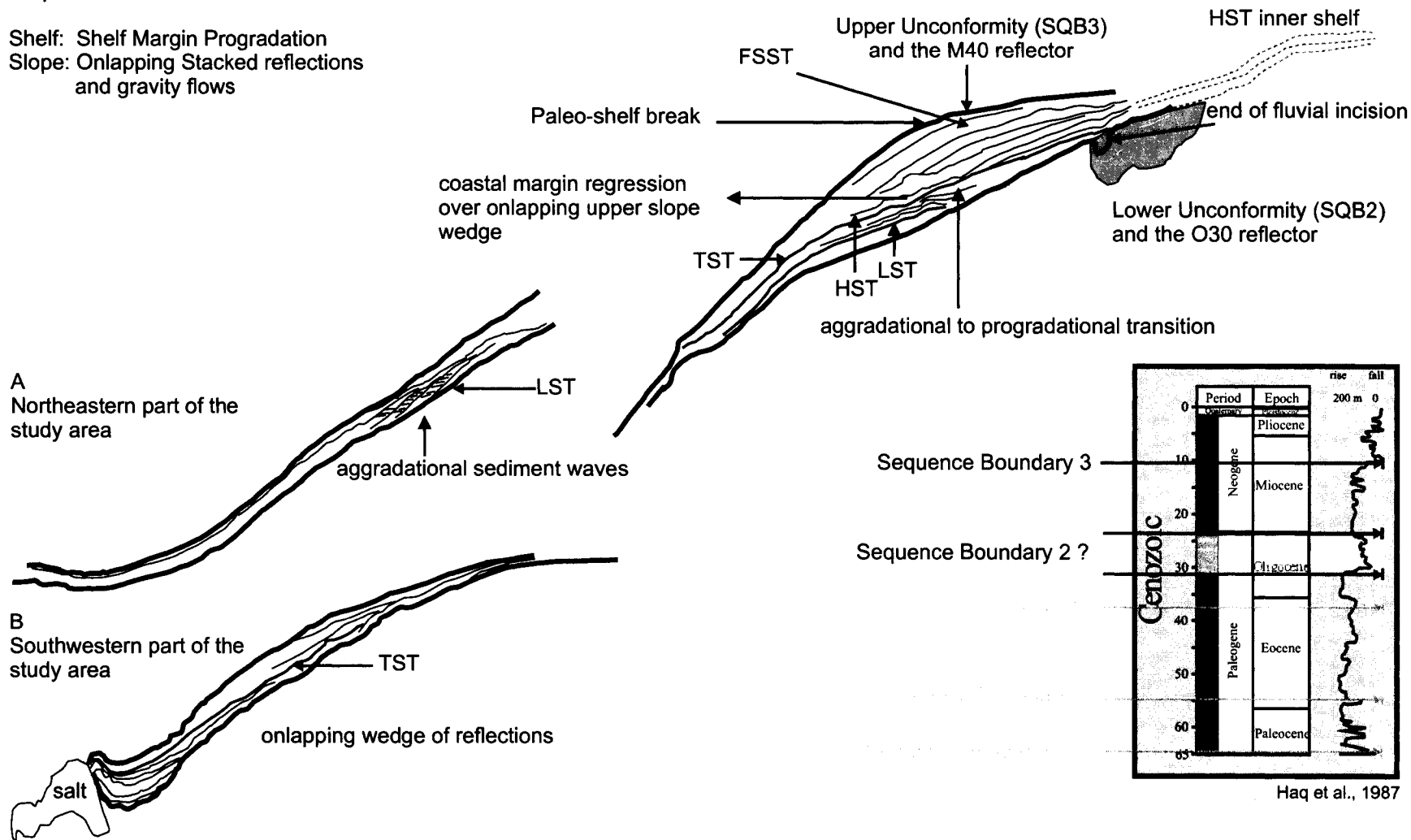
4.10). Sequence 3 forms a complete sequence stratigraphic succession. LST aggrading reflections on the paleo-slope transition into a TST recognized on the upper slope and paleo-outer shelf. A FSST migrates over the TST late in Sequence 3 before moving into the TST in the end of Sequence 3 (Figure 4.10).

Compared to Sequence 3 and Sequence 2, Sequence 4 forms a thinner package of oblique downlapping reflections on the paleo-outer shelf. Sequence 4 is more tightly constrained to late Middle to Late Miocene times. Outer shelf FSST reflections in Sequence 4 are steeply dipping and form a shelf margin wedge (SMW) (Weimer and Posamentier 1993). On the lower paleo-slope, onlapping reflections form a lowstand wedge, where as the upper slope is a zone of sediment bypass (Figure 4.11). This pattern could be the result of the onset of North Atlantic currents sweeping across the paleo-outer shelf and the upper paleo-slope. Evidence of paleo-channel incision on the upper paleo-slope is minor and indicative of some sediment bypass through channel flow in Sequence 4. Surface amplitude extraction of Sequence Boundary 4 (M50), shows slope trending parallel striations on the upper to upper middle paleo-slope, which will be discussed in more detail in the next chapter.

Sequence 5 is constrained by the lower Sequence Boundary 4 (M50), and the seafloor reflection boundary (SRB). Most of this section on the central Scotian Slope has been cut by erosion from shelf crossing glaciation in the Pleistocene. However, below the reflector dated as mid Pliocene (P60), a 3-D time surface render shows paleo-seafloor morphology with broad shallow canyons and dendritic low lying ridges onto the lower slope. Above

Sequence Three:

Shelf: Shelf Margin Progradation
 Slope: Onlapping Stacked reflections and gravity flows



Haq et al., 1987

Figure 4.10. Reflection geometry of Sequence 3 (Figure 4.3), showing a relatively complete sequence stratigraphic succession of coastal margin regression FSST over upper slope reflections of the LST and TST. A) sediment waves in the upper to middle slope. B) Onlapping reflections on the upper to lower slope.

Sequence Four:

Shelf: Shelf Margin Progradation
 Slope: Onlapping Stacked reflections on the slope

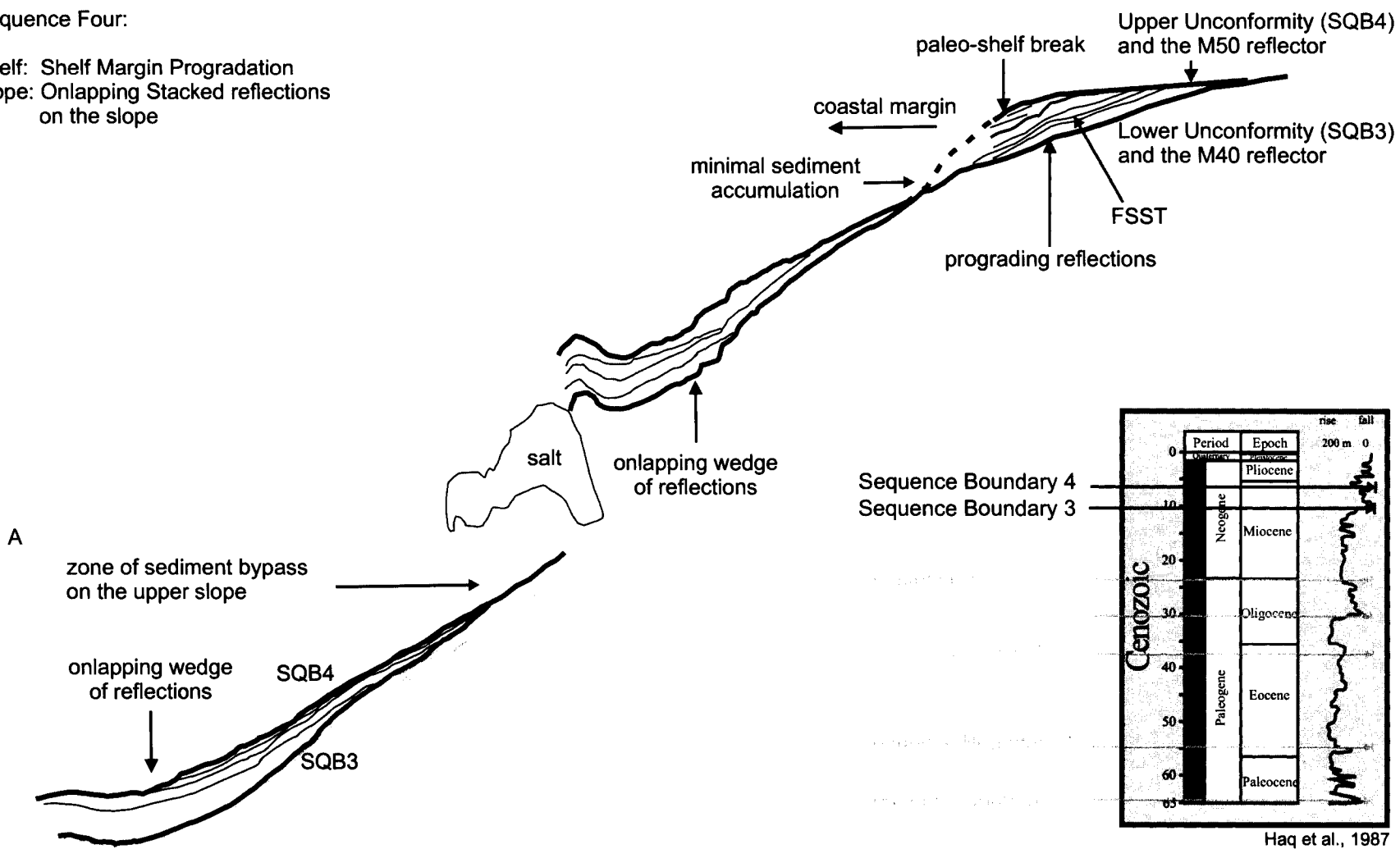


Figure 4.11. Reflection geometry of Sequence 4 (Figure 4.3), indicating a wedge of reflections onlapping the middle lower paleo-slope and downlapping reflections on the paleo-outer shelf in close proximity of the shelf break, forming a shelf margin wedge. A) Sequence Boundary 4 onlapping Sequence Boundary 3 on the upper paleo-slope.

Sequence Boundary 4 and below the P60 reflection, a period of mass transport deposition occurred on the middle to lower paleo-slope (Figure 4.5). Mass transport complexes (MTCs) are commonly cited as basal units in a stratigraphic cycle (Weimer 1991; Beaubouef and Freidman 2000), and the onset of a new sedimentary cycle is often defined by the lowest surface of the mass transport deposit (MTD). This corresponds to Sequence Boundary 4 and the basal reflection of the LST in Sequence 5. The previous three sequences (4, 3 and 2) had aggradational reflections of a typical lowstand wedge on the middle to lower paleo-slope, which preceded the HST - FSST recognized by outer paleo-shelf progradation. In Sequence 5, outer paleo-shelf prograding reflections are generally of low amplitude and poor continuity. Onlapping paleo-slope reflections of the LST are limited to the lower paleo-slope and the lowest portion of Sequence 5 (Figure 4.12).

Reflections above P60 are paleo-slope draping reflections. Through the middle to late Pliocene, the paleo-slope went through numerous FSSTs and HSTs. Periods of HST in the middle to late Pliocene likely correspond to periods of rare MTDs on the paleo-slope and to the building of the outer paleo-shelf edge. During LST, the paleo-shelf edge likely became unstable due to the increased sediment load and gravitational stresses.

In the latest section of Sequence 5, during the latest Pliocene through the Pleistocene, shelf-crossing glaciation created an environment dominated by proglacial fluvio-deltaic and glacio-marine deposition (King and MacLean 1976; Piper 1988; Pickrill et al. 2001). This section represents approximately the upper 100-200 meters of section below the

Sequence Five:

Shelf: Glacial fluvial deposition and erosion
 Slope: Proglacial fluvial deposition and erosion

shelf edge prism at modern day
 shelf break with reflections
 downlapping onto the upper slope

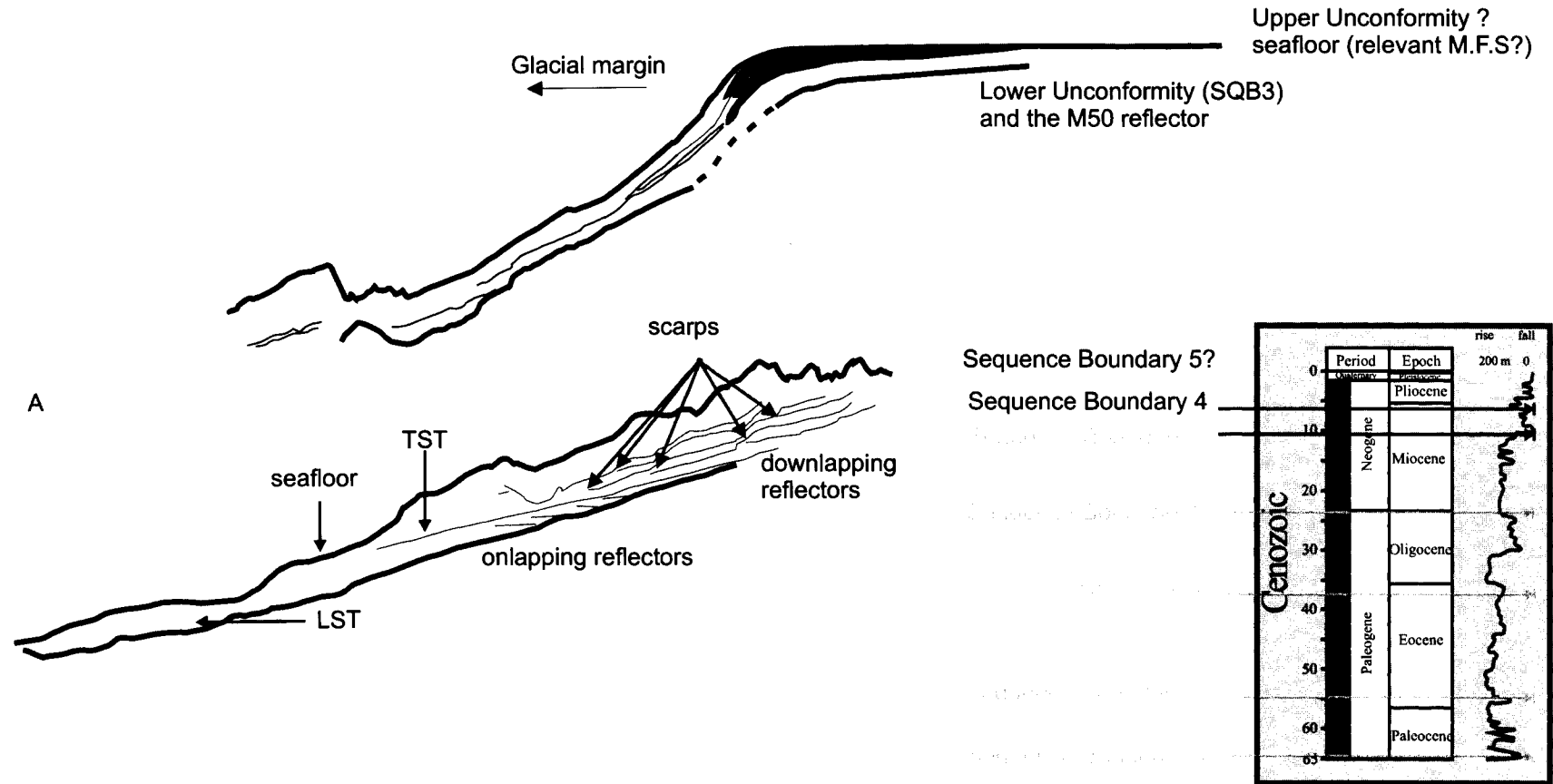


Figure 4.12. Reflection geometry of Sequence 5 (Figure 4.3), showing complexity of onlapping / downlapping reflections of the paleo-slope in response to glacial influence. (A) scarps and associated erosional horizons.

SRB (Piper et al. 2002). On the outer paleo-shelf, downlapping reflections are replaced with an outer paleo-shelf wedge of glacial till, typical of glaciated margins (Fader 1991; King et al. 1991). Generally, Sequence 5 is dominated by early lowstand deposition on the paleo-slope followed by erosion, which removed Pliocene strata and which was then followed by pro-glacial slope draping.

4.4 Stratigraphic Relationships to Salt Mobility

Periods of salt mobility are recognized to have affected the stratigraphic architecture in this study. Each sequence discussed previously in this chapter is represented by a unique stratigraphic element related to the mode of deposition and to sedimentation rates. Evidence for salt tectonics in this study are recognized in stratigraphy as fault offsets above and around salt diapirs, pull-ups, top collapse and flanking subsidence. Seismic reflection data show structural reorganization through the Cenozoic section. An attempt is made to identify the timing of these events and their relationship to the five sequence stratigraphic units.

4.4.1 Sequence 1

Deposition in the Paleogene to Early Eocene (Sequence 1) was minimal as a high sealevel restricted sedimentation on the slope. Deepwater condensed reflections of Sequence 1 onlap salt diapirs, passing through salt withdrawal basins in the middle and lower paleo-slope (Figure 3.11). The recognition of Sequence 1 reflections onlapping a

salt diapir indicates that salt tectonics and minibasins were active in the area of the lower paleo-slope before the Cenozoic Era.

Sequence 2

In salt withdrawal basins on the middle to lower paleo-slope (Figure 4.3), Sequence 2 deposition generally consisted of onlapping and laterally aggrading reflections typical of a lowstand wedge. Lowstand wedge reflections are not recognized outside of salt minibasins. This result suggests that sedimentation was preferential to the minibasins during the LST of Sequence 2. Reflection onlap and pull-ups, due to frictional drag along diapir edges, are recognized in Sequence 2, increasing up-section towards Sequence Boundary 2. Pull-up reflections along the salt flanks between the C10 and O30 reflections suggest that the salt diapirs rose upward from the Early Eocene to the Late Oligocene. On each side of the minibasin, growth faults offset strata. On the lower paleo-slope, above the salt tongue, sediment overburden is minimal. A thin section beneath the O30 reflection implies that the salt tongue may not have been fully in place until near the end of Sequence 2.

4.4.2 Sequences 3 and 4

In Sequence 3, which encompasses the middle Oligocene (O30) to the end of the Middle Miocene (M40), stratigraphic architecture suggests that a salt tongue was already fully in place on the lower paleo-slope. A sediment drift package above the salt tongue suggests

that the salt high was in place by the middle Oligocene (O30) and that preferential conditions may have been created for drift packages to form along the lower paleo-slope in the Late Oligocene to Early -Middle Miocene. In the Middle Miocene, minibasins filled until the Late Miocene (Figure 4.3), at which time they were completely filled. Increased offset of minibasin growth faults are recognized, typically with an increasing normal offset up section. No stratigraphic alterations related to salt minibasins are recognized in Sequence 4. However, both Sequence 4 and Sequence 3 reflections are bent upwards towards the dome crest and faulted near the salt dome apex (Figure 4.11). The general geometry of stratigraphy from M40 to M50 suggests that a considerable seafloor relief feature was present during the Miocene, with packages of reflections thinning towards the crest on both sides of the salt high. Seaward of the salt dome, above the salt tongue, Sequence 4 and 3 reflections are uplifted and tilted seaward and incoherent reflections are recognized on its up-dip side.

4.4.3 Sequence 5

Sequence Boundary 5 (M50) truncates uplifted strata at the dome crests above salt highs. Internal reflections in Sequence 5 are relatively absent above salt domes and are offset by minibasin growth faults, which commonly have a seafloor expression.

5. Facies types

Seismic facies analysis is the recognition of distinctive packages of reflections and their reflection characteristics (Brown and Fisher 1980). Integration of facies units into a seismic stratigraphy framework is to recognize distinct stratigraphic units that correspond to a distinct depositional process. Within these packages, separated by bounding surfaces, reflection characteristics such as geometry, continuity, amplitude, frequency, external form and three-dimensional associations can be used for the interpretation of depositional environments and processes, sediment transport direction and lithology (Mitchum et al. 1977b; Roksandic 1978; Brown and Fisher 1980). Reflection continuity is interpreted to correspond to continuity of strata and the reflection amplitude to the contrast in lithology (Mitchum et al. 1977b). Geometry of reflections can be subdivided into packages of reflections composing a unit or seismic “package” of reflections. Commonly, in this study, reflection geometry is described as parallel (concordant), sub-parallel (discordant), divergent, progradational, aggradational, sigmoidal (shelf margin progradation), reflection-free, incoherent or chaotic. The external morphology and three-dimensional character of seismic packages is described as sheets, lenses, mounds, wedges or drapes (Mitchum et al. 1977b). Geologic interpretation made by integrating the facies units to seismic sequences allows respective inferences to be made on depositional systems, paleo-environments, facies boundaries, paleo-shelf edges and other stratigraphic features (Brown and Fisher 1980).

Within the study area, 9 facies are identified from 2-D and 3-D seismic reflection data. These facies are distinguished by the overall reflection character and geometry of the facies unit in seismic reflection data. Reflection amplitude strength, continuity and location within the above and below stratigraphy altogether helped defining these facies.

5.1 Outer Shelf Deltas

Outer shelf deltas are depositional systems which result from a river flow entering the unconfined marine environment. Outer shelf deltas in the study area are identified by a characteristic parasequence of oblique, prograding clinoform reflections that are tangential to parallel reflections onto a lower bounding reflector (Cummings, 2004). In strike section, reflection characteristics differ by showing parallel to sub-parallel reflections forming a large mounding geometry. The geometry of outer shelf deltas in dip section is described as an outer shelf wedge of internally dipping reflectors (Figure 4.8). Seaward to the outer limits of the wedge, a smaller wedge of incoherent reflections may be present. This feature is interpreted to be a healing wedge formed at the transition period between one sedimentary sequence and the next (Figure 4.7).

3-D seismic reflection coverage is limited to the slope, and information on the 3-D geometry of the deltas is therefore limited to 2-D seismic reflection interpretation.

5.2 Submarine Fans

Submarine fans are deep-water morphological features that are deposited at the end of submarine channels or canyons, and that form as a result of turbidite flow deposition. In seismic sections, this facies consists of offlapping sub-parallel reflections forming small (<10 km) or broad (>10 km) lenses or mounds downslope from an incised channel and/or canyon (Deptuck 2003).

Two types of fans are recognized within the study area: immature fans and mature fans, following the terminology of Deptuck (2003). Immature fans are small, high gradient fans with low sinuosity channels, well developed lobes, and a high sand to mud ratio (Deptuck 2003). Mature fans are large, low gradient fans with low sand to mud ratio and sinuous channels. These fans are better characterized by sheet deposits (sands or other) and lobes rather than the mounds of immature fans.

Typical acoustic characters of immature submarine fans within the study area are subtle to large mounds of moderate to high amplitude reflections. Internal acoustic character varies from incoherent to well defined dipping reflections. In 3D amplitude surface renders, high amplitude values in sinuous, braided or coalescing patterns over fan lobes are interpreted as paleo-channels feeding the submarine fan complex (Figure 4.8) and are inferred to be the seismic expression of a more sand-prone facies. The paleo-channels form a immature fan system downslope. Apparent channel deposits have higher amplitude than the apparent overbank deposits, inferred to have lower sand to mud ratios.

In the lower slope, high amplitude anomalies are recognized with variable geometric character. These deposits demonstrate a more sheet-like geometry, and have a high amplitude central area with a rimming moderate amplitude response (Figure 4.8). In 2-D seismic reflection profiles, these mature fans are recognized as large (<10 km), low gradient lobes in strike section, and as relatively flat-lying reflections in dip section. Paleo-channels and associated overbank deposits occur on fan lobes as the submarine fan evolves. Figure 5.1 illustrates a submarine fan complex that may have levee deposits on it. However, the shape geometry of levee wedges is not directly obvious, and it is interpreted as a submarine fan complex with multi-staged growth.

5.3 Paleo-Channels

Paleochannels are common in slope environments. In 2-D seismic reflection data, paleochannel geometry is defined by high amplitude seismic reflections that imply coarser grained sediment in channel fills, and a strong acoustic impedance contrast at the erosional boundaries of the channel walls. Characteristic packages of isolated or stacked reflections of an asymmetric to symmetric u- or v-shape geometry (Figure 5.2) are common elements for paleochannel recognition. Basal erosional fairways bordered by outer levees on the upper and middle paleo-slope are common. Inner levee deposits, thalwegs and slumps can form, creating an inter-channel architecture that is chaotic and not commonly recognized in this study.

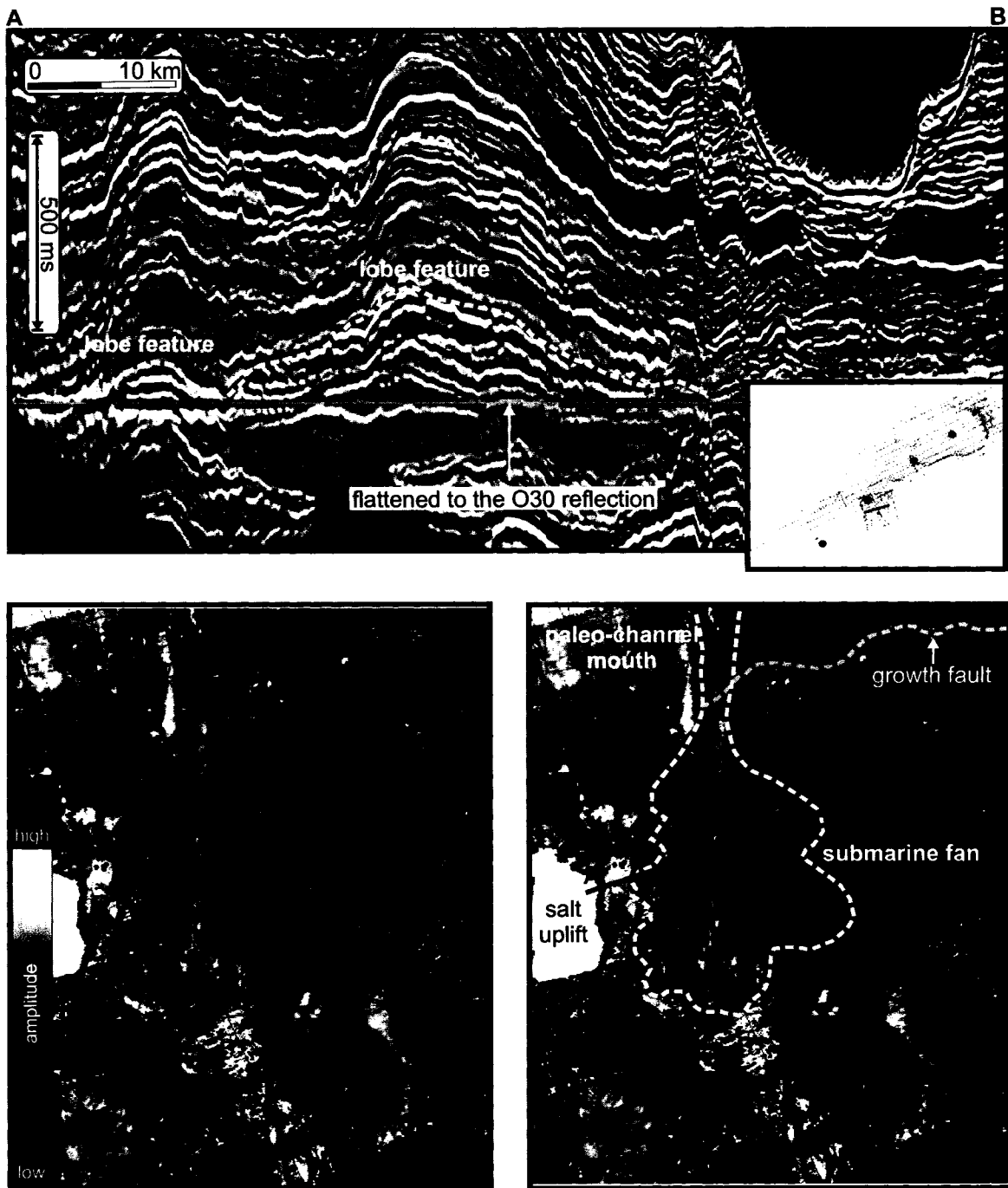


Figure 5.1. 3-D seismic reflection profile flattened to the O30 unconformity reflection and to the base of a sheet-like lobe of a mature submarine fan of the Late Oligocene. Note: dotted orange lines represent a possible alternative interpretation of a channel levee.

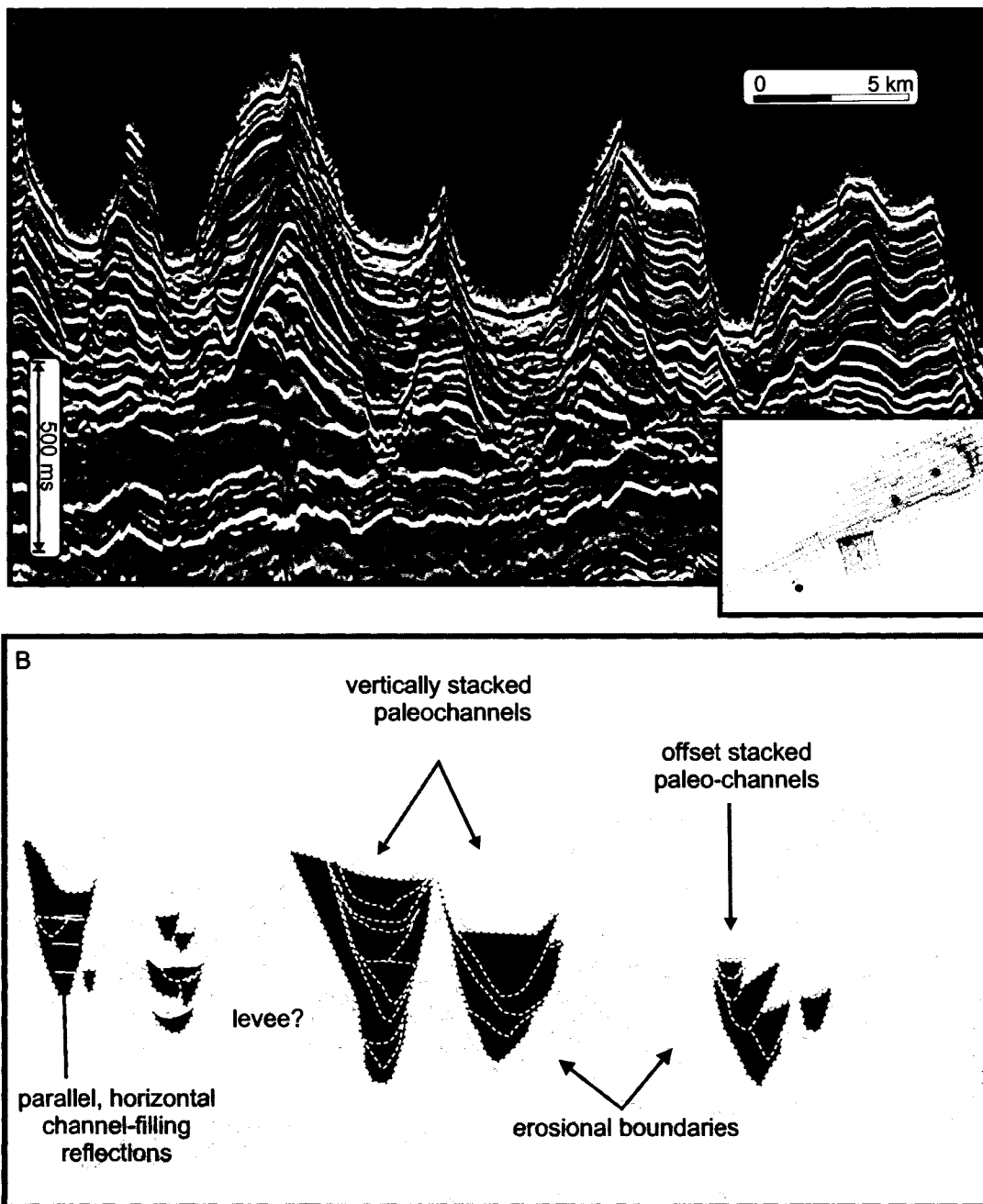


Figure 5.2. A) 3-D seismic reflection profile from the upper slope, which is heavily incised by paleo-channel erosion and deposition. B) Interpreted paleo-channel evolution.

In the study area, 3-D seismic reflection data shows that the Cenozoic section is highly degraded by paleo-channel erosion on the outer paleo-shelf and paleo-slope during Quaternary glaciation. In 3-D seismic reflection data, channel and channel levee architectures are recognized as lower impedance facies flanking the paleo-channels in 3-D seismic time slices (Figure 5.3).

5.4 Mass Transport Complexes

Mass transport complexes (MTCs) are generally recognized in seismic reflection profile by their complex reflection characteristics caused by failure scarps, underlying erosional boundaries and associated mass transport deposits (MTDs). The MTD facies unit has a chaotic and / or incoherent internal acoustic character with a hummocky or smooth appearance at the upper limits (Figure 5.4A and Figure 5.4B). In 2-D seismic reflection profiles MTCs, which encompass the full spectrum of slope failure sedimentation, can generate reflections that show a depression-filling lobe geometry that is generally above erosional boundaries, as well as abrupt stops in stratigraphic successions followed by an incoherent facies. MTDs are associated with local or regional unconformities and failure scarps, both laterally and upslope. Paleo-channels are also filled with MTDs on the paleo-slope with incoherent and / or chaotic reflections typical of MTDs (Figure 5.3). Multiple periods of MTC formation are recognized below the middle to lower paleo-slope with stacked packages of MTDs separated by erosional boundaries (Figure 4.5). Relating MTDs to the source of material and the initiation point of failure is done by correlating

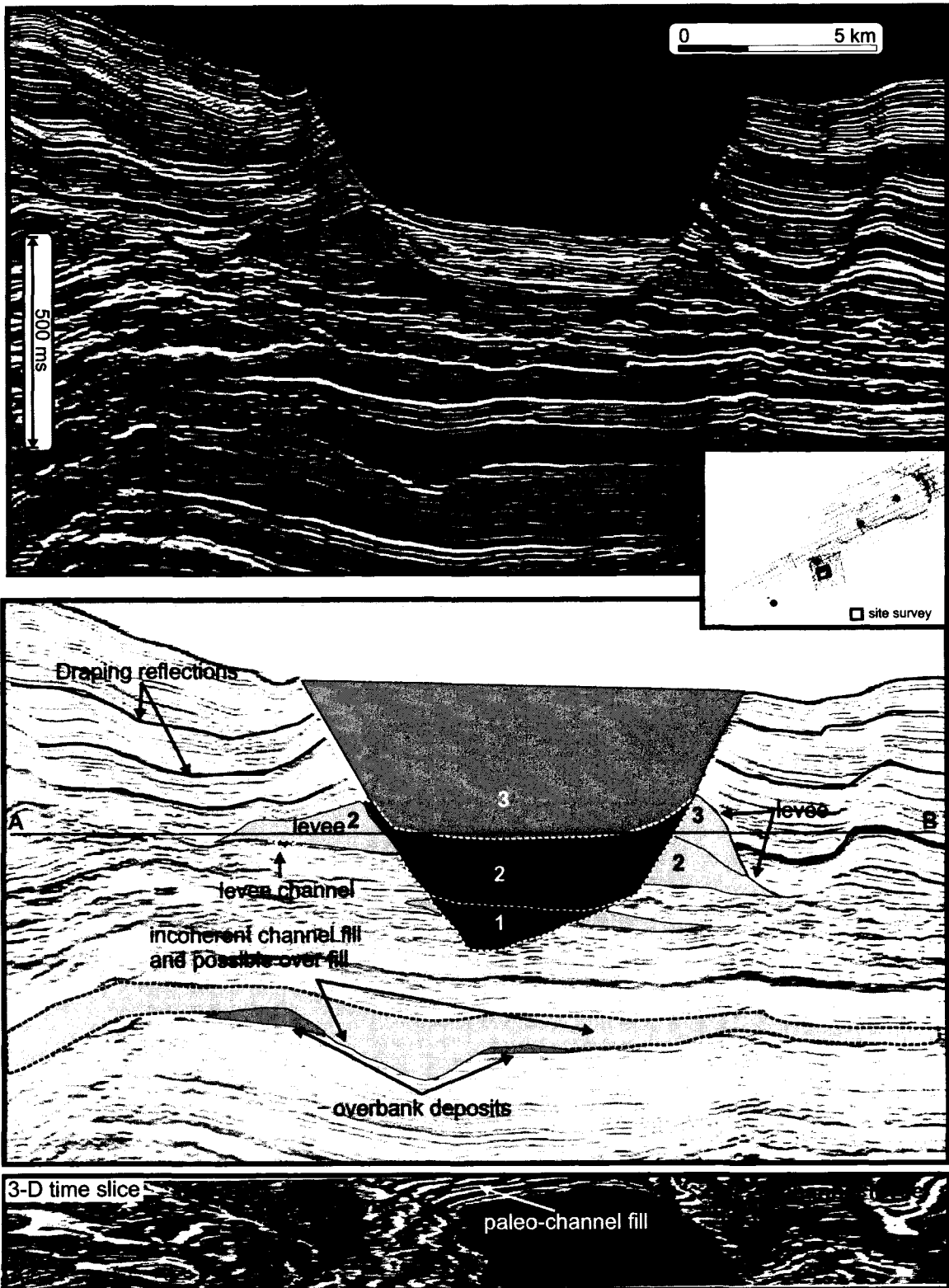


Figure 5.3. 3-D seismic reflection profile from the middle slope with multiple stage growth leveled paleo-channels. A-B: 3-D time slice showing the lateral lower amplitude nature of overbanking deposits. Note: seismic reflection profile graininess is an artifact of higher (2 ms) sample rate to increase resolution.

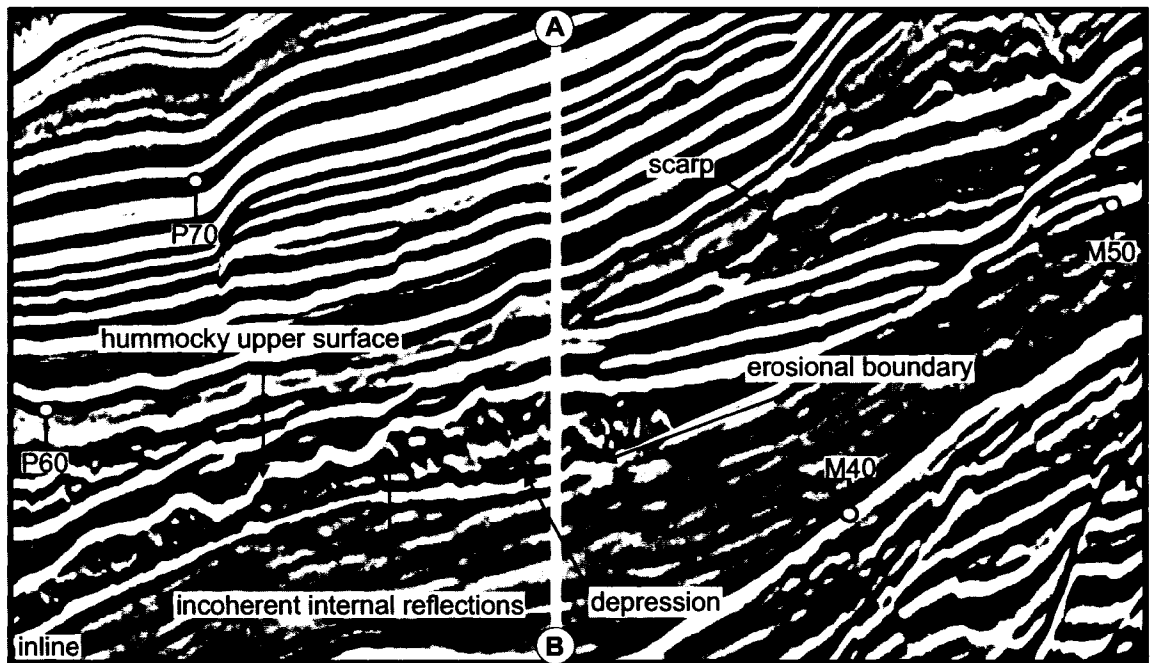
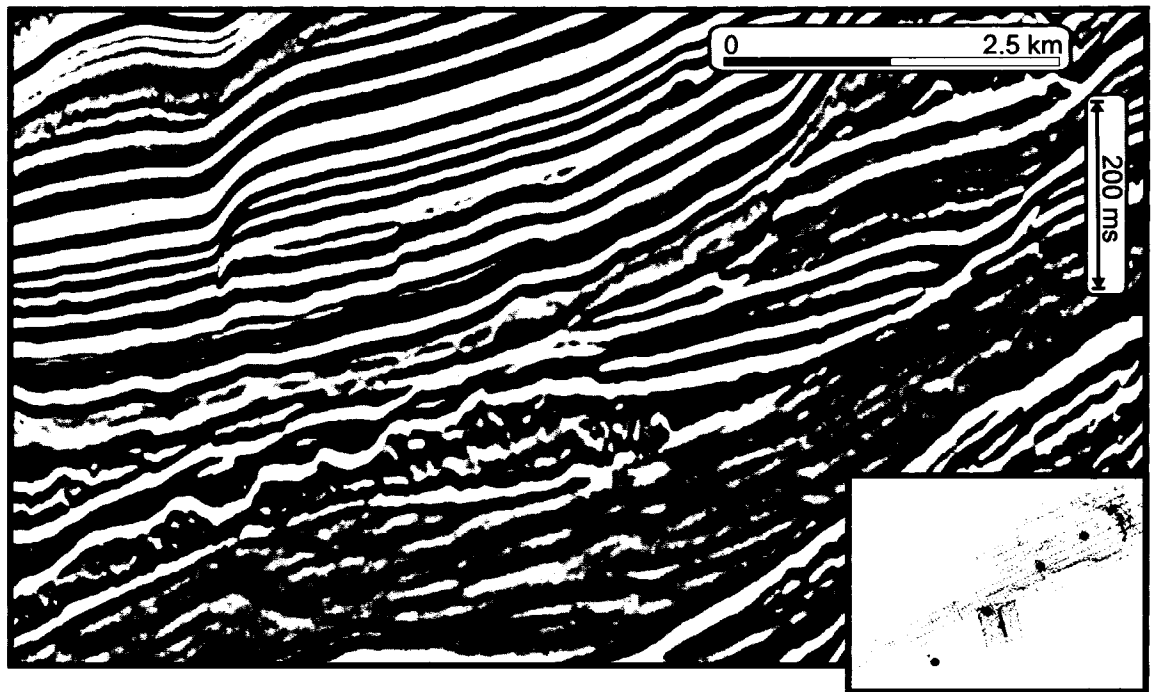


Figure 5.4A. In-line seismic reflection profile with MTD outlined in yellow with depression filling geometry and hummocky upper surface. Typical incoherent internal reflections. Note: failure scarp labelled on inline profile and above draping unit. Crossline Profile A-B Figure 5.4B.

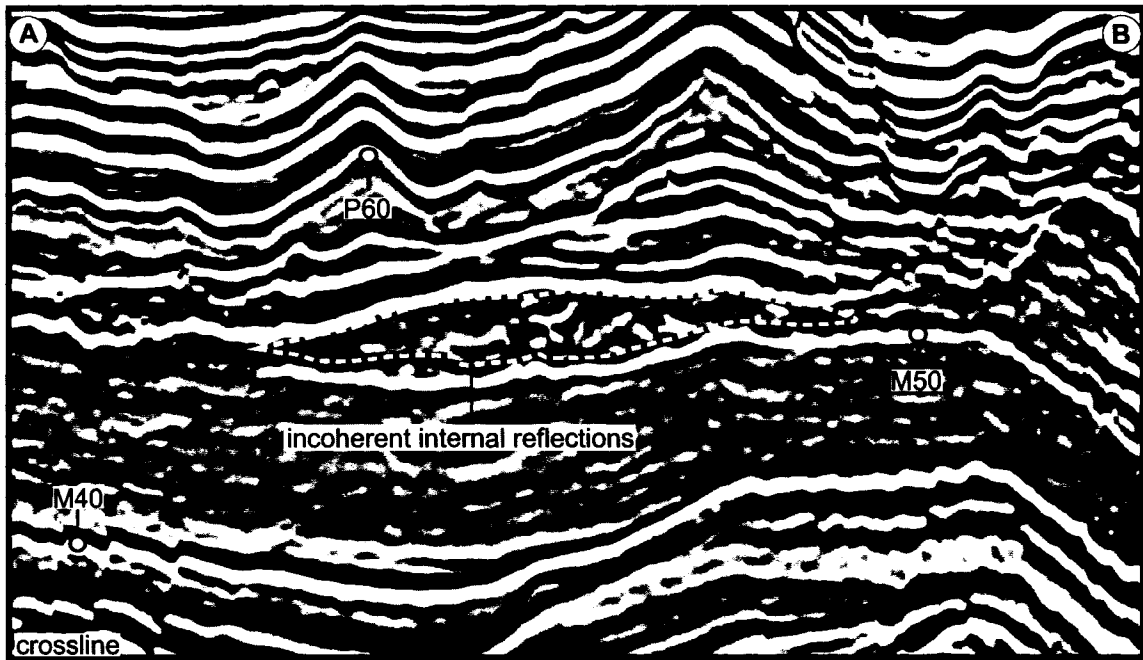
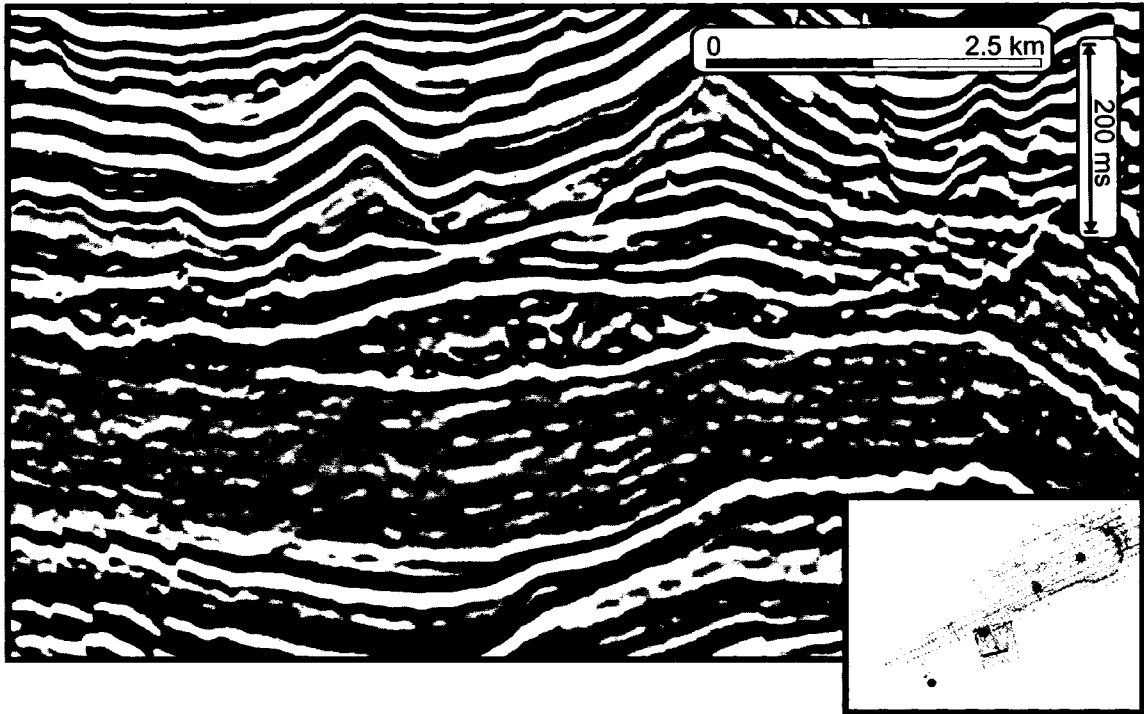


Figure 5.4B. Crossline seismic reflection profile with MTD outlined in yellow with a lense shape depression filling geometry with typical incoherent internal reflections. Note: This is A-B crossline through Figure 5.4A

top and bottom surface reflections to the surrounding undisturbed stratigraphy (Figure 4.5).

5.5 Sediment waves I

Sediment waves on the upper paleo-slope are recognized in seismic reflection data as symmetric, aggradational, wave shape reflections above the O30 reflection and below the M40 reflection. Wave lengths average 800-1000 meters and migrate vertically approximately 200 milliseconds through seismic reflection data in dip section. Sediment waves are separated by high amplitude surfaces which migrate up the paleo-slope along the high amplitude surface. In 2-D strike profile, type 1 sediment waves appear as packages of convex depression filling lenses with internal reflections (Figure 5.5). In a time slice amplitude surface from 3-D data, sediment waves are striking west southwest (WSW), very closely parallel to the modern day slope edge and possibly parallel to the paleo-slope (Figure 5.5). The aggradational and slope-parallel nature of type 1 sediment waves is consistent with observations made by studies of sea-floor sediment waves to the overbanking of turbidity currents (Normark et al. 1980; Migeon 2000; Normark et al. 2001; Ercilla et al. 2002; Keith and Pantin 2002; Lee et al. 2002). In this type of setting, sediment waves aggrade up current. Type 1 sediment waves generally form perpendicular to a channel axis Normark et al. 2001. Some authors previously interpreted this facies as rotational slumps (Lee et al. 2002).

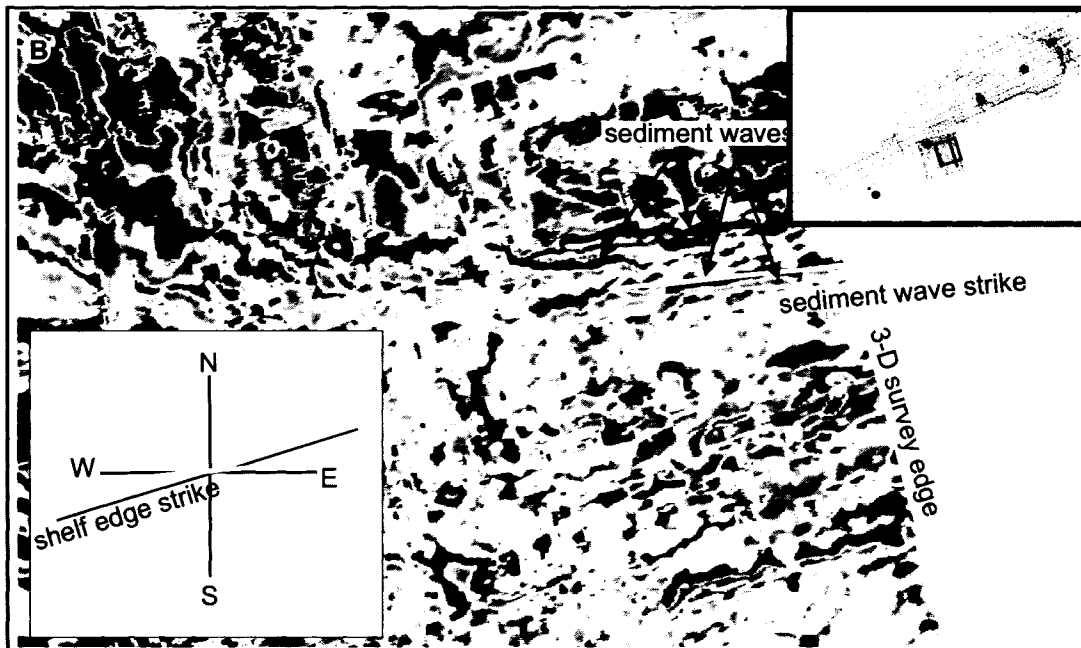
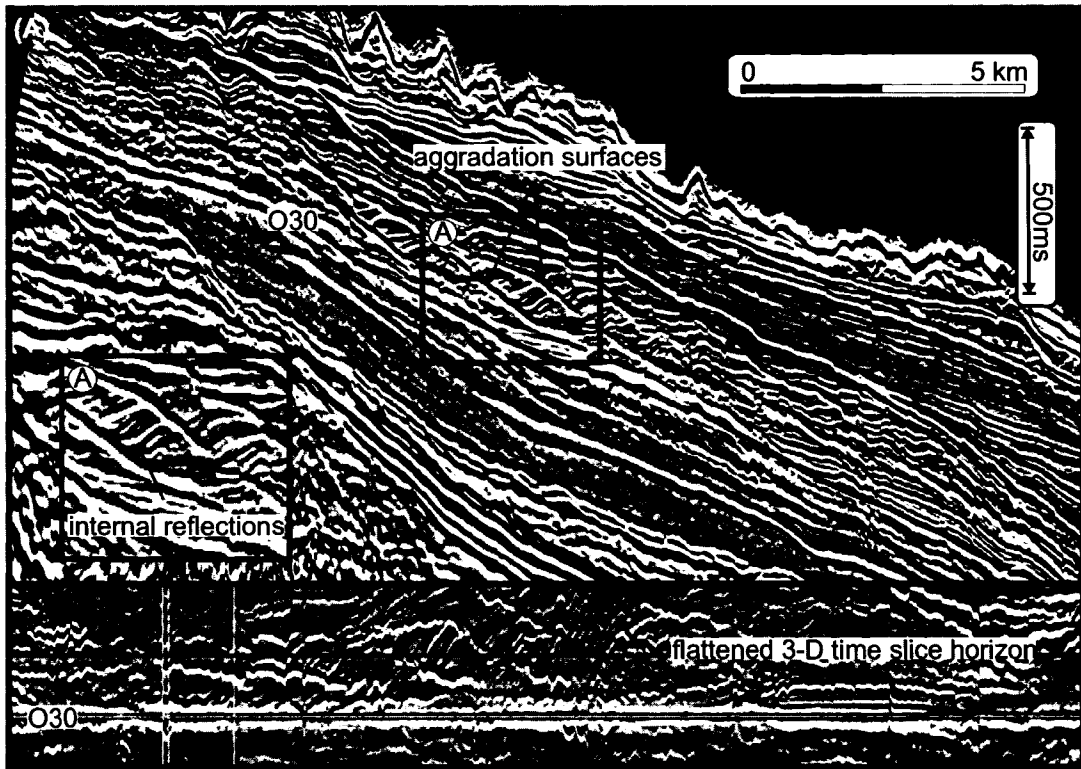


Figure 5.5. (A) Type 1 sediment waves on the upper to middle slope recognized in seismic reflection profile as a convex lenses of aggrading reflections (inset top) internal to the upper and lower bounding high amplitude aggradation surfaces. (B) sediment wave trending ENE-WSW seen through 3-D seismic flattened time slice.

5.6 Sediment waves II

Sediment waves on the lower paleo-slope are recognized in seismic reflection data as symmetric, aggradational wave shape reflections above the O30 reflection and below the M40 reflection. Wave lengths average 600-800 meters and migrate vertically through approximately 150-200 milliseconds of seismic reflection data. Similar to sediment wave type 1, type 2 sediment waves are separated by high amplitude aggradational surfaces which migrate in the upslope direction. In 2-D strike profile, type 2 sediment waves show stratigraphically cross-bedded geometry with internal reflections bounded by the inferred high amplitude aggradation surfaces (Figure 5.6). In a time slice amplitude surface from 3-D data, sediment waves are recognized as striking WNW, oblique to the modern day shelf edge (Figure 5.6). The upslope migration of type 2 sediment waves is consistent with observations made in other studies where packages of 'sediment drift' form on the lower paleo-slope or in deepwater highs and migrate upslope (Fulthorpe and Carter 1991). As it would appear in the lower paleo-slope, type 2 sediment waves are limited to the lowermost paleo-slope and occur above a salt-generated high.

5.7 Slope drape

Slope drape is recognized as continuous to semi-continuous reflections that are relatively homogenous across section, and reasonably consistent thickness across slope (Figure 5.7). Generally, slope drape gently conform to the sub-unit morphology, and reflections mimic the subsurface geometry (Figure 5.8). The P60 draping reflection in time surface render

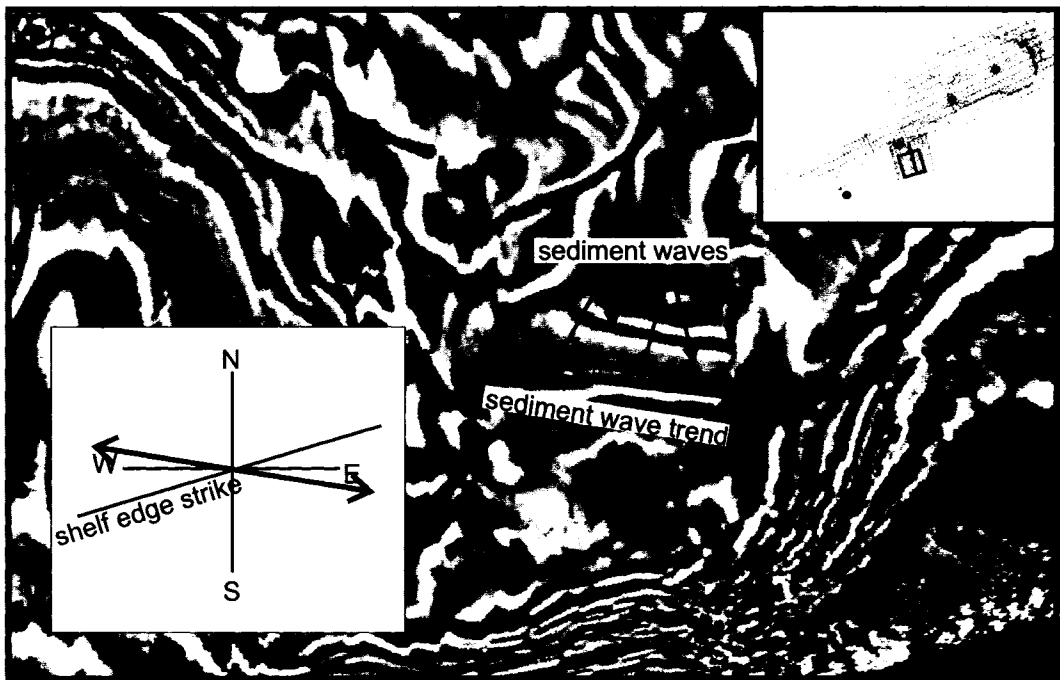
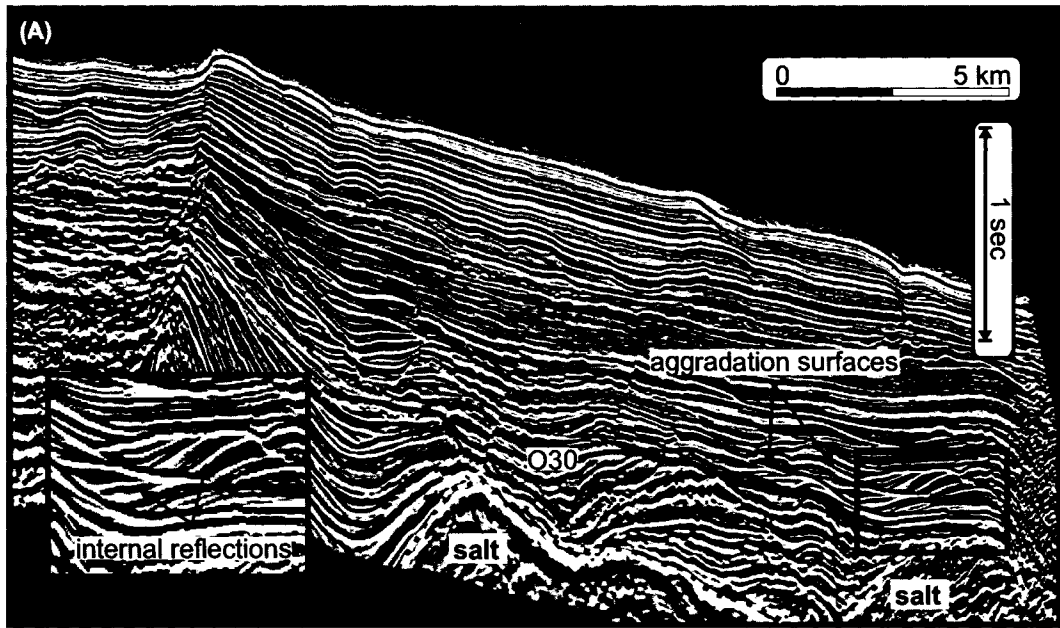


Figure 5.6. (A) Type 2 sediment waves in seismic reflection profile on the lower slope with aggrading reflections (inset) internal to the upper and lower bounding high amplitude aggradation surfaces. (B) sediment waves striking WNW seen on a 3-D seismic time slice.

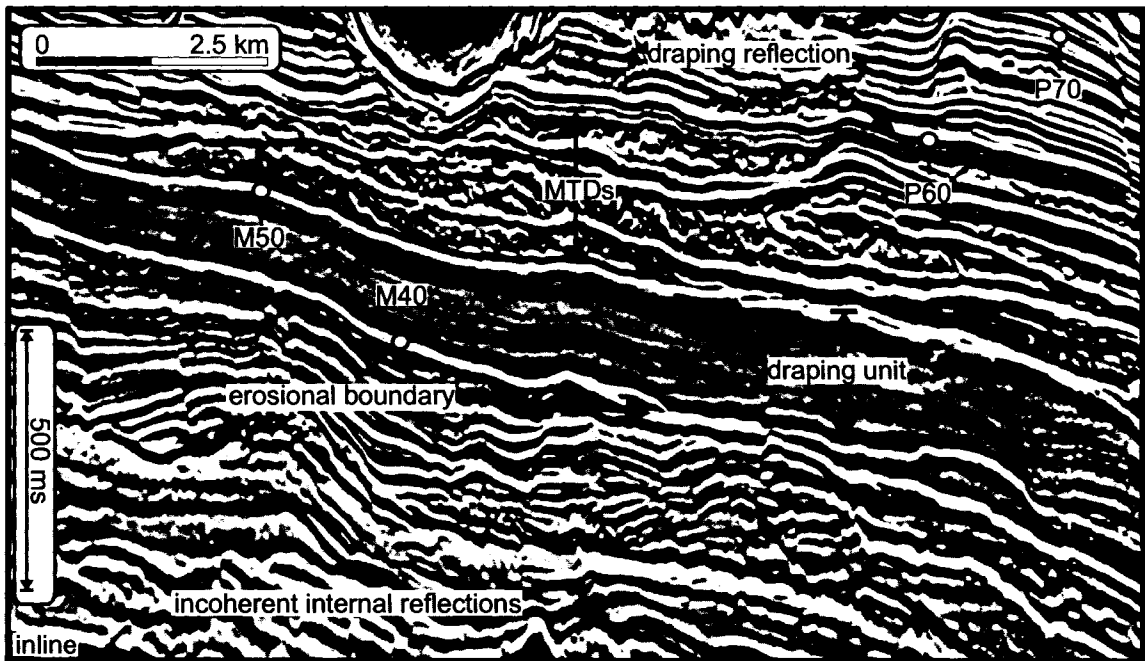
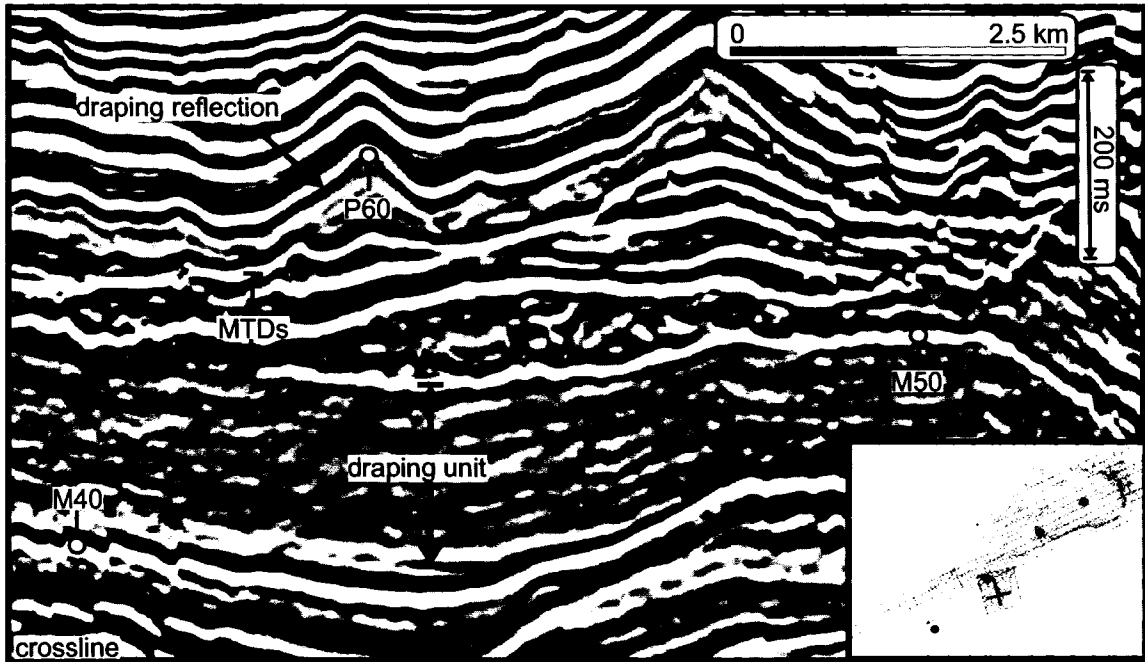


Figure 5.7. Crossline (top) and inline (bottom) seismic reflection profile with a seismic unit of slope drape indicating relatively homogenous facies with low acoustic impedance, inferred here as fine grained sediment. Also, P60 draping of another acoustically weak sub-unit with considerably more upper surface morphology (Figure 5.9).

(Figure 5.8) shows the mimicking nature of slope drape, which creates a softer impression of the sub-surface morphology. Draping reflections generally have high continuity and range from high to low amplitude (see Chapter 2). Inferences can be made on the sedimentology of slope drape based on the acoustic response, which suggests a hemipelagic fined grained sediment. In 2-D strike and dip seismic profiles, draping reflections maintain continuity and amplitude character, but generally thin and lose strength in amplitude seaward and on edges of bathymetric highs such as salt. In the 3-D amplitude surface render of the upper surface of a slope drape package in Sequence 3, the M50 reflector (Figure 5.7) shows slope parallel striations expressed as subtle amplitude variations across the upper to lower paleo-slope (Figure 5.9).

5.8 Proglacial slope drape

Proglacial slope drape facies are generally recognized as high amplitude, continuous reflections across the slope. Unlike 'slope drape' discussed above, proglacial drape is a unit of high- and low-amplitude reflections of excellent continuity. Proglacial slope drape will also gently conform to the sub-unit morphology, if any (Figure 5.10). Sedimentological inference of proglacial drape suggests high sedimentation rates due to possible ice-margin plume fallouts and turbidites from prodeltaic deposition (Piper et al. 2002). Significant processes such as MTCs and large deep seated faults offset proglacial slope drape. In 2-D strike and dip profiles, proglacial draping reflections maintain continuity and amplitude character. However, they thin and lose amplitude seaward and on the edges of bathymetric highs such as salt. The P70 draping reflection in the time

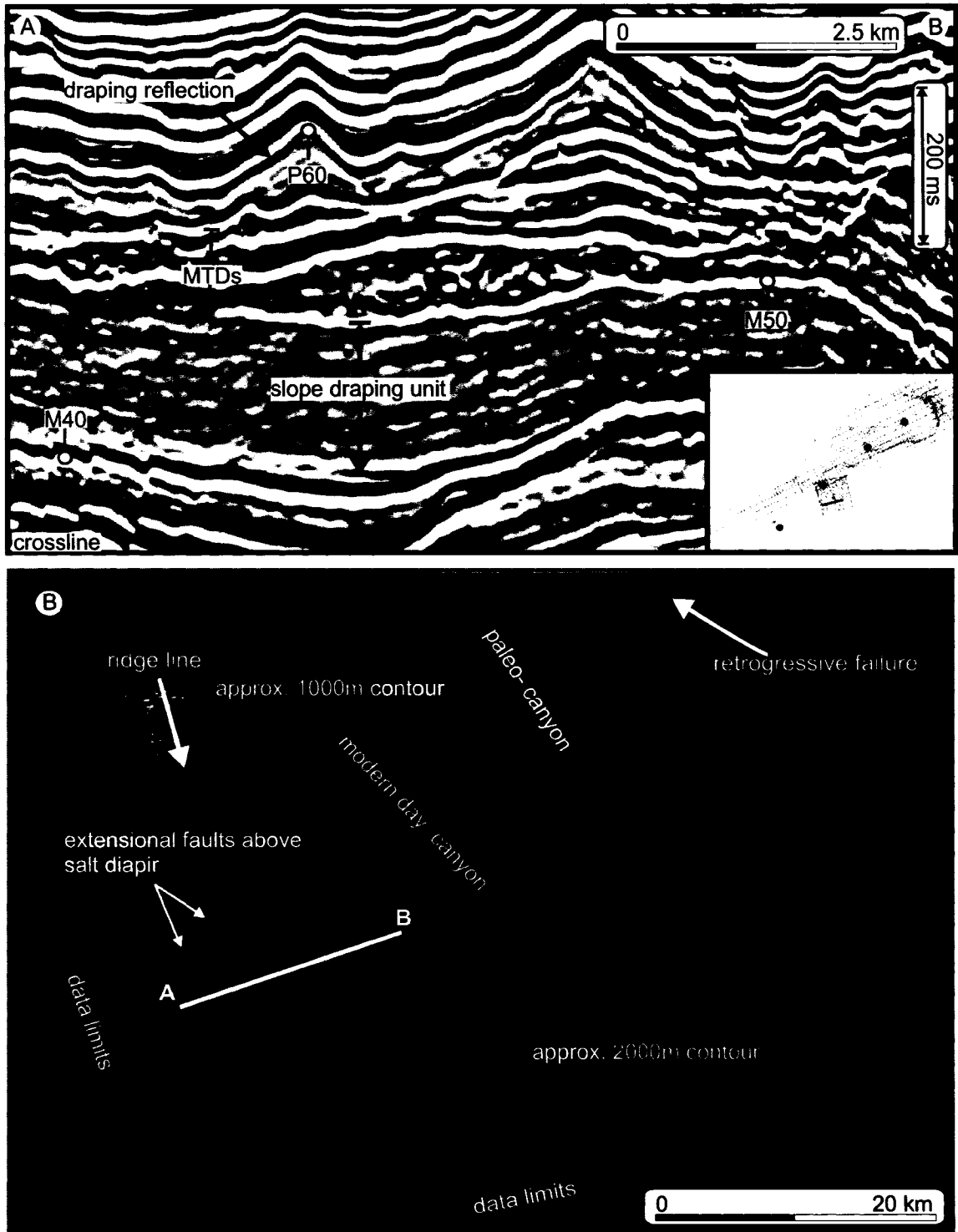


Figure 5.8. (A) Seismic reflection profile from the middle slope. (B) time surface render of P60.

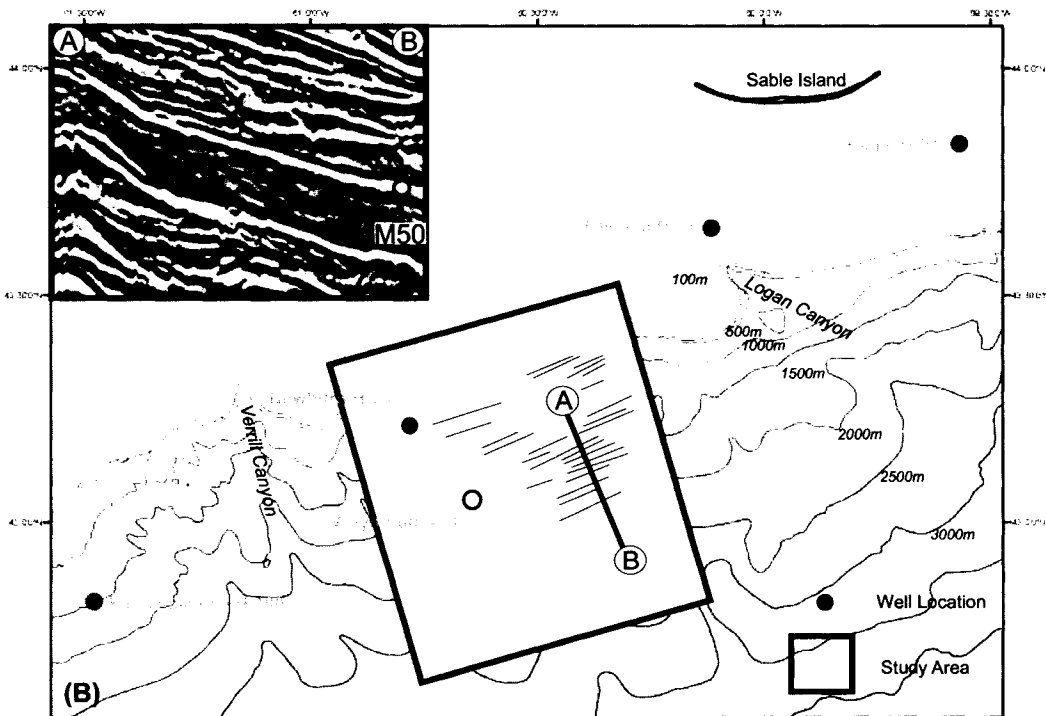
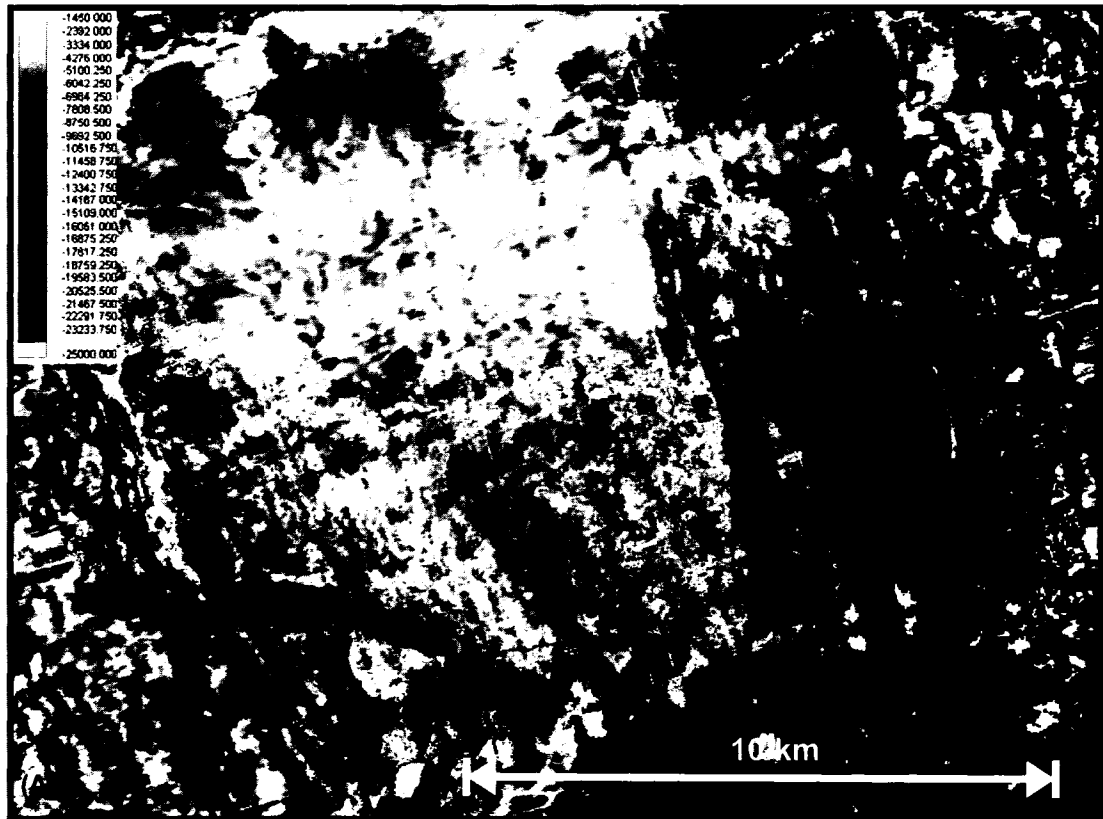


Figure 5.9. (A) Slope-parallel striations seen in a 3-D amplitude extraction of the M50 reflector, which is also the top of a slope drape unit. (B) Striations in relation to the study area.

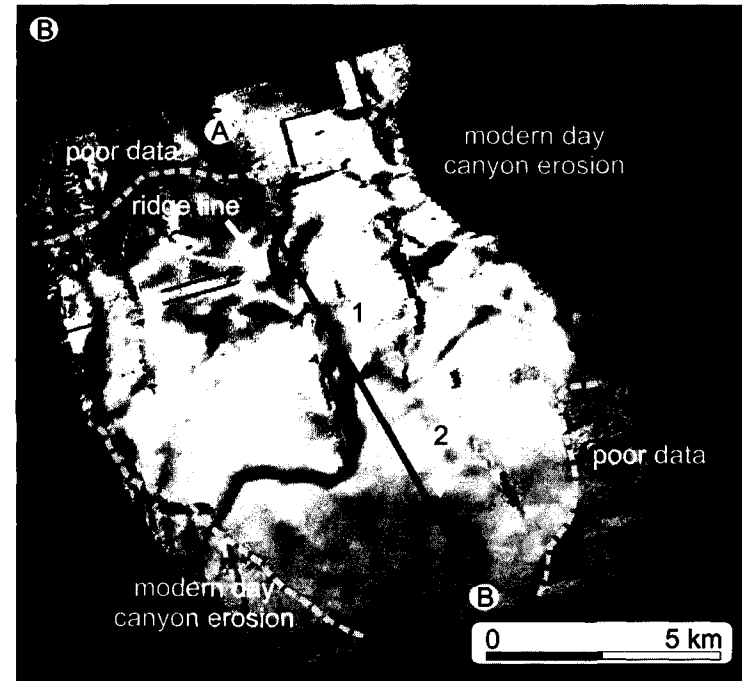
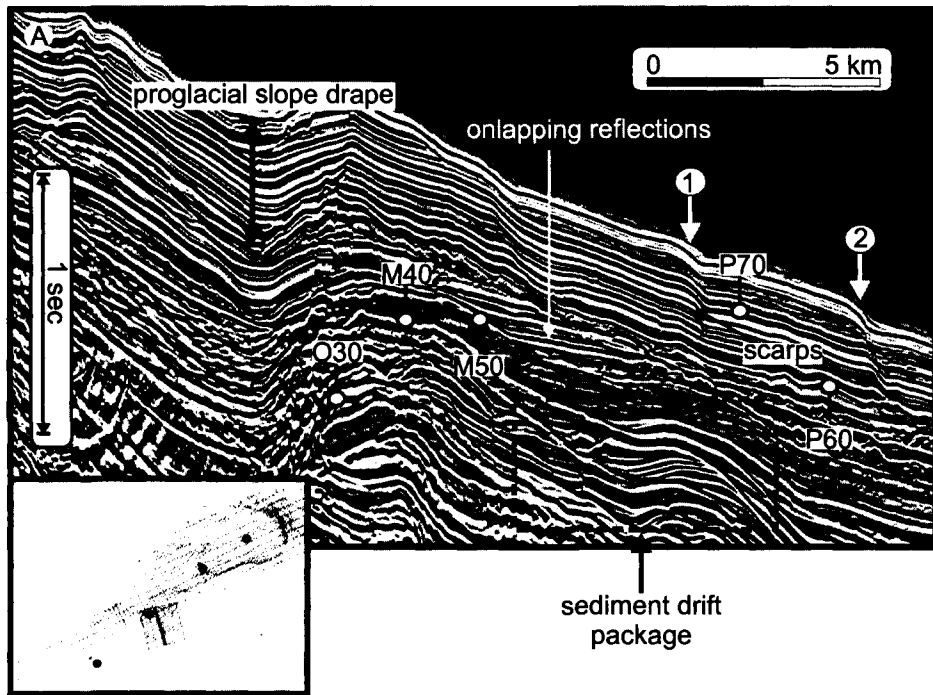


Figure 5.10. (A) Inline seismic reflection profile showing proglacial slope draping reflections that drape over paleo-failure scarp surfaces, and paleo-channels, which generally conform to the sub-surface morphology. (B) Time surface render of the P70, which is gently draping older retrogressive failure scarps.

surface render of Figure 5.11 shows a relatively uniform surface, with moderate relief that gently mimics the underlying paleochannels and sub-surface undulations. The general strength in reflection character of proglacial drape allows for easy recognition of fault offset with breaks in continuity.

5.9 Sediment drift

Sediment drift on the Scotian Slope is recognized in the lower paleo-slope above O30 and below the M40 in Sequence 3. Diagnostic features of sediment drifts are: 1) surfaces and internal reflections that do not conform to deeper surfaces; 2) thickness of the drift that exceeds that of the adjacent sedimentary cover; 3) drift deposit that is thickest at the drift axis and that thins on one side of the drift, which is the area inferred to have the greatest rate of current flow; 4) drifts that are commonly “mantled” by sediment waves and; 5) internal reflections that are weaker than the bounding reflections of the outer drift (Fulthorpe and Carter 1991). The accreted drift in the lower paleo-slope (Figure 5.12), in 2-D strike profile, shows stratigraphically cross-bedded geometry with internal reflections bounded by the inferred high amplitude aggradation surfaces. In dip profile, this lower slope drift system is made up of type 2 sediment waves. Observations of sediment drift are similarly described by others in deep marine settings affected by bottom current flow (McCave and Tucholke 1986; Fulthorpe and Carter 1991; Mosher and Thomson 2002).

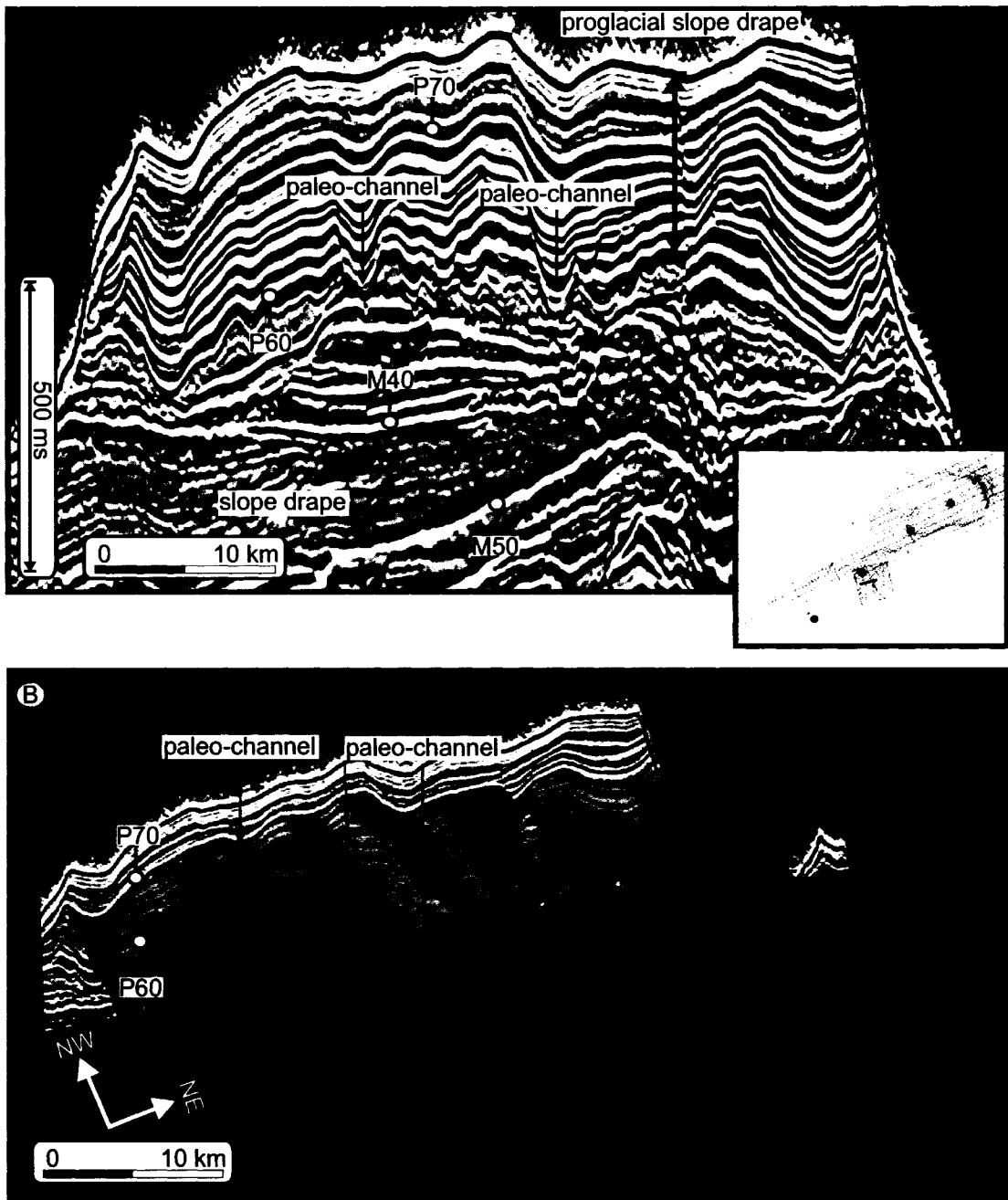
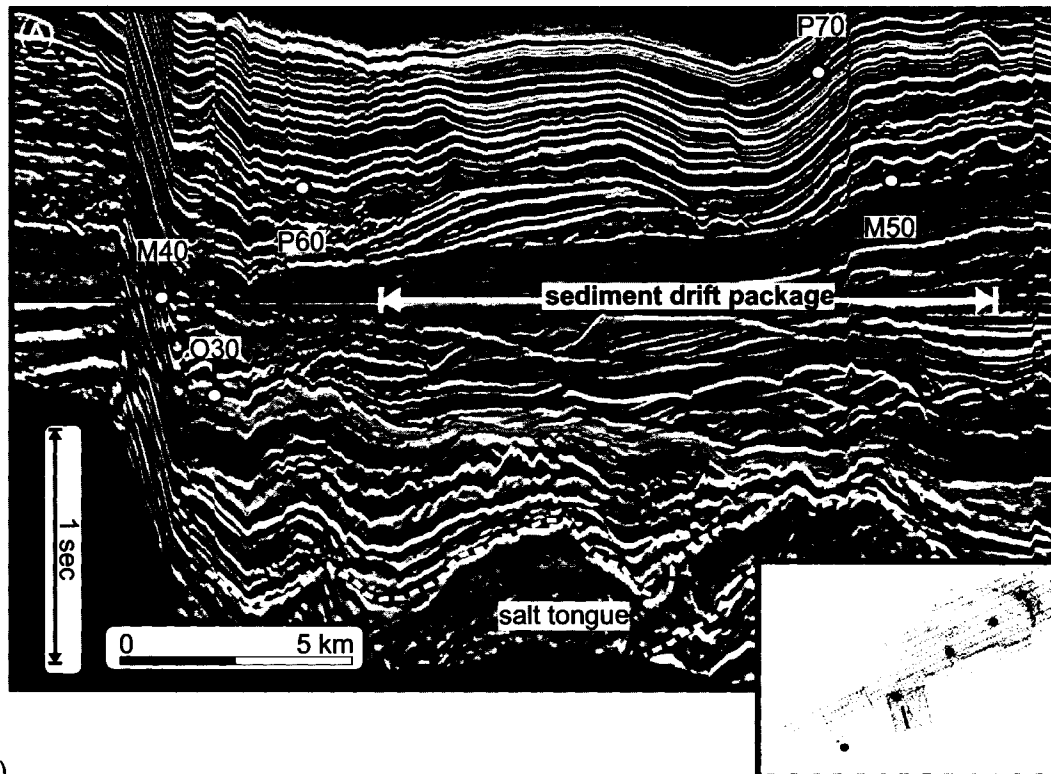


Figure 5.11. (A) Crossline seismic reflection profile showing proglacial slope draping reflections that form a unit of high amplitude reflections over paleo-channels, and which generally conform to the sub-surface morphology. (B) P70 time surface render on the upper slope draping of paleo-channels.



(B)

Accreted drift

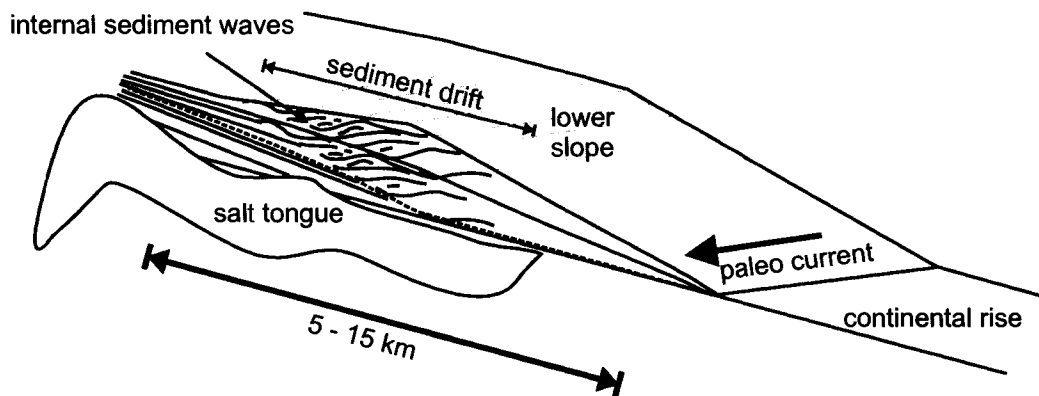


Figure 5.12. (A) Seismic reflection profile flattened to the M40 reflector and showing a thick sediment drift package above the O30 reflection and on top of a salt high. (B) Sediment drift model in the lower slope of the study area with aggrading sediment waves on top of a salt induced high. Paleocurrent direction is inferred as parallel-to-slope (Modified from Fulthroup and Carter, 1991).

6. Integration of Stratigraphy and Facies Units

In this section, the architecture of Cenozoic sediments within the study area is presented by placing facies interpretations within a sequence stratigraphic framework. At the Newburn H-23 well site, gamma ray log interpretation is used to indicate lithological changes and to make inferences on facies types based on the log signature.

6.1 Sequence Unit 1

Sequence unit 1 is the outer shelf delta system (Chapter 5) of a complex FSST, which perhaps overlays a thin HST. However, none of the prograded deltas appear to have reached the paleo-shelf break (Figure 4.7). On the paleo-slope, Sequence unit 1 comprises a condensed package of two high amplitude reflections, C10 and SB0 (Wyandot marker), which are correlated to the outer paleo-shelf as the top and bottom of the outer shelf delta facies (Figure 4.2). C10 is recognized across the paleo-slope as a high amplitude reflection with good reflection continuity and is dated as early Eocene. Subtle mounding and shingling is a common feature on the upper paleo-slope. In dip seismic reflection profile, internal, oblique, clinoform reflections of the prograding delta downlap the SB0 reflector in a variation of high angle or tangential-to-parallel reflections. In strike section, reflection characteristics differ, appearing as stacked parallel to sub-parallel reflections of a gentle mounding geometry that is representative of the depositional layering of the prograding clinoform reflections.

The C10 reflection marks the end of delta progradation and it is inferred to represent a MFS and a change in sea-level. At the Newburn H-23 well site, a simple gamma ray log interpretation for facies types shows a distinct change in gamma ray signature at the level of the C10 reflection (Figure 6.1). A low gamma measurement in this case is most likely indicative of a carbonate rich facies of a MFS in the paleo-deepwater setting. In seismic reflection profile, C10 is at the base of a mounded submarine fan facies. Furthermore, an amplitude surface extraction of C10 shows a distinct submarine fan (~ 5 km wide) in the middle paleo-slope. This submarine fan is again indicative of a deepwater facies after sealevel has fallen (i.e. after the MFS) and canyon cutting on the outer paleo-shelf and upper paleo-slope is conveying sediment at the canyon mouths to the upper and middle slopes.

6.2 Sequence Unit 2

Sequence unit 2 is recognized in the outer paleo-shelf and paleo-slope, bound from below by the C10 reflector and from above by the erosional O30 reflector. The reflection character of Sequence unit 2 is variable across the paleo-slope and is divided into upper and lower facies units. The lower package of Sequence unit 2, between C10 and E20, is a submarine fan facies in which the E20 reflector is interpreted as a possible transgressive surface, and the above package as a paleo-slope drape (Chapter 5). The submarine fan facies of Sequence unit 2 is characterized in seismic reflection profile by relatively small mounds of offlapping sub-parallel reflectors that prograde into the minibasin of the middle paleo-slope. Mounding reflections thin and decrease in amplitude in the lower

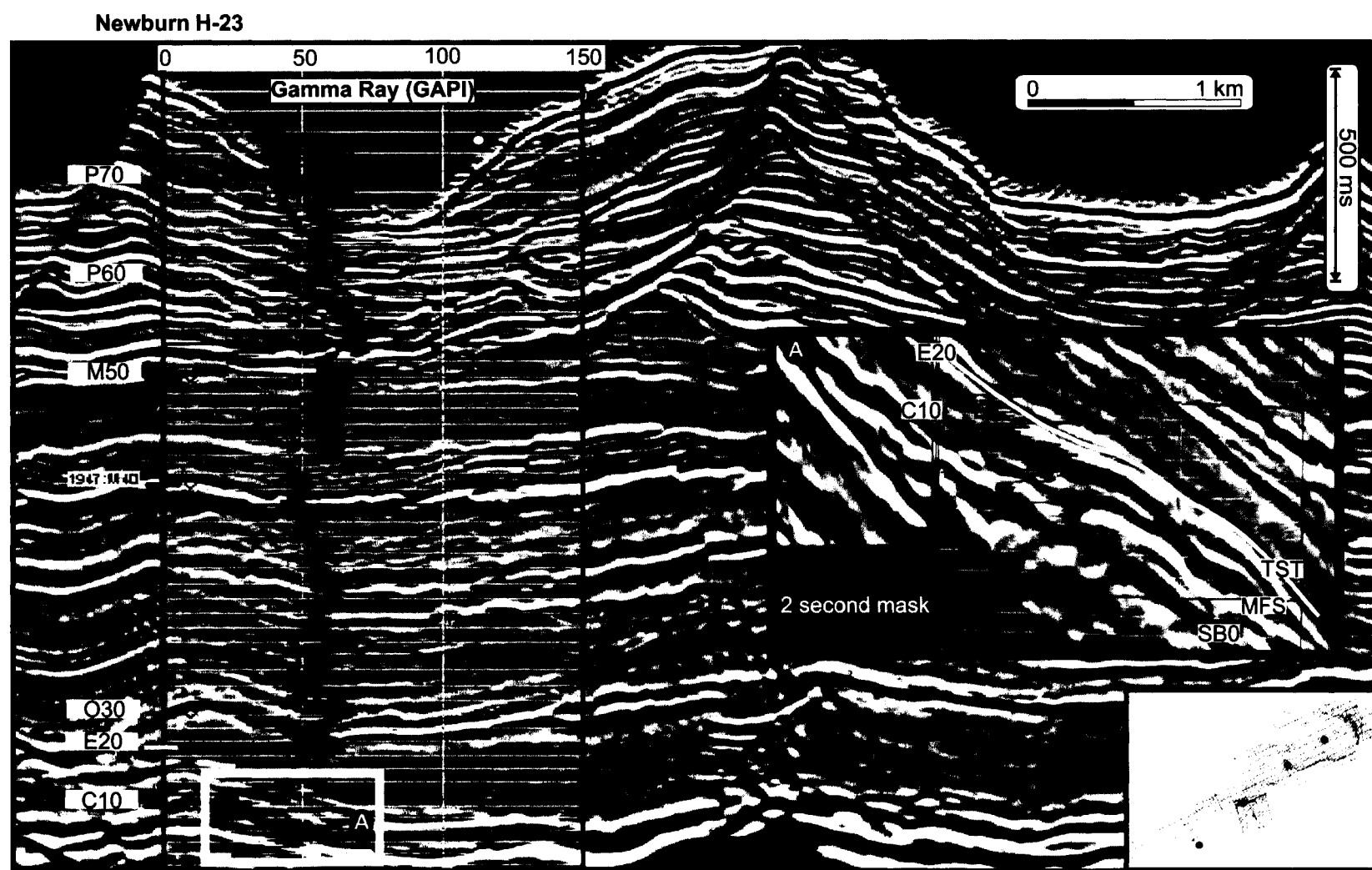


Figure 6.1. Strike section through the Newburn H-23 well site, with Gamma Ray log superimposed and used for indications of lithologic changes throughout the section. A) Sequence Unit 1 shows changes to a very low gamma signature at the C10 reflection, similar to Sequence boundary 0 (SB0) (Wyandot marker) below, which has been described as a chalky marl.

paleo-slope before lapping out. The submarine fan facies increases relative to slope drape towards the northeast, where Sequence unit 2 is thickest. In the southwest, the lower portion of Sequence unit 2 is thinner, with fan mounds that form smaller lenses, and internal parasequence-like reflections in 3-D seismic reflection data (Figure 4.8 and 4.9). Commonly, at the paleo-shelf edge in the southwest, the lower submarine fan facies of Sequence unit 2 has been removed beneath the O30 reflector, or is unresolved in seismic reflection data.

The later portion of Sequence unit 2, from E20 to O30, is not a submarine fan facies. Reflections above the E20 reflection onlap the paleo-slope front and are recognized as slope drape of moderate amplitude reflections. On the outer paleo-shelf, parallel sigmoid reflections represent shelf margin progradation which has been heavily incised by paleochannels in the Oligocene (Figure 4.2).

Gamma ray log observations made from the Newburn H-23 well site show a distinct change in facies at the E20 reflection. Below E20, a more sand-rich log signature is typical of the LST submarine fan facies. Above E20, the clay-rich signature is consistent with a more distal hemipelagic type of sedimentation during the formation of the HST (Figure 6.2). Generally, from C10 to O30 the gamma ray signature suggests a fining-upward sequence inferred to be the LST, with clastic deposition aggrading on the slope and fining upward as sea-level increased (Figure 6.2). At the same time, sediment delivery across the paleo-shelf diminished and the shelf margin prograded seaward in a

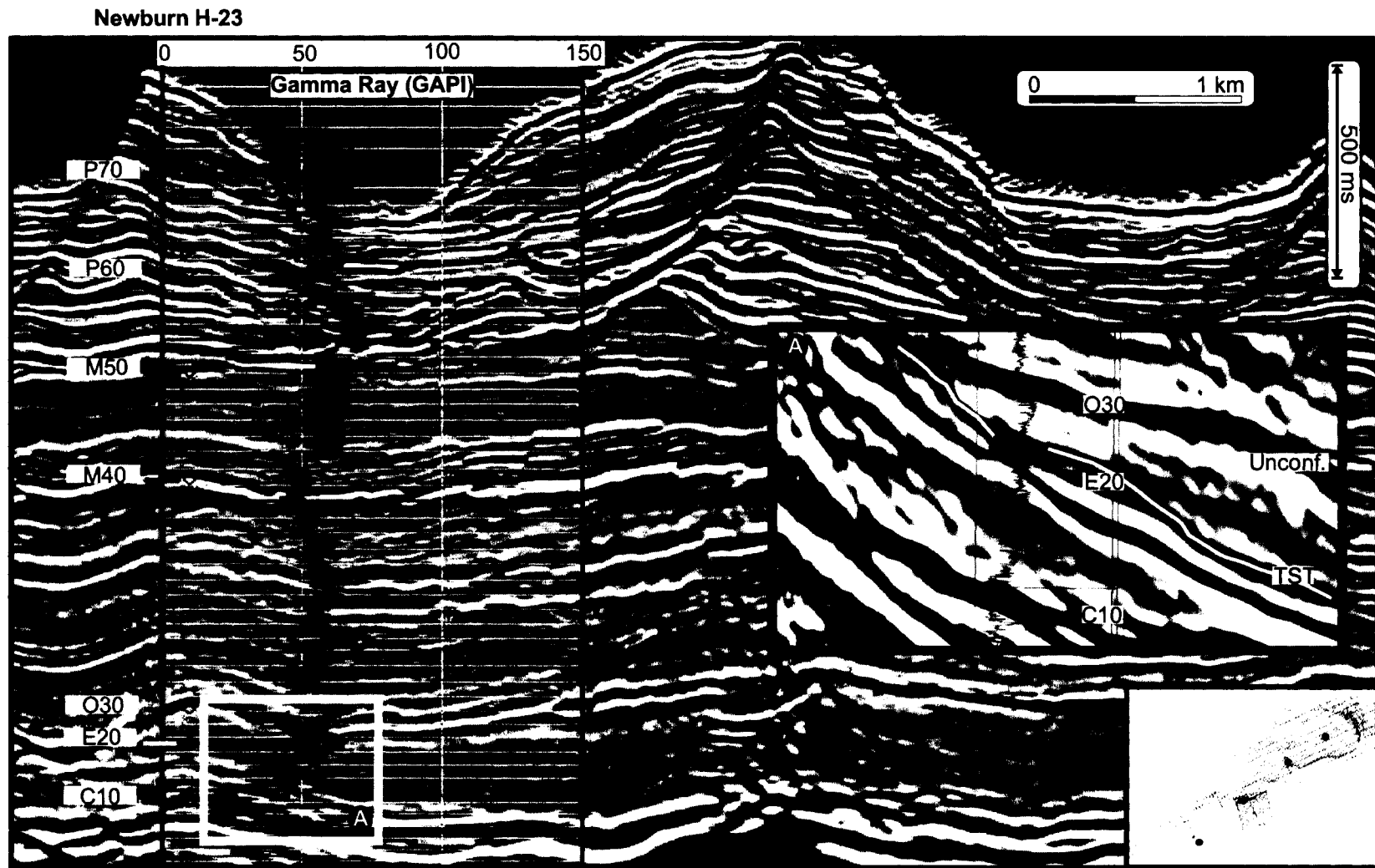


Figure 6.2. Strike section through the Newburn H-23 well site, with Gamma Ray log superimposed and used for indications of lithologic change through out the section. A) Sequence Unit 2 shows changes in gamma signature at the C10 reflection, increasing toward the E20 reflection and again increasing from the E20 to the O30 reflection, indicating a fining-upward succession.

FSST of parallel-sigmoid reflections in the outer paleo-shelf. Deposition on the paleo-slope became more distal and hemipelagic in nature (Figure 4.2).

6.3 Sequence Unit 3

Sequence unit 3 is recognized in the outer paleo-shelf and paleo-slope. It is bound below by O30 and from above by the erosional M40. The outer paleo-shelf consists of the thick package of shelf margin prograding reflections of a FSST above LST deposits in the outer paleo-shelf and paleo-slope. The early part of Sequence unit 3 (O30 to M40) is dominated in the upper paleo-slope by paleochannels. Paleochannel incision occurred in the early stages of Sequence 2 and persisted into the middle of Sequence unit 3 (Figure 4.9). In the middle to lower paleo-slope, overbanking channel levee complexes resulted in thick deposits of deepwater MTCs and turbidite sandy splays into the salt withdrawal basins during a middle Oligocene lowstand. Below the northeastern part of the upper and middle paleo-slope, type 1 sediment waves (Figure 5.6) are recognized and are interpreted to be related to overbanking turbidity currents. Sediment waves are cut by perpendicular paleochannels and are aggrading upslope above the O30 reflector. In the deeper basin, evidence for relatively small MTDs are recognized in seismic reflection profile (Figure 4.4) and possibly related to slumping and wasting upslope. In the lower paleo-slope, type 2 sediment waves (Figure 5.7) are recognized in Sequence unit 3 on top of a salt-generated high, forming an accreted drift package in the lower paleo-slope.

The general filling of paleochannels in the paleo-slope and outer paleo-shelf occurred late in Sequence unit 3 during transgression that followed the LST (Figure 4.6). During this transition, sedimentation on the outer paleo-shelf became more progradational to the shelf margin as it moved into the HST of Sequence unit 3. In the HST, channels on the paleo-slope and paleo-shelf became choked with back-filling sediment and marked the end of overbanking deposits and paleo-channel erosion. The late portion of Sequence unit 3 is recognized as slope draping units above sediment waves and drift packages, which are correlated with a thick package of shelf margin prograding reflections in the outer paleo-shelf. According to the correlation of facies observations in Sequence unit 3 and gamma ray log observations at the Newburn H-23 well site, the lower portion of Sequence unit 3 is sandier than the upper part (Figure 6.3).

6.4 Sequence Unit 4

Sequence unit 4 is bound from below by M40 and from above by M50. The outer paleo-shelf consists of a package of eroded shelf margin prograding reflections of a probable FSST, but possible HST. Sequence unit 4 is a slope drape unit that thins upslope with some ponding in minibasins. Shelf margin progradation of the FSST / HST allowed for the homogenous distal sedimentation needed to form the slope drape unit. On the upper paleo-slope, Sequence 4 appears to have a bypass zone, where little sediment has accumulated (Figure 4.11). In a surface amplitude extraction of Sequence Boundary 4 at the top of Sequence unit 4 (M50 reflector) (Figure 5.10), slope parallel striations appear in the upper to upper middle paleo-slope and are interpreted as deep-sea current scours.

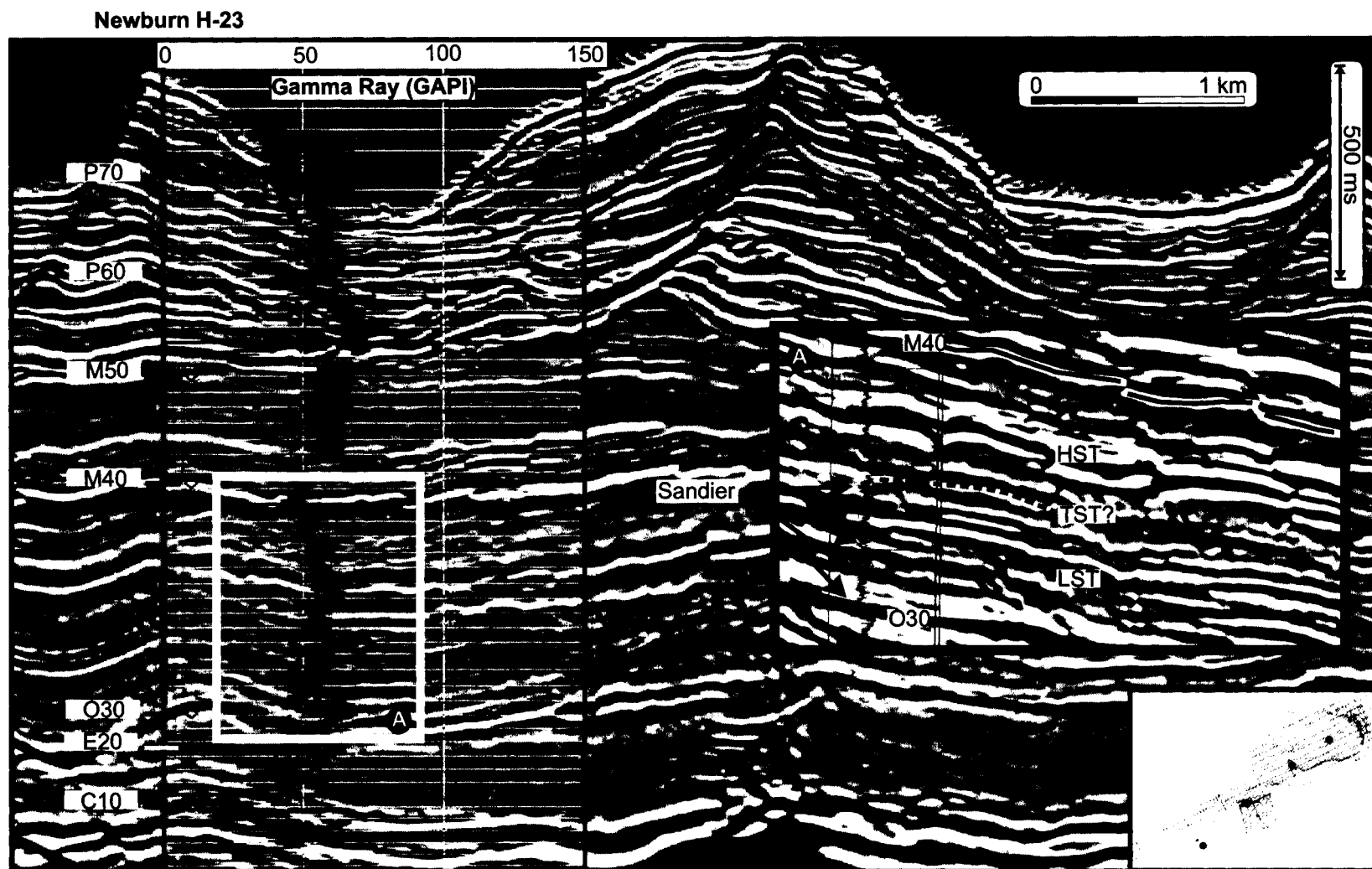


Figure 6.3. Strike section through the Newburn H-23 well site, with Gamma Ray log superimposed and used for indications of lithologic changes through out the section. A) Sequence Unit 3 shows a change in gamma signature at the O30 reflection with a fairly homogeneous sandy gamma signature due to increased channel discharge and overbanking.

Similar striations have been noted by other workers, who have also interpreted them as deep-sea current scours (Cochonat et al. 1989; Barnes 1992; Hughes Clarke et al. 1992). The effects of current scouring on the paleo-slope could account for the minimal accumulation of sediment on the paleo-upper slope. The outer paleo-shelf sigmoid reflections are more steeply dipping close to the upper paleo-slope. In the outer paleo-shelf to paleo-slope transition area, outer shelf reflections are not recognized in seismic reflection profile. It is postulated that late in Sequence unit 4, the shoreface may have been closer to the paleo-shelf edge than in previous time periods, and that more shallow water currents may have partially eroded and scoured the seafloor. Outer paleo-shelf and upper paleo-slope reflections show minor paleo-channel erosion.

The HST that followed on the paleo-shelf was a short-lived shelf margin progradation that allowed for a relatively homogenous slope drape to be deposited across the paleo-slope. Facies observations in Sequence 4 are consistent with log observations made from the Newburn H-23 well site, which include a homogeneously fine-grained facies unit of slope drape above a non-homogenous lowstand wedge deposit in the upper paleo-slope (Figure 6.4).

6.5 Sequence Unit 5

Sequence unit 5 is recognized in the outer paleo-shelf and paleo-slope and is bound from below by M50 and from above by the seafloor reflection. The outer paleo-shelf sigmoid reflections of Sequence 5 are steep and relatively close to the paleo-shelf edge. In the

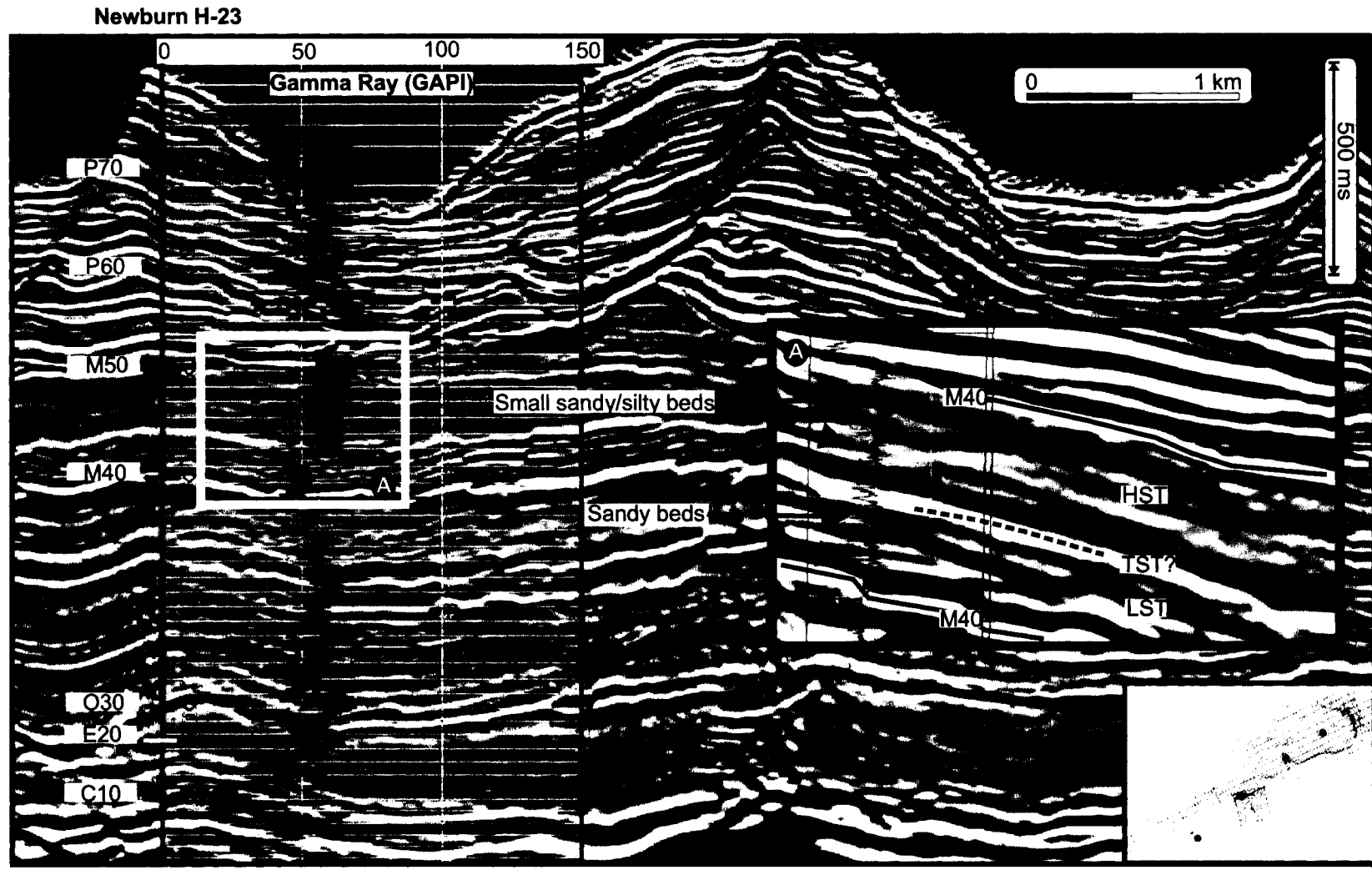


Figure 6.4. Strike section through the Newburn H-23 well site, with Gamma Ray log superimposed and used for indications of lithologic changes through out the section. A) Sequence Unit 4 shows a change in gamma signature at the M40 reflection, with slightly sporadic values indicative of the overbanking deposits moving into to a more homogeneous signature of the slope drape.

early part of Sequence 5, below the P60 reflection, the northeastern lower paleo-slope was a depocenter for mass transport deposits (Figure 4.5). The LST deposits of Sequence unit 5 are recognized in the middle to lower paleo-slope as aggrading and onlapping the M50 reflection where there are no MTDs (Figure 4.3). In the southwestern study area, early LST deposits were ponded in salt withdrawal basins. The increased sediment load, amplified by the higher rates of sedimentation on the upper paleo-slope combined with the relative sea-level fall, may have favored the development of MTCs in the study area. Similar suggestions of sediment failure due to gravity loading and of slope overstepping due to high rates of sedimentation have been made by other workers on the Scotian Margin (Piper 1988; Mulder and Moran 1995; Mosher et al. 2004). Relatively smaller scale MTDs occur later in the section, above the P60 reflection, and are sourced from failure scarps up slope or from the edges of canyon walls.

On the paleo-slope, proglacial slope drape with common MTDs is the predominant facies above the P60 reflection in the later part of Sequence 5. On the outer paleo-shelf, this late stage Sequence 5 forms a wedge of incoherent facies which interfingers with the stratified proglacial drape (till tongues), which is also seen elsewhere on the margin (Piper et al. 2002). On the outer shelf, till tongue reflection character is recognized as far as the uppermost paleo-slope (Figure 4.6). Proglacial drape on the slope was heavily incised by canyons in the latest stages of Sequence 5 due to shelf crossing glaciations in the Pleistocene.

Seismic facies observations in Sequence 5 and gamma ray log at the Newburn H-23 well site suggest interbedded sand and mud beds in the proglacial slope facies (Figure 6.5).

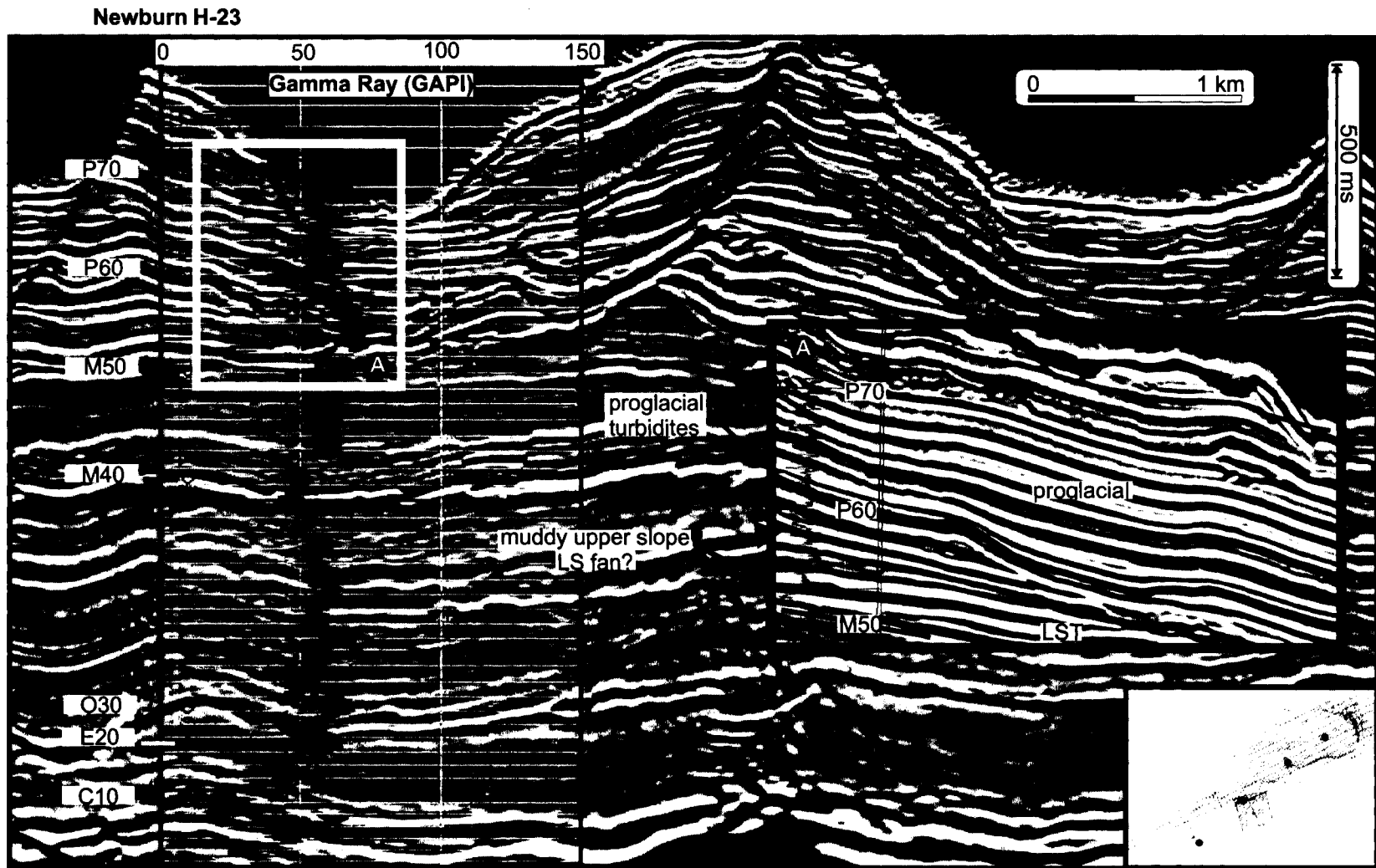


Figure 6.5. Strike section through the Newburn H-23 well site, with Gamma Ray log superimposed and used for indications of lithologic changes through out the section. A) Sequence Unit 5 shows a change in log signature at the M50 reflection into sporadic values indicative of interbedded turbidite muds and sands consistent with proglacial sedimentation.

7. Discussion

7.1 Chronology of sea-level variations and associated depositional sequences

The effects of sea-level change are recognized in the stratigraphic record across the central Scotian Slope and outer shelf. Studies elsewhere have suggested that since the mid-Cretaceous, sea level has been oscillating, superimposed on a gradual rise (Vail et al. 1977; Mitchum et al. 1977a; Haq et al. 1988; Christie-Blick et al. 1998; Miller et al. 1998). Previous work done by Vail et al. (1977) and Haq et al. (1988) suggested that sea-level variations, grouped into global eustatic cycles, are reflected in the seismo-stratigraphic records of the world's continental shelf margins, from which they have established a eustatic sea-level curve (Haq curve used in several figures herein) representative of sea-level rise and fall through the Cenozoic Era (Figure 7.1). The eustatic Haq curve provides a useful point of reference from a global scale. However, it has been suggested that relative sea-level is defined qualitatively with respect to tectonic influence or a datum within a sedimentary succession on a non-global but independent basin scale (Posamentier and Vail, 1988), such as in the Scotian Basin. Studies that have focused on the Cenozoic sea-level and how it has affected stratigraphic evolution have generally been skeptical of the accuracy of the Haq curve for this time period (Miller et al., 1996, 1996; Brown et al., 1996).

It has been recognized that the deep-sea sediments of the Cenozoic contain a proxy for a suggested glacially-driven eustatic change (glacioeustasy), which is recorded by the oxygen isotope record from benthic foraminifera deposited in deep-sea sediments

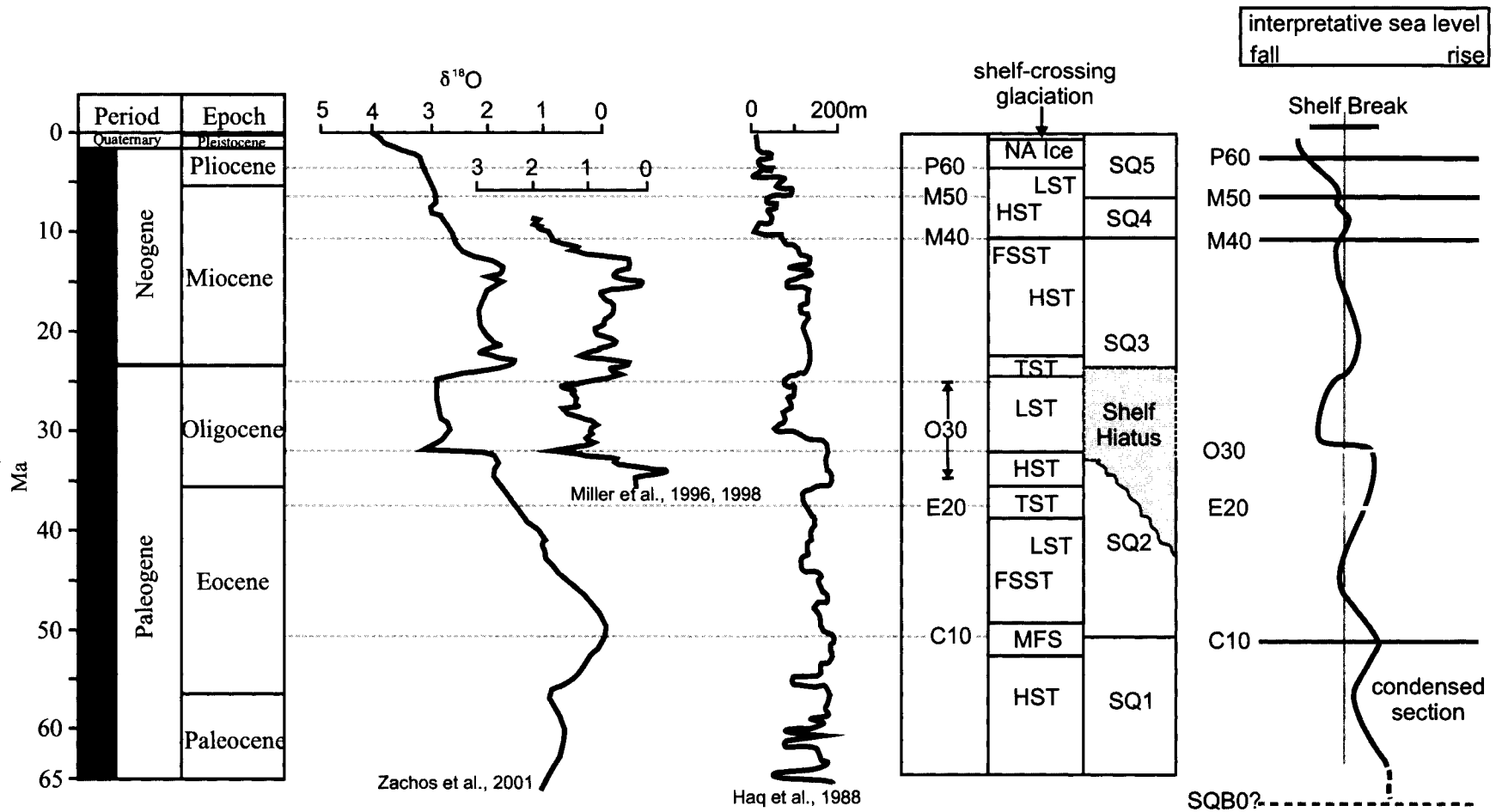


Figure 7.1. Three oxygen isotope curves derived from global data (Zachos et al., 2001) and from the New Jersey Margin (Miller et al., 1996, 1998) as well as, the global eustatic curve from Haq et al. (1988) derived on the basis of sequence stratigraphy. Sea-level curves are correlated to key reflectors and sequence stratigraphic interpretations of relative sea-level from this study.

(Broecker and Van Donk 1970; Imbrie et al. 1984; Christie-Blick et al. 1998; Miller et al. 1998; Zachos et al. 2001). Since the early 1970's, ^{18}O isotope data served as the principal means for reconstructing global and regional climate change variability (Zachos et al. 2001). Glacio-eustasy is controlled by the ratio of global ice volume to free water through the formation of polar ice sheets since the late Eocene (Browning et al. 1996). Fluctuations in global ice volume causes change in sea-level, which are reflected in the oxygen isotope record (Miller et al. 1998). The formation of polar ice caps in the Eocene (Miller et al., 1998) and Oligocene (Zachos et al., 2001) (both still debated) increased the amount of ^{18}O in the oceans, as lighter oxygen isotopes (^{16}O) are preferentially sequestered by evaporation. Thus, higher ratios of $^{18}\text{O} / ^{16}\text{O}$ correlate with sea-level falls (Broecker and Van Donk 1970; Imbrie et al. 1984; Browning et al. 1996; Miller et al. 1998). When ice melts, sea-level rises and $^{18}\text{O} / ^{16}\text{O}$ ratios decrease. Oxygen isotopic records are multidimensional in that they provide a mechanism to make both climatic and stratigraphic predictions that are correlated with observations made in this study. Two oxygen isotope curves are used in this study for the purpose of correlation: (1) from the New Jersey margin (Miller et al., 1998) and (2) a compilation of isotopic records from ODP and DSDP sites around the world to form a proxy-eustatic record of the complete Cenozoic (Zachos et al., 2001) (Figure 7.1).

Key reflectors (sequence boundaries) from the study area were correlated to the eustatic Haq curve in Chapter 4.2 (see Figures 4.8- 4.12). Relative positions of reflections were based on inflections on the sea level curve and biostratigraphy age-dates (Table 4.1). Comparison of the oxygen isotope curves from the New Jersey margin (NJM) (Miller et

al, 1998) and the global data, (Zachos et al., 2001) with the eustatic Haq curve shows similarities and differences (Figure 7.1).

For the purpose of discussion, an interpretative sea-level curve has been made for this study area (central Scotian Slope). Sea-level interpretation is based on the interpretation of stratigraphic architecture, paleo-shelf breaks and sequence stratigraphy (Figure 7.2).

7.1.1 Paleocene through Early Eocene

The earliest package recognized in this study is Sequence 1, bound by SB0 (the Wyandot marker) and SB1(the C10 reflection). These were respectively dated as Late Cretaceous (Wyandot) (McIver 1972; Jansa and Wade 1975; Wade and MacLean 1990; MacLean and Wade 1993; Kidston et al. 2002) and early Eocene (this study). Sequence 1, is a Paleogene prograding paleo-outer shelf delta of early Eocene HST deposits that comprises of smaller order cycles. Slope deposits from Wyandot to C10 consist of a condensed deepwater section of probable carbonate-rich muds. Correlation to sea-level curves is consistent with stratigraphic interpretations of a highstand sea-level that lasted from the early Paleogene to the end of the early Eocene (Figure 7.1). The C10 reflector is recognized as a MFS at the end of the prolonged formation of a HST and a FSST in Sequence 1.

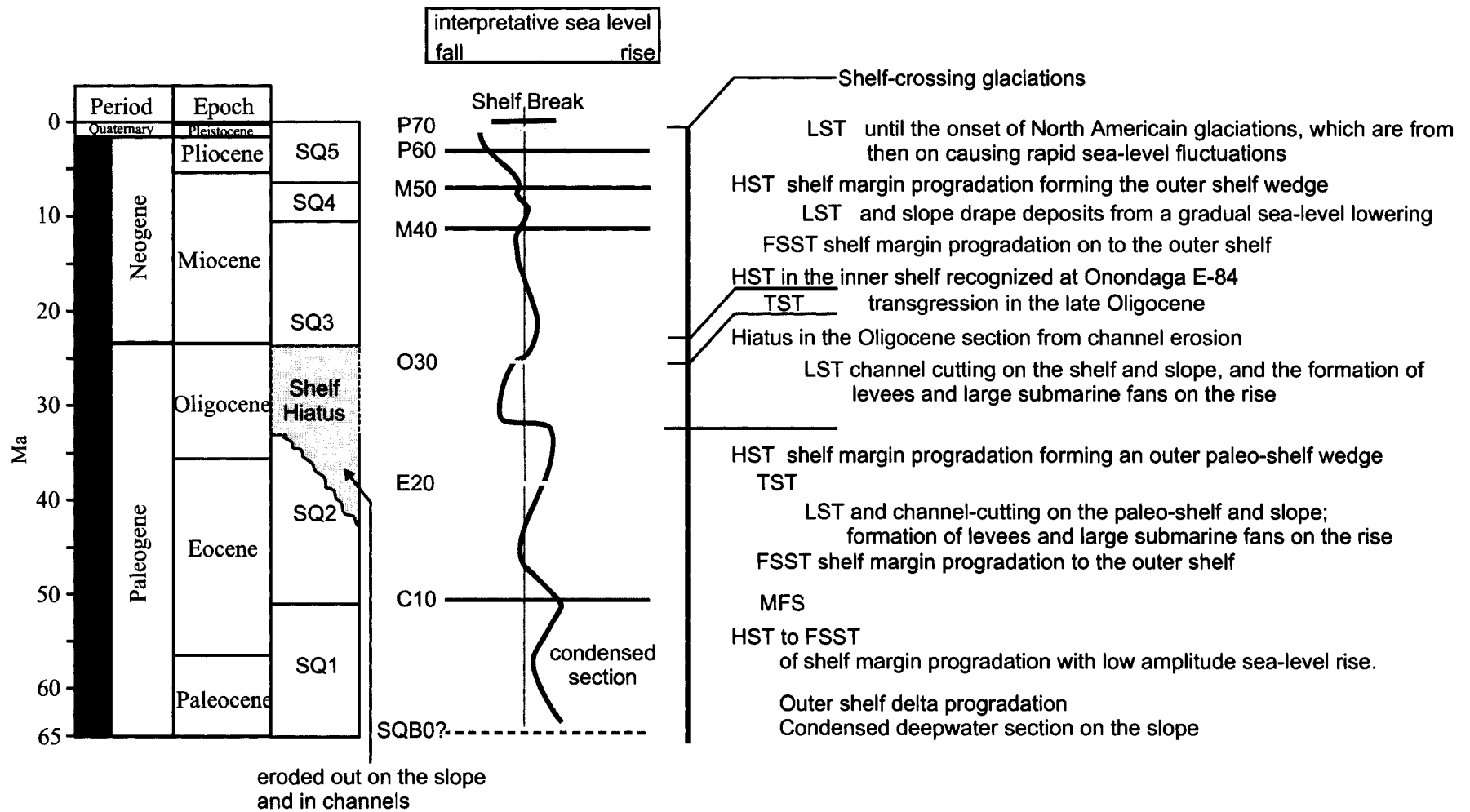


Figure 7.2. Interpretive sealevel curve in relation to the study. Interpretation is based on stratigraphic architecture, paleo-shelf breaks and sequence stratigraphy.

7.1.2 Early Eocene through middle Early Oligocene

Sequence 2 was formed in the Early Eocene through the middle Early Oligocene. From the Early Eocene to the mid Late Eocene (E20), a FSST is inferred to have developed on the inner shelf. Early Eocene LST submarine fans were deposited on the paleo-middle slope, followed by a TST that developed as a package of onlapping and aggrading reflections on the upper paleo-slope above the submarine fan deposits (Figure 4.6). The E20 reflection represents a Middle Eocene TST. A relatively low amplitude sea-level rise corresponding to E20 is recognized from the Early Eocene to the Middle Eocene on the eustatic curves (Figure 7.1). From the Middle Eocene to the middle Early Oligocene, a FSST developed on the paleo-outer shelf. Reflection dip of the FSST, on the paleo-outer shelf, is at a relatively low angle to low amplitude outer shelf sigmoid reflections of Sequence 1 and 3, indicating a gradual sea-level fall through the Late Eocene, which is consistent with sea-level curves to date (Figure 7.1).

7.1.3 Middle Early Oligocene to end Middle Miocene

The middle Early Oligocene to end Middle Miocene is recognized in this study as Sequence 3. A LST developed above the O30 reflector, but its precise age is unknown. This LST is interpreted to be the result of a sea-level drop in the middle Early Oligocene. The O30 reflector, base of Sequence 3, is recognized throughout the study area as an Oligocene unconformity. It corresponds to an abrupt drop in sea-level during the middle

Early Oligocene recognized as a sharp inflection point on oxygen isotope curves and on the Haq sea-level curve. The middle Early Oligocene was a lowstand period with channel incision on the paleo-outer shelf and erosional bypass on the paleo-slope. Channel cutting on the paleo-shelf edge and -upper slope removed most, and in some cases all, of the Late Eocene to Oligocene section, creating a hiatus in the stratigraphic record of the central Scotian Slope in the study area and other areas of the margin (Wade and MacLean 1990; MacLean and Wade 1993; Wade et al. 1995) (Figure 7.1). This Oligocene unconformity is recognized as the O30 reflection. Between the middle Early Oligocene and the Late Oligocene, channelized flow in the paleo-outer shelf and upper slope deposited sediment to the paleo-middle and lower slope in overbank levee deposits and later as submarine fans infilling minibasins. During the LST of the late Early and Late Oligocene, sediment bypassed the upper slope and was likely deposited on the continental rise in large (<100 km), passive-margin-scale submarine fans.

Near the end of the Oligocene, a sharp rise in sea-level is recognized on the oxygen isotope curves and the Haq sea-level curve (Figure 7.1). This ended LST deposition on the paleo-slope and generated a transgression surface (TST) (Figure 4.10). Sometime in the late Oligocene to earliest Miocene, infilling of channels occurred in correlation with the general rise in sea-level (Figure 7.1). The formation of an inner shelf HST (Figure 4.10), as discussed in Chapter 4.3, is recognized around the Onondaga E-84. Late Oligocene deposition on the slope of submarine fans and / or levee deposits (Figure 5.2) continued to develop as some of the largest Oligocene channels remained open during the

Miocene, as seen in industry 2-D seismic reflection profiles directly adjacent to the 3-D survey coverage.

In the early Middle Miocene, a sea-level fall (Figure 7.1) produced a basinward shift below the present inner shelf with a FSST recognized through seismic observations on the paleo-outer shelf (Figure 4.10). The FSST migrated over the LST on the paleo-slope during the Middle Miocene. In the Middle Miocene, FSST sedimentation filled any remaining Oligocene channels on the paleo-outer shelf and upper slope that remained open through the Early Miocene. Sea level curve interpretations of the Early Miocene through to the end of the Middle Miocene indicate a relatively still sea-level until the Middle Miocene.

During the middle Early Oligocene to the end of the Middle Miocene time period, sediment waves developed from overbanking turbidity flows from Oligocene channels that cut the outer shelf and upper paleo-slope. Some of the largest (700 ms twtt) Oligocene channels remained active into the early Miocene. These paleo-channels back filled with the Late Oligocene TST and continued to fill while sea-level remained relatively still through to the Middle Miocene (Figure 7.1) On the lower paleo-slope, contourite drift packages accumulated in the Early Miocene through the late Middle Miocene. Sediment drifts on the lower Scotian Slope are most likely related to the Western Boundary Undercurrent, recognized to have been in effect from the Oligocene through the early Miocene (Carter and Schafer 1983; McCave and Tucholke 1986;

Davies et al. 2001) and related to similar deep water drift deposits across the eastern margin (Piper et al. 2005).

Generally, sedimentation of Sequence 3 is recognized as Middle to Late Oligocene lowstand wedge deposits that formed by ponding sediment in minibasins during the LST on the lower paleo-slope. Sediment waves formed in the same time period on the upper paleo-slope and are due to overbanking turbidity flows from Oligocene channels that were active since the middle Early Oligocene to end Middle Miocene. Sediment drift packages are also recognized below the modern day lower slope above salt highs. These are associated with the onset of bottom currents and are controlled by the availability of sediment being delivered to the lower paleo-slope during the Late Oligocene.

During most of the Oligocene, the paleo-outer shelf was under a period of hiatus in which erosion removed the majority of Oligocene record and transported it downslope. From the Latest Oligocene to the early Middle Miocene, Sequence 3 is recognized as a HST on the inner paleo-shelf and is interpreted as corresponding to a period of minimal sedimentation on the paleo-outer shelf and paleo-slope. During the Middle Miocene, the paleo-outer shelf was a FSST of shelf margin regression that migrated over the TST recognized on the paleo-slope.

7.1.4 End Middle Miocene to Latest Miocene

The late Middle Miocene to latest Miocene is recognized in this study as Sequence 4. From the end of the Middle Miocene, sea-level curves correlate to a gradual sea-level lowering that continued through the Late Miocene (Figure 7.1). A FSST developed across the paleo-outer shelf in the Late Miocene and an ensuing LST developed on the paleo-slope. Paleo-slope facies during this time period consisted of large packages of slope drape, indicative of a low sediment input and distal sedimentation. These sedimentation rates and facies types are consistent with a deepwater FSST section. As sea-level continued to fall in the Late Miocene, the shelf margin prograded proximal to the paleo-shelf edge and maximized deposition on the paleo-slope. Steeply dipping reflections (Figure 4.11) on the paleo-outer shelf and upper paleo-slope are indicative of the shelf margin wedge system tract that developed at that time. Between the area extending the paleo-outer shelf and middle paleo-slope, almost no sediment accumulated. It is suggested that there was a sediment bypass zone in the latest Miocene on the upper paleo-slope, which was affected by nearshore currents, and which only allowed minimal sediment accumulation. Sequence Boundary 4 (M50) truncates underlying strata and onlaps Sequence Boundary 3 (M40) below the top of the middle paleo-slope. The age of the M50 reflection roughly corresponds to a small rise in sea-level, noted on the Haq and oxygen isotope curves of Figure 7.1. A sea-level rise in the Late Miocene possibly indicates a TST surface at the end of Sequence 4. In amplitude surface extraction of the M50 reflection, possible indications of bottom current activity are recognized.

7.1.5 Latest Miocene to end Quaternary

The latest Miocene to end Quaternary is recognized as Sequence 5. Although no Quaternary bounding unconformity is recognized in this study, the base of glacial till is an erosion surface and a deeper unconformity of proglacial outwash over the Banquereau Formation, recognized on the shelf (King and MacLean 1976; King and Fader 1986). Sequence Boundary 4 (M50) amplitude extraction shows slope parallel striations of higher and lower amplitude contrast (Figure 5.9). These striations suggest that a possible paleo-current was in affect and acted as a scouring mechanism giving cause to little sedimentation during the end of the Miocene. Sea-level lowering suggests that these amplitude striations are related to currents generated possibly in response to the strengthening of the Labrador or Western Boundary Undercurrent. Sea-level curve interpretation shows a continuous lowering of sea-level with a sharp drop in the Late Pliocene (Figure 7.1).

A FSST was formed due to this relative drop in sea level. After a short and relatively small rise in the latest Miocene, erosion on the paleo-outer shelf and upper paleo-slope occurred in the Early to Middle Pliocene, below the P60 reflection. In effect, the increased sediment accumulation on the paleo-outer shelf and upper paleo-slope may have generated instability on the upper paleo-slope. Sediment failures in the Latest Miocene through the Early Pliocene wasted to the middle and lower paleo-slope, forming stacked packages of MTDs and associated scarps (Figure 4.5). Lowstand reflection stratigraphy of the latest Miocene to Middle Pliocene has generally been obliterated on

the slope by subsequent canyon cutting. Early Pliocene LST reflections of onlapping strata are still recognized in some areas of the central slope not affected by erosion.

From the base of the Middle Pliocene onward, proglacial deposition (approximately 100-200 mbsf) on the slope has been characterized by an alteration of sandy and muddy layers. Deposition on the paleo-slope during this time was controlled by the fluctuation of sea-level. Interbedded periods of increased shelf margin prodeltaic deposition during highstand periods only permitted muddy deposition on the slope. During periods of lowstand, sandier facies delivered to the paleo-slope by shelf-crossing outwash were deposited. This deposition may have made the upper paleo-slope relatively unstable as increased sedimentation rates caused progradation onto the slope gradient. It is suggested that such variable mixing of depositional and differential loading on the paleo-slope is related to the interbedded, relatively small scale MTDs recognized across the slope from the latest Miocene to the Seafloor Reflection Boundary.

The onset of proglacial slope drape began at the end of the Late Pliocene (P70) with shelf-crossing glaciation. Paleo-outer shelf deposits of the Pleistocene are glacial tills which often reached as far seaward as the upper paleo-slope. Proglacial prodeltaic deposition dominated across the central slope with periods of channel cutting on the upper paleo-slope and shelf. Deeply incising canyons cut the paleo-slope from the Pleistocene to the beginning of the Holocene with the melting and retreat of the Wisconsinan ice sheet (King and Fader 1986; Stea et al. 1998). Various stages of

channel / canyon growth and re-growth are recognized with the waxing and waning of shelf-crossing ice sheets.

7.2 Timing of salt movement in relationship to the stratigraphic architecture

Salt tectonics played a major role in the mode of sedimentation on the Scotian Slope. Scotian Basin salt is part of the Triassic-Jurassic Argo Formation (Figure 1.3). Down-dip gravity sliding due to sediment loading on the prograding Scotian Shelf is considered the primary mechanism for salt movement. This study area falls into Subprovince 3 of Shimeld (2004) and Wade and MacLean (1995), which is described as allochthonous tongue canopies overlying Lower Cretaceous units (Figure 7.3). These authors suggested that salt tectonics was active in the Cenozoic during the Miocene and is still active today. Evidence from the present study shows a similar result. Uplifted post-Oligocene strata observed in seismic reflection profile display structural reorganization above salt diapirs and tongues through extensional spreading at dome crests, crestal grabens and outward extensional normal faulting (Figure 3.4). Cenozoic salt movement features in the study area can only be locally correlated and show little to no regional pattern. Inferences on salt mobility and timing are made based on stratigraphic architecture and are correlated with the sequence stratigraphy units discussed previously in Chapter 7.1.

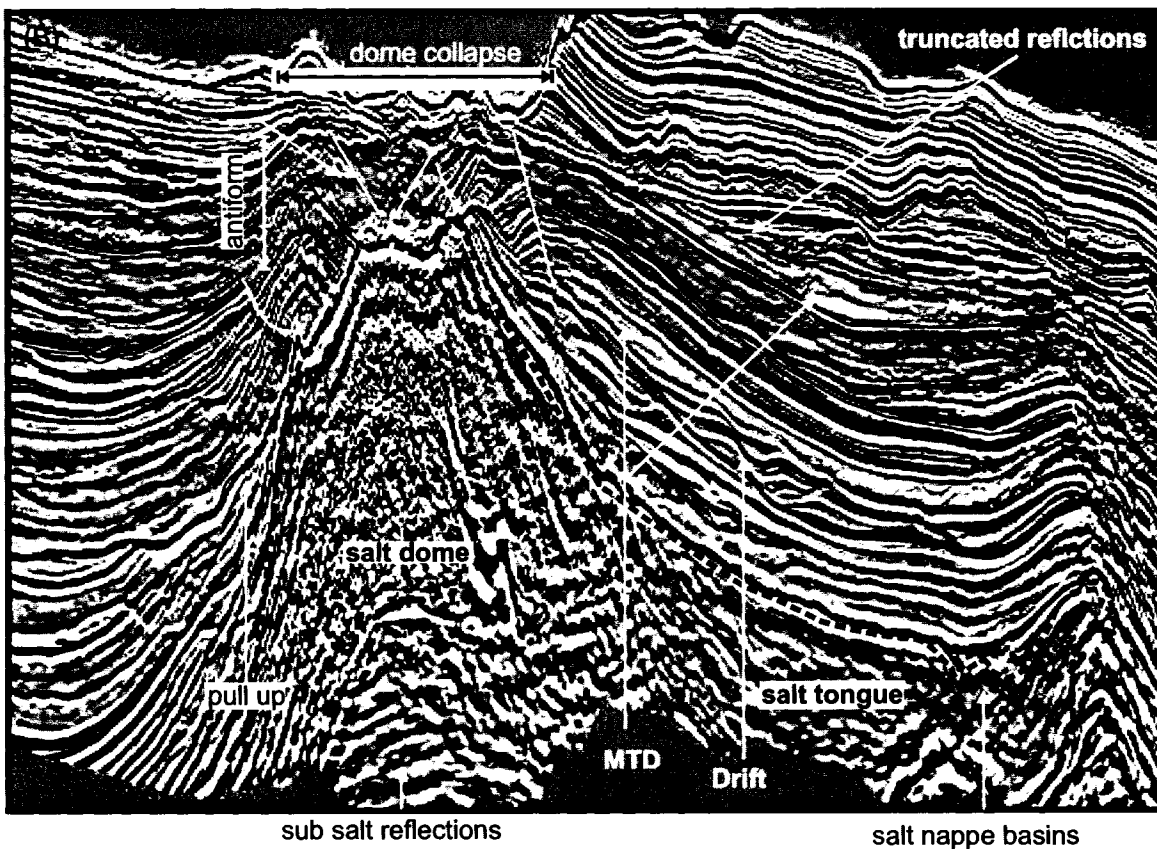
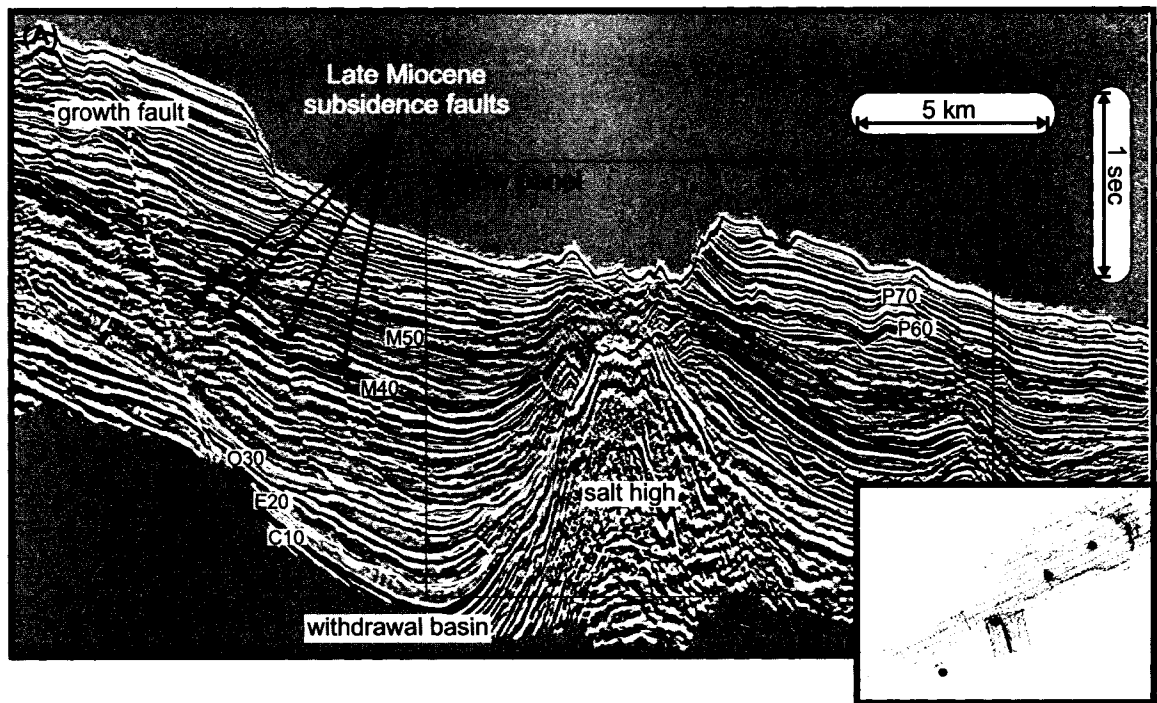


Figure 7.3. (A) Seismic reflection dip profile through the middle of the study area, with features described in text relative to key seismic reflections. (B) features such as frictional drag (pull up), salt domes and tongues, antiform structures and dome crest collapse. MTD source is from out of page.

7.2.1 Paleogene

The stratigraphic architecture of Sequence 1 suggest that salt was in place below the lower paleo-slope in the Early Cenozoic. During this time, the Scotian Shelf was loaded with prograding deltas in the HST of Sequence 1. It is likely that a salt diapir was already in place in the Late Cretaceous in association with a slope withdrawal basin. From the Paleogene to the Middle Eocene, sediment accumulation rates were low in the minibasins. During the LST of the late Middle Eocene there was an increased sediment accumulation in the minibasins, which caused an increase in salt withdrawal, and is indicated by movement along growth faults (Figure 7.3). During the Middle Eocene to the Late Oligocene LST, sedimentation on the paleo-slope was preferential into the minibasins (Figure 7.4). During this time period the increased filling and loading of minibasins likely caused or contributed to the uplift of salt, and to the possible seaward movement of a salt tongue towards the lower paleo-slope.

From the Late Oligocene to the end of the Middle Miocene (Sequence 3), stratigraphic architecture indicates that a salt tongue was in place on the lower paleo-slope, creating a bathymetric high. A contourite sediment drift package accumulated on the upslope flank of and an antiform developed above this high in relation to bottom currents. Elsewhere in the study area, drift packages are not recognized beneath the lower slope, suggesting preferential conditions for the plastering of drift along this bathymetric high.

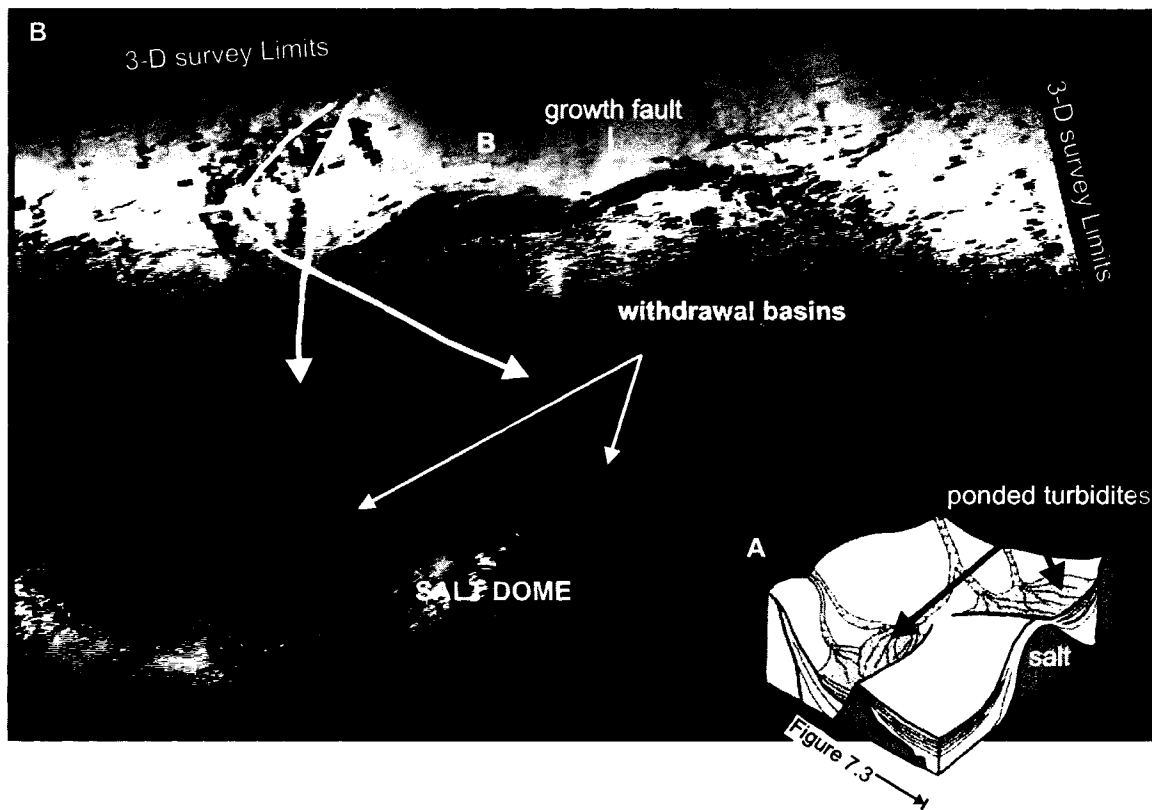
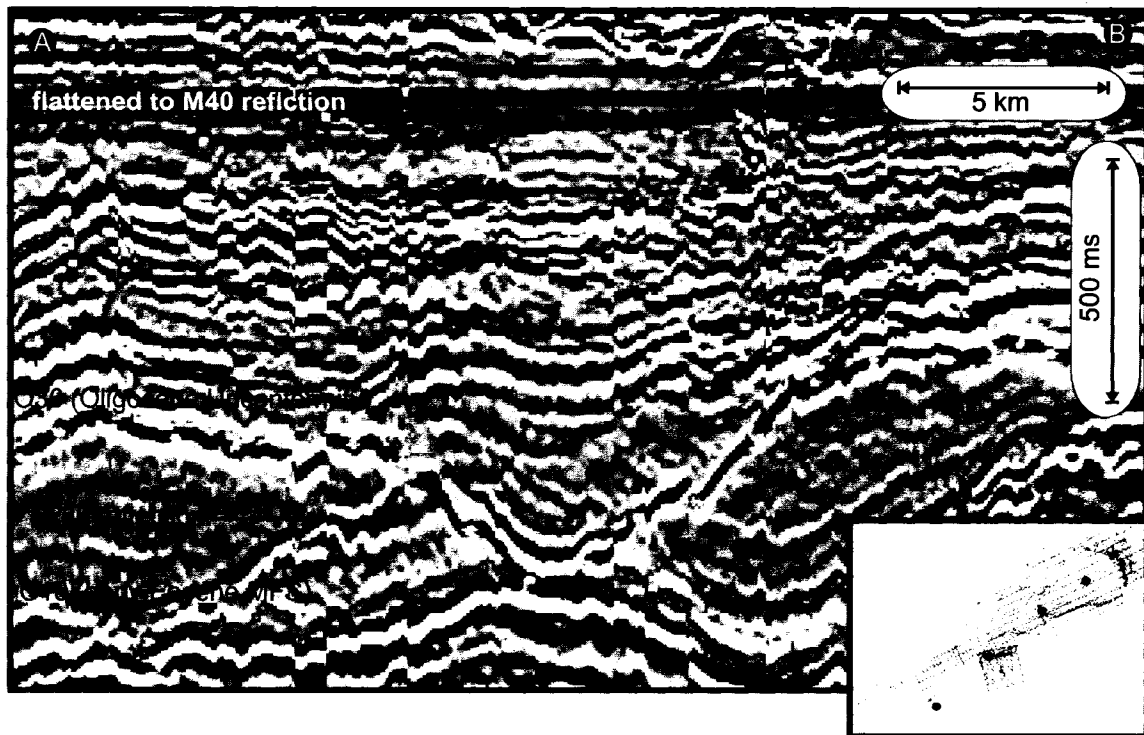


Figure 7.4. (A) Seismic reflection profile across a Oligocene channel. (B) time surface render of the O30 reflection indicating preferential deposition into salt withdrawal basin from channel flow. Inset: Similar observations made by Booth et al., 2003 in the Gulf of Mexico and analogous to Figure 7.3.

7.2.2 Neogene

Middle Oligocene to late Middle Miocene (Sequence 3) sediments filled a large part of the withdrawal basins beginning in the late Oligocene until the Middle Miocene. As sediment was ponded into the minibasins, growth faults on their outer edges were rejuvenated. With relative minibasin subsidence, a period of salt rejuvenation also occurred. Salt uplift rose until almost reaching the seafloor by the middle Early Miocene. Seafloor relief due to salt uplift in the Early to Middle Miocene is indicated by packages of thinning reflection towards the crest, which were later faulted and offset seaward.

From the Early Miocene to the Late Middle Miocene, minibasins were mostly full, and salt was not mobile having come close to, or reaching the seafloor. In the Late Miocene, a rejuvenation of salt mobility occurred. It is inferred that this salt rejuvenation is related to the complete filling of the minibasins by the Middle Miocene and to the exhaustion of the subsurface salt supply. In effect, a collapse of the salt diapir and downward withdrawal occurred in the latest Miocene, tilting Late Miocene through Oligocene reflections seaward above the salt tongue. Furthermore, the onset of MTDs in the middle and lower paleo-slope during the latest Miocene indicate a possible trigger mechanisms for MTCs, which have been recognized by others to be caused by ground accelerations due to salt tectonics (Piper et al. 1985; Gauley 2001; Piper and Ingram 2003; Mosher et al. 2004). MTDs are noted to preferentially fill basin lows. However, on the lower paleo-slope, they are seen in uplifted strata, indicating post-depositional uplift constrained to the Miocene section (Figure 7.3). Proglacial slope drape from the end of the Miocene through the

Pliocene is minimally affected by subsurface salt in the study area. Directly above salt highs, reflections are distorted, but otherwise thin as they drape the salt highs.

Canyon erosion during the proglacial period of the Pleistocene occurred in areas of minimal salt uplift, inferring the deflection of paleo-flow due to salt highs. Fault offsets around minibasins are relatively minimal compared to earlier sections implying, movement through the Quaternary.

8. Conclusions

This study explored the stratigraphic architectural evolution of the outer central Scotian Shelf and Slope and the stratigraphic relationships between the two depositional environments.

A composite seismic-stratigraphy based on a 3-D seismic volume around the Weymouth A-45 wellsite and adjacent 2-D seismic reflection data was completed for the central Scotian Slope. This stratigraphy is age constrained through the last 55 Ma. Seven key reflectors are recognized across the study area in 3-D and 2-D seismic reflection data, which are correlated to biostratigraphic ties in 4 offshore wells. The reflections are respectively dated as Early Eocene, middle Late Eocene, approximately middle Oligocene, late Middle Miocene, Late Miocene, Middle Pliocene and Late Pliocene. Key reflectors can be placed into five stratigraphic sequences constrained by unconformities below the modern day slope and outer shelf. Reflection geometries are put into the sequence stratigraphic context of highstand, lowstand, falling stage and transgressive system tracts, with maximum flooding surfaces. Highstand system tracts are generally recognized on the slope as condensed sections of reflections and as clinoform prograding deltas on the middle to outer shelf. Falling stage system tracts are recognized above maximum flooding surfaces by the basinward shift in onlapping gently dipping prograding reflections on the outer shelf to upper slope. Lowstand system tracts show onlapping and aggrading reflections against the slope face and correlate to paleochannel incision on the outer shelf and slope, with associated submarine fan and turbidite deposits.

Generally, highstand system tracts and lowstand system tracts on the slope are separated by an unconformable transgression surface and a package of onlapping and aggrading reflections that have transgressed upslope. In periods of sharp sea-level fall, erosion removes complete sections of the stratigraphic record.

During periods of low sea-level, in the Middle Eocene and middle Oligocene, the paleo-outer shelf and upper slope were cut by channel erosion. Channel flow preferentially entered salt withdrawal basins, depositing submarine fans and turbidites which accumulated into lowstand wedges. During periods of high sea-level and sea-level lowering in the Early Eocene, late Middle and Late Miocene, sedimentation rates decreased on the paleo-slope with distal and muddy facies draping and onlapping it. Deltas or shelf margin progradation built seaward on the paleo-outer shelves.

In the Oligocene and Miocene, bottom currents affected the central Scotian Slope. Sediment drift in the Oligocene section indicates that currents existed on the lower slope, and deposition was then favored on bathymetric highs generated by subsurface salt. Bypass zones recognized in the Late Miocene with evidence of current scours are likely related to paleoceanographic currents that swept the paleo-outer shelf and slope from the middle Oligocene to the Late Miocene.

The study area was characterized by short-lived sea-level rises and falls from the Late Miocene to the end of the Pliocene. This time period was marked by high sedimentation rates, canyon cutting events, and by the infilling of the lowermost slope basin. These sea-

level fluctuations were related to the waxing and waning of glaciers in Antarctica, Greenland, Europe and North America. Great amounts of proglacial outwash accumulated on the paleo-shelf and –slope during this time period. Shelf-crossing glaciations began in the Middle to Late Pleistocene and deposited up to 200 meters of glacial prodeltaic sediments, which draped across the slope. These deposits were later cut by glacial melt waters, resulting in the formation of canyon systems and a dendritic pattern of seafloor morphology still recognized today.

Salt tectonics were active in the Early Eocene, Late Oligocene, Late Miocene, and most probably today. These periods of activity were associated with preferential deposition into minibasins during periods of channel flow in the Middle Eocene, Middle Oligocene and Early Miocene, suggesting that minibasin loading contributed to the driving mechanisms for uplifting strata, but also generated minibasin subsidence along growth faults. Salt collapse in the latest Miocene to Middle Pliocene indicated a pause in diapirism. During proglacial canyon cutting events in the Pleistocene, salt highs deflected channel and canyon flow. Generally, areas of uplift became the intra canyon areas, where canyon incision was minimal if present. Unfortunately, intra-canyon areas are not complete packages of Cenozoic strata but are zones of stratigraphic uplift where strata thin. Stratification on the slope are structurally reorganized with respect to the regional architecture, or are ponded in withdrawal basins as turbidites and MTDs.

In summary, the evolution of the central Scotian outer Shelf and Slope can be constrained within at least five sequences which are age constrained by biostratigraphic data and

correlated to paleoceanographic sea-level changes. Intra-canyon regions below the central Scotian Slope are generally salt cored, and their Cenozoic stratigraphy is not complete due to the influence of salt tectonics during and after deposition. Overall, the stratigraphic architecture of the central Scotian Slope is recognized as having: 1) stratigraphic development influenced by sea-level changes; 2) salt tectonics active through the Cenozoic which influenced deposition and stratigraphic evolution; and 3) evidence for paleoceanographic currents during the Oligocene on the lower slope and across the slope in the Late Miocene.

REFERENCES

- Barnes, P. M., 1992, Mid-bathyal current scours and sediment drifts adjacent to the Hikurangi deep-sea turbidite channel, eastern New Zealand; evidence from echo character mapping: *Marine Geology*, v. 106, p. 169-187.
- Barss, M. S., Bujak, J. P., and Williams, G. L., 1979, Palynological zonation and correlation of sixty-seven wells, eastern Canada, Dartmouth, Geological Survey of Canada, p. 118.
- Beaubouef, R. T., and Freidman, S. J., 2000, High resolution/sequence framework for the evolution of Pleistocene intra slope basins, Western Gulf of Mexico: depositional models and reservoir analogues: GCSSEPM Foundation Bob F. Perkins 20th Annual Research Conference, Houston, Texas, p. 82-103.
- Bolli, H. M., and Saunders, J. B., 1985, Oligocene to Holocene low latitude planktic foraminifera, *in* Saunders, J. B., and Perch-Neilsen, K., eds., *Plankton Stratigraphy*: Cambridge Earth Science Series, Cambridge, UK, Cambridge University Press, p. 155-262.
- Bouma, A. H., 1969, *Methods for the study of sedimentary structures*: New York, Wiley - Interscience, 458 p.
- Broecker, W., and Van Donk, J., 1970, Insolation changes, ice volumes and the ^{18}O record in deep-sea cores.: *Reviews of Geophysics and Space Physics*, v. 8, p. 169-198.
- Brown, L. F., and Fisher, W. L., 1980, *Seismic Stratigraphic Interpretation and Petroleum Exploration: Continuing Education*, v. 16: Austin, American Association of Petroleum Geologists.

- Browning, J. V., Miller, K. G., and Pak, D. K., 1996, Global implications of Eocene Greenhouse and Doubthouse sequence on the New Jersey Coastal Plain - The Icehouse cometh: *Geology*, v. 24, p. 639-642.
- Carter, L., and Schafer, C. T., 1983, Interactions of the Western Boundary Undercurrent with the continental margin off Newfoundland: *Sedimentology*, v. 30, p. 751-768.
- Chevron Canada Ltd, 2007, Newburn H-23 WELL HISTORY REPORT, Dartmouth, Nova Scotia, CNSOPB, unpublished report, record file 300 H23 43200 60450.
- Christie-Blick, N., Austin, J. A., Jr., and Shipboard Scientific Party, 1998, Introduction: Oligocene to Pleistocene eustatic change at the New Jersey continental margin - a test of sequence stratigraphy, *Proceedings of the Ocean Drilling Program, Initial reports, ODP*, p. 5-16.
- Cochonat, P., Ollier, G., and Michel, J. L., 1989, Evidence for slope instability and current-induced sediment transport, the RMS Titanic wreck search area, Newfoundland Rise: *Geo-Marine Letters*, v. 9, p. 145-152.
- Crane, G., 2003, Framework, Architecture and Exploration Potential of the Tertiary Strata - Offshore, Southwestern Nova Scotia (abstract): *AAPG Annual Meeting 2003: Energy - Our Monumental Task*.
- Davies, R., Cartwright, J., Pike, J., and Line, C., 2001, Early Oligocene initiation of North Atlantic Deep Water formation: *Nature*, v. 410, p. 917-920.
- Davison, I., Alsop, G. I., and Blundell, D. J., 1996, Salt tectonics: Some aspects of deformation mechanics, *in* Alsop, G. I., Blundell, D.J., Davidson, I., ed., *Salt tectonics*, London, Geological Society Special Publication 100, p. 1-10.

- Davison, I., Alsop, I., Birch, P., Elders, C., Evans, N., Nicholson, H., Rorison, P., Wade, D., Woodward, J., and Young, M., 2000, Geometry and late-stage structural evolution of Central Graben salt diapirs, North Sea: *Marine and Petroleum Geology*, v. 17, p. 499-522.
- Deptuck, M. E., 2003, Post-rift geology of The Jeanne D'Arc Basin, with a focus on the architecture and evolution of early Paleogene submarine fans, and insights from modern deep-water systems: Unpub. PhD thesis, Dalhousie University 369 p.
- Deptuck, M. E., Steffens, G. S., Barton, M., and Pirmez, C., 2003, Architecture and evolution of upper fan channel-belts on the Niger Delta slope and in the Arabian Sea: *Marine and Petroleum Geology*, v. 20, p. 649-676.
- EnCana, 2003, Canadian Offshore Petroleum Board, Geophysical Program Record: NS24-E43-02E, Dartmouth, CNSOPB.
- Ercilla, G., Alonso, B., Wynn, R. B., and Baraza, J., 2002, Turbidity current sediment waves on irregular slopes: observations from the Orinoco sediment-wave field: *Marine Geology*, v. 192, p. 171-187.
- Fader, G. B., 1991, Surficial geology and physical properties 3: subsurface features, East Coast Basin Atlas Series: Scotian Shelf, Atlantic Geoscience Centre, Geological Survey of Canada, p. 115.
- Fensome, R., 2000, Palynological Analysis of Shell et al. Shubenacadie H-100 well, Scotian Slope, Internal report, Dartmouth, Nova Scotia, Geological Survey of Canada Atlantic internal report, p. 7.
- Fulthorpe, C. S., and Carter, R. M., 1991, Continental-shelf progradation by sediment-drift accretion: *Geological Society of America Bulletin*, v. 103, p. 300-309.

- Gauley, B. L., 2001, Lithostratigraphy and sediment failure on the Scotian Slope.:
Unpub. M.Sc. thesis, Dalhousie University 214 p.
- Haq, U. B., Hardenbol, J., and Vail, P. R., 1987, Chronology of Fluctuating Sea Levels
since the Triassic: *Science*, v. 235, p. 1156-1166.
- Hardenbol, J., Thierry, J., Farley, M. B., Jacquin, T., de Graciansky, P. C., and Vail, P.
R., 1998, Mesozoic and Cenozoic Sequence Chronostratigraphic Framework of
European Basins, *in* de Graciansky, P. C., ed., *Mesozoic and Cenozoic Sequence
Stratigraphy of European Basins.*, SEPM Special Publication, no. 60, p. 3-13.
- Hart, B. S., 1999, Definition of subsurface stratigraphy, structure and rock properties
from 3-D seismic data: *Earth Science Reviews*, v. 47, p. 189-218.
- Hogg, J., 2000, The Scotian Basin, New Exploration Trends for the next decade,
Offshore Nova Scotia: *GeoCanada 2000*, Abstract No. 1096, p. 4.
- Hughes Clarke, J. E., O'Leary, D. W., and Piper, D. J. W., 1992, Western Nova Scotia
continental rise: relative importance of mass wasting and deep boundary-current
activity, *in* Poag, C. W., and deGraciansky, P. C., eds., *Geologic evolution of the
Atlantic continental rise*, New York, vanNostrand Reinhold, p. 266-281.
- Imbrie, J., Hays, J. D., Martinson, D. G., McIntyre, A., Mix, A., Morely, J., Pisias, N. G.,
Prell, W., and Shackleton, N., 1984, The orbital theory of Pleistocene climate:
support from a revised chronology of the marine 18O record, *in* Berger, A.,
Imbrie, J., Hays, J. D., Kulka, G., and Saltzman, B., eds., *Milankovitch and
Climate*, Dordrecht, The Netherlands, Riedel, p. 269-305.
- Jansa, L. F., and Wade, J. A., 1975, Geology of the continental margin off Nova Scotia
and Newfoundland: *Geological Survey of Canada Paper 74-30*, Offshore geology
of eastern Canada, v. 2, p. 51-105.

- Kearey, P., and Brooks, M., 1991, *An introduction to geophysical exploration*: Oxford, Blackwell Scientific Publications, 254 p.
- Keith, B. L., and Pantin, H. M., 2002, Channel-axis, overbank and drift sediment waves in the southern Hikurangi Trough, New Zealand: *Marine Geology*, v. 192, p. 123-151.
- Kennett, J. P., 1982, Sea-Level History and Seismic Stratigraphy, *in* Caughey, E. W., ed., *Marine Geology*, New Jersey, Prentice-Hall Inc., p. 752.
- Kidston, A., Brown, D., Alheim, B., and Smith, B., 2002, Hydrocarbon Potential of the Deep-Water Scotian Slope, Halifax, Canada-Nova Scotia Offshore Petroleum Board, p. 111.
- King, L. H., and Fader, G. B. J., 1986, Wisconsinan glaciation of the continental shelf, southeastern Atlantic Canada, *Geological Survey of Canada, Bulletin 363*, 72 p.
- King, L. H., and MacLean, B., 1976, *Geology of the Scotian Shelf*: Geological Survey of Canada Paper 74-31, *Marine Science Paper*, v. 7, p. 31.
- King, L. H., Rokoengen, K., Fader, G. B., and Gunleiksrud, T., 1991, Till-tongue stratigraphy: *Geological Society of America Bulletin*, v. 103, p. 637-659.
- Koyi, H., 1998, The shaping of salt diapirs: *Journal of Structural Geology*, v. 20, p. 321-338.
- Lee, H., Syvitski, J. P. M., Parker, G., Orange, D., Locat, J., Hutton, E., and Imran, J., 2002, Distinguishing sediment waves from slope failure deposits: field examples, including the 'Humboldt slide', and modelling results: *Marine Geology*, v. 192, p. 79-104.

- MacLean, B., and Wade, J., 1993, Seismic Markers and Stratigraphic picks in the Scotian Basin wells: East Coast Basin Atlas: Dartmouth, Geological Survey of Canada.
- Martini, E., 1971, Standard Tertiary and Calcareous Nannoplankton Zonation: Proceedings of the Second Planktonic Conference Roma, p. 739-785.
- McCave, I. N., and Tucholke, B. E., 1986, Deep current-controlled sedimentation in the western North Atlantic. Chapter 27, *in* Vogt, P. R., and Tucholke, B.E., ed., The Geology of North America, USA, Decade of North American Geology, p. 451-486.
- McIver, N. L., 1972, Cenozoic and Mesozoic Stratigraphy of the Nova Scotia Shelf: Canadian Journal of Earth Sciences, v. 9, p. 54-70.
- Miller, K.G, Liu, C., and Feigenson, M., 1996, Oligocene to middle Miocene Sr-isotopic stratigraphy of the New Jersey continental slope: Proceedings of the Ocean Drilling Program, Scientific Results, v. 150, p. 97-114.
- Miller, K. G., Mountian, G. S., Browning, J. V., Kominz, M., Sugarman, P. J., Christie-Blick, N., Katz, M. E., and Wright, J. D., 1998, Cenozoic global sea level, sequences, and the New Jersey transect: Results from coastal plain and continental slope drilling: Reviews of Geophysics, v. 36, p. 569-601.
- Migeon, S., 2000, Dunes Geantes et Levees Sedimenraires en domaine marin profond: Approches Morphologique, Sismique et Sedimentologique: Unpub. Docteur thesis, l'University Bordeaux I 287 p.
- Mitchum, R. M., Vail, P. R., and Thompson, S., 1977a, Seismic stratigraphy and global changes of sealevel, part 2: The depositional sequence as a basic unit for stratigraphic analysis, *in* Payton, C. E., ed., AAPG Memoir 26, Seismic stratigraphy - application to hydrocarbon exploration, Tulsa, Oklahoma, p. 53-62.

- Mitchum, R. M., Vail, P. R., and Sangree, J. B., 1977b, Seismic stratigraphy and global changes of sealevel, part 6: Stratigraphic interpretation of seismic reflection patterns in depositional sequences, *in* Payton, C. E., ed., AAPG Memoir 26, Seismic stratigraphy - application to hydrocarbon exploration, Tulsa, Oklahoma, p. 117-133.
- Mitchum, R. M., Vail, P. R., Todd, R. G., Widmier, J. M., Thompson, S., Sangree, J. B., Bubb, J. N., and Hatlelid, W. G., 1977a-b, Seismic stratigraphy and global changes of sealevel, *in* Clayton, C. E., ed., Seismic Stratigraphy - Applications to Hydrocarbon Exploration, Tulsa Oklahoma, American Association of Petroleum Geologists, p. 49-212.
- Mosher, D., Piper, D. J. W., Campbell, D. C., and Jenner, K. A., 2004, Near-surface geology and sediment-failure geohazards of the central Scotian Slope: AAPG Bulletin, v. 88, p. 703-723.
- Mosher, D., and Thomson, R. E., 2002, The Foreslope Hills: large-scale, fine-grained sediment waves in the Straight of Georgia, British Columbia: Marine Geology, v. 192, p. 275-295.
- Mosher, D., and Simpkin, P. G., 1999, Status and Trends of Marine High-Resolution Seismic Reflection Profiling: Data Acquisition: Geoscience Canada, v. 26, p. 174-188.
- Mosher, D. C., Moran, K., and Hiscott, R. N., 1994, Late Quaternary Sediment, Sediment Mass Flow Processes and Slope Stability on the Scotian Slope, Canada: Sedimentology, v. 41, p. 1039-1061.
- Mosher, D. C., Piper, D. J. W., Vilks, G., Aksu, A. E., and Fader, G. B., 1989, Evidence for Wisconsinan Glaciations in the Verrill Canyon Area, Scotian Slope: Quaternary Research, v. 31, p. 27-40.

- Mulder, T., and Moran, K., 1995, Relationship among submarine instabilities, sealevel variations and the presence of an ice sheet on the continental shelf: An example from the Verrill Canyon area, Scotian Shelf: *Paleoceanography*, v. 10, p. 137-154.
- Normark, W. R., Piper, D. J. W., Posamentier, H. W., Pirmez, C., and Migeon, S., 2001, Variability in form and growth of sediment waves on turbidite channel levees: *Marine Geology*, v. 192, p. 23-58.
- Normark, W. R., Hess, R., Stow, D. A. V., and Bowen, A. J., 1980, Sediment waves on the Monterey Fan levees: a preliminary physical interpretation: *Marine Geology*, v. 37, p. 1-18.
- North, F. K., 1985, Well Logs, *Petroleum Geology*, Allen and Unwin Inc., p. 127-151.
- Parker, T. J., and McDowell, A. N., 1955, Model Structures of Salt Dome Tectonics: *Bulletin of the American Association of Petroleum Geologists*, v. 39, p. 2384-2470.
- Pe-Piper, G., and Piper, D. J. W., 2004, The effects of strike-slip motion along the Cobequid - Chedabucto -southwest Grand Banks fault system on the Cretaceous - Tertiary evolution of Atlantic Canada: *Canadian Journal of Earth Sciences*, v. 4, p. 799-808.
- Pickrill, R. A., Piper, D. J. W., Collins, J. T., Kleiner, A., and Gee, L., 2001, Scotian Slope mapping project: the benefits of an integrated regional high-resolution multibeam survey: *Offshore Technology Conference*, Paper OTC 12995.
- Piper, D. J. W., 1988, Glaciomarine sedimentation on the Continental Slope off Eastern Canada: *Geoscience Canada*, v. 15, p. 23-28.

- , 2000, Pleistocene ice outlets on the central Scotian Slope, offshore Nova Scotia., Geological Survey of Canada, Current Research, no. 2000-D7, Ottawa, Geological Survey of Canada, p. 1-8.
- Piper, D. J. W., and DeWolfe, M., 2003, Petrographic evidence from the eastern Canadian margin of shelf-crossing glaciations: *Quaternary International*, v. 99-100, p. 99-113.
- Piper, D. J. W., and Ingram, S., 2003, Major Quaternary Sediment Failures on the East Scotian Rise, eastern Canada: *Current Research*, v. 2003-D1, p. 7.
- Piper, D. J. W., MacDonald, A., Ingram, S., Williams, G. L., and McCall, C., 2005, Late Cenozoic evolution of the St. Pierre Slope, offshore Newfoundland: *Canadian Journal of Earth Sciences*, v. in press.
- Piper, D. J. W., Mosher, D. C., and Newton, S., 2002, Ice-margin seismic stratigraphy of the central Scotian Slope, eastern Canada: Geological Survey of Canada, Current Research, no. 2002-E16, p. 1-10. (<http://www.nrcan.gc.ca/gsc/bookstore>).
- Piper, D. J. W., Mudie, P. J., Fader, G. B. J., Josenhans, H. W., MacLean, B., and Vilks, G., 1990, Quaternary Geology, *in* Keen, M. J., and Williams, G. L., eds., *Geology of the continental margin off Canada: Geology of Canada*, Geological Survey of Canada, p. 475-607 (also Geological Society of America, *The Geology of North America*, v. I-1).
- Piper, D. J. W., Normark, W. R., and Sparkes, R., 1987, Late Cenozoic Stratigraphy of the Central Scotian Slope, Eastern Canada: *Bulletin of Canadian Petroleum Geology*, v. 35, p. 1-11.

- Piper, D. J. W., Shor, A. N., Farre, J. A., O'Connell, S., and Jacobi, R., 1985, Sediment slides around the epicenter of the 1929 Grand Banks earthquake: *Geology*, v. 13, p. 538-541.
- Posamentier, H. W., and Allen, G. P., 1993, Variability of the sequence stratigraphic model: effect of local basin factors: *Sedimentary Geology*, v. 86, p. 91-109.
- , 1999, Fundamental Concepts of Sequence Stratigraphy, *in* Dalrymple, R. W., ed., *Siliclastic Sequence Stratigraphy - Concepts and Applications*, Tulsa Oklahoma, SEPM Special Publications, p. 9-51.
- Posamentier, H. W., Allen, G. P., James, D. P., and Tesson, M., 1992, Forced Regression in a Sequence Stratigraphic Framework: Concepts, Examples, and Exploration Significance, *AAPG Bulletin*, Tulsa, v. 76, p. 1687-1709.
- Posamentier, H. W., and Kolla, V., 2003, Seismic geomorphology and stratigraphy of depositional elements in deep-water settings: *Journal of Sedimentary Research*, v. 73, p. 367-388.
- Posamentier, H. W., and Vail, P. R., 1988, Eustatic Controls on Clastic Deposition II - Sequence and System Tract Models, Sea Level Changes - An Integrated Approach, SEPM Special Publications, p. 125-154.
- Roksandic, M. M., 1978, Seismic facies analysis concepts, *in* Roksandic, M. M., ed., *Geophysical Prospecting*, v. 26, p. 383-398.
- Shaw, J., and Courtney, R. C., 2002, Postglacial coastlines of Atlantic Canada: digital images: *Geological Survey of Canada Open File 4302*, p. 13.

- Shell Canada Resources Ltd., 1986, Glenelg N-49, WELL HISTORY REPORT, Dartmouth, Geological Survey of Canada Atlantic, unpublished report, GSCA file num.10276.
- Shimeld, J. W., 2004, A Comparison of Salt Tectonic Subprovinces Beneath the Scotian Slope and Laurentian Fan: GCSSEPM: Salt Sediment Interactions and Hydrocarbon Prospectivity: Concepts, Applications, and Case Studies for the 21 Century, Houston, Texas, p. 502-532.
- Shimeld, J. W., Warren, S. N., Mosher, D. C., and MacRae, R. A., 2003, Tertiary-aged megaslumps under the Scotian Slope, South of the LaHave Platform, Offshore Nova Scotia (abstract): The Geological Society of America (GSA), Halifax, # 32-2.
- Stea, R. R., Piper, D. J. W., Fader, G. B. J., and Boyd, R., 1998, Wisconsinan Glacial and Sea-Level History of Maritime Canada and the Adjacent Continental Shelf: A Correlation of Land and Sea Events.: Geological Society of America Bulletin, v. 110, p. 821-845.
- Swift, S. A., 1985, Late Pleistocene Sedimentation on the Continental Slope and Rise off Western Nova Scotia: Geological Society of America Bulletin, v. 96, p. 832-841.
- , 1987, Late Cretaceous-Cenozoic development of outer continental margin, southwestern Nova Scotia: AAPG Bulletin, v. 71, p. 678-701.
- Thomas, F. C., 1994, Cenozoic foraminiferal biostratigraphy and depositional environments of Shell Mobil Tetco Eagle D-21, unpublished report, Geological Survey of Canada Atlantic.
- Toumarkine, M., and Luterbacher, H., 1985, Paleocene and Eocene planktonic foraminifera, *in* Bolli, H. M., Saunders, J. B., and Perch-Nielsen, K., eds., Plankton Stratigraphy, Cambridge, UK, Cambridge University Press, p. 87-154.

- Turcotte, D. L., and Schubert, G., 1982, *Geodynamics: Applications of Continuum Physics to Geologic Problems*: New York, Wiley, 450 p.
- Uchupi, E., and Austin, J. A., Jr., 1979, The geologic history of the passive margin off New England and the Canadian Maritime provinces: *Tectonophysics*, v. 59, p. 53-69.
- Vail, P. R., Mitchum, R. M., Todd, R. G., Widmier, J. M., Thompson, S., Sangree, J. B., Bubb, J. N., and Hatlelid, W. G., 1977, Seismic stratigraphy and global changes of sealevel, *in* Payton, C. E., ed., *Seismic Stratigraphy - Applications to Hydrocarbon Exploration*, AAPG Mem., v.26, p. 49-212.
- Wade, J. A., and MacLean, B., 1990, The geology of the southeastern margin of Canada, Chapter 5, *in* Keen, M. J., and Williams, G. L., eds., *Geology of the Continental Margin of Eastern Canada*, Geological Survey of Canada, p. 167-238.
- Wade, J. A., MacLean, B. C., and Williams, G. L., 1995, Mesozoic and Cenozoic stratigraphy, eastern Scotian Shelf, New interpretations: *Canadian Journal of Earth Sciences*, v. 32, p. 1462-1473.
- Weimer, P., 1991, Seismic facies, characteristics, and variations in channel evolution, Mississippi Fan (Plio- Pleistocene), Gulf of Mexico, *in* Weimer, P., and Link, M. H., eds., *Seismic Facies and Sedimentary Processes of Submarine Fans and Turbidite Systems: Frontiers in Sedimentary Geology*, New York, Springer-Verlag, p. 323-348.
- Weimer, P., and Posamentier, H. W., 1993, Recent development and applications in siliciclastic sequence stratigraphy, *in* Weimer, P., and Posamentier, H. W., eds., *Siliciclastic Sequence Stratigraphy - Recent Developments and Applications*, Tulsa, AAPG Memoir, v.58, p. 3-12.

Wright, L. D., Coleman, J. M., and Erickson, M. W., 1974, Analysis of major river systems and their deltas: morphologic and process comparisons, Louisiana State University, Coastal Studies Institute, unpublished report, Technical Report #156.

Yilmaz, O., 1987, Seismic Data Processing, v. 2: Tulsa, Society of Exploration Geophysicists, 525 p.

Zachos, J., Pagani, M., Sloan, L., Thomas, E., and Billups, K., 2001, Trends, Rhythms, and Aberrations in Global Climate 65 Ma to Present: *Science*, v. 292, p. 686-693.